

Laboratory Investigations of
Silicon Dioxide Nanoparticle Enhanced Oil Recovery
for Application in the Offshore Reservoir, Hebron Field

by
© Jenny Kim.

A Thesis submitted to the
School of Graduate Studies
in partial fulfillment of the
requirements for the degree of

Master of Engineering in Oil and Gas

Faculty of Engineering and Applied Science
Memorial University of Newfoundland

May 2018

St. John's

Newfoundland and Labrador

Canada

Abstract

The silicon dioxide nanoparticles for enhanced oil recovery as a water additive is a growing research field. The challenge of using silicon dioxide nanoparticles offshore, such as Hebron Field, is an instability of the nanoparticles in the seawater. The use of hydrochloric acid is proposed as a silicon dioxide nanoparticle stabilizer in seawater, and its effectiveness was investigated at room temperature, and at Hebron Field temperature (62 °C) over a 14-day period, via visual examination and particle size measurements. The nanofluids were then prepared by adding hydrochloric acid to the nanoparticles, then dispersing the resulting mixture in seawater for the coreflood experiments. The coreflood experiments conducted at Hebron Field conditions on the Berea sandstone cores, in which 0.01, 0.03 and 0.05 wt% silicon dioxide nanofluids were injected as a tertiary method, showed increasing oil recovery (3.3, 9.3, and 14.9% increments, respectively) with increasing nanoparticle concentration. The coreflood experiment on the Hebron Field core with 0.05 wt% nanofluid also exhibited 11.9% incremental oil recovery. The hydrochloric acid added in the nanofluid was found to have minimal effect on the recovery factor.

Acknowledgements

My thesis project was an exciting platform for me to explore the world of engineering and deepen my understanding in chemistry. I would like to thank Dr. Lesley James for giving me the opportunity to embark on this journey. It was a privilege to work in the Hibernia EOR Laboratory, and I am grateful for Dr. James' academic support, financial assistance, and advice. I would also like to thank Dr. Yahui Zhang for his generous input and insights. My thank you also extends to the Hibernia EOR Research staff – Edison Sripal, Shervin Ayazi, and Kim Power – for their support.

I was fortunate to have Daniel Sivira as a research partner. We helped and pushed each other every step of the way – I will always pride the dedication and hard-work we put into our projects.

IA's, LI's, and Dan Wade at Memorial University Chemistry Department: Thank you for your words of encouragements and sense of humour, helping me to push through my studies while working full-time. I appreciate the instructional staffs being extremely flexible with the scheduling, allowing me to attend classes, group meetings, and conferences around the work hours.

My friends Kelli-Nicole Croucher, Gabriela Estrada, Wilson Humphries, and Kerry-Lynn Williams: You are my chosen family – thank you for the never ending moral support and accepting me for who I am.

My deepest gratitude goes to my family, and the Beresfords. Your unconditional love and support keeps me strong and propels me to become the best version of myself. I dedicate all my accomplishments to you, including this thesis.

Table of Contents

Abstract.....	ii
Acknowledgements	iii
Table of Contents	iv
List of Tables	viii
List of Figures.....	ix
List of Abbreviations and Symbols	xii
Notes on Units.....	xiv
List of Appendices.....	xvi
Chapter 1. Introduction.....	1
1.1. Overview	1
1.2. Hebron Field Overview.....	2
1.3. Enhanced Oil Recovery	4
1.4. Nanoparticle Enhanced Oil Recovery.....	5
1.4.1. Advantages	5
1.4.2. Nanofluid Coreflood Experiments.....	6
1.5. Silicon Dioxide Nanoparticle.....	9
1.5.1. Structure and Surface Chemistry	9
1.5.2. Stability.....	12

1.6. Stability Evaluation Method	14
1.7. Thesis Organization	16
Co-authorship Statement	18
Chapter 2. Stability of Hydrophilic Silicon Dioxide Nanoparticles Dispersed in Seawater for the Enhanced Oil Recovery Application in the Offshore Reservoirs ...	19
2.1. Abstract	19
2.2. Introduction	20
2.3. Experimental Methodology	22
2.3.1. Experiment Overview	22
2.3.2. Materials	25
2.3.3. Instruments for the Particle Size and pH Measurements	26
2.3.4. Experimental Procedures	26
2.4. Experimental Results and Discussion	30
2.4.1. Aggregation Behaviour of Silicon Dioxide Nanoparticles in Ionic Salt Solutions.....	30
2.4.2. Optimization of Silicon Dioxide Nanofluid Preparation Method.....	36
2.4.3. The Effect of Hydrochloric Acid Concentration on the Stability of Silicon Dioxide Nanofluid	38
2.4.4. The Effect of Hydrochloric Acid Concentration on the Stability of Silicon Dioxide Nanofluid over Time and Temperature.....	41
2.5. Conclusions.....	44

Acknowledgements.....	45
References.....	45
Chapter 3. Experimental Investigation of Enhanced Oil Recovery by Injecting SiO₂ Nanoparticles as Water Additive with Application to the Hebron Field.....	48
3.1. Abstract.....	48
3.2. Introduction.....	49
3.3. Method.....	54
3.4. Results and Discussion.....	59
3.5. Conclusions.....	63
Acknowledgements.....	64
References.....	64
Chapter 4. A Coreflood Study of Injecting Silicon Dioxide (SiO₂) Nanoparticles as a Water Additive for the Enhanced Oil Recovery on the Hebron Field Cores.....	68
4.1. Abstract.....	68
4.2. Introduction.....	69
4.3. Experimental Methodology.....	72
4.4. Results and Discussion.....	79
4.5. Conclusions.....	87
Acknowledgements.....	88

References	88
Chapter 5. Concluding Remarks	91
5.1. Summary	91
5.2. Lessons Learned and Future Recommendations.....	93
5.2.1. SiO ₂ Nanoparticle Stability.....	93
5.2.2. Optimization of SiO ₂ Nanoparticle Concentration	94
5.2.3. Coreflooding Experiments.....	94
5.2.4. Nanoparticle Retention due to Adsorption	95
5.2.5. Nanoparticle Enhanced Oil Recovery Mechanisms	95
Bibliography	96
Appendices.....	102

List of Tables

Table 1.1 Selected coreflood experiments using silicon dioxide nanofluid	8
Table 2.1 The composition of Grand Banks seawater (Valencia, James, & Azmy, 2017)	25
Table 2.2 Ionic salt solution compositions and concentrations used to identify the ion affecting the stability of SiO ₂ nanoparticles the most	27
Table 2.3 The HCl to SiO ₂ ratio ranges prepared to study the effect of HCl	29
Table 2.4 The concentrations of hydrochloric acid and silicon dioxide to generate range of ratios between the two, and the pH measurements of resulting fluids	39
Table 3.1 Coreflood Experiments Using Silicon Dioxide Nanoparticles.....	51
Table 3.2 Nanofluid properties in seawater	55
Table 3.3 Grand Banks seawater composition (Valencia et al. 2017)	55
Table 3.4 Standard Berea cores specifications for coreflood experiments	56
Table 3.5 Composition of synthetic formation water used to generate connate water.....	57
Table 4.1. Grand Banks seawater composition (Valencia et al. 2017).....	73
Table 4.2. Physical properties of the cores used in coreflood experiments	74
Table 4.3. Composition of synthetic formation water used to generate connate water in Berea and Hebron Cores	75
Table 4.4 The summary of pH measurements and recovery factor from coreflood run 1	84
Table 4.5 The summary of pH measurements and recovery factor from coreflood run 2	84
Table 4.6 The summary of pH measurements and recovery factor from coreflood run 3	84
Table 5.1 Summary of coreflooding experiment results.....	92

List of Figures

Figure 1.1 Hebron field location	3
Figure 1.2 Cross-section of Hebron asset (CNLOPB, 2011)	4
Figure 1.3 Tetrahedral geometry (left) and linear geometry (right).....	9
Figure 1.4 Three-dimensional arrangement of amorphous silicon dioxide nanoparticles (Bergna, 2005)	10
Figure 1.5 Formation of silanol group via rehydroxylation process (Modified after Comas-Vives, 2016)	10
Figure 1.6 The surface of amorphous silicon dioxide (Modified after Comas-Vives, 2016)	11
Figure 1.7 Stability of Colloidal System Evaluation via Particle Size Measurements	14
Figure 2.1 The experimental design.....	22
Figure 2.2 The relationship between the stability of colloidal system and the particle size measurements.....	24
Figure 2.3 Three method of preparing silicon dioxide nanofluid	28
Figure 2.4 The particle size measurement at Na ⁺ concentrations of 0 ppm to 50000 ppm from two ionic salts: sodium chloride and sodium sulfate	31
Figure 2.5 The particle size measurement at Mg ²⁺ concentrations of 0 ppm to 2000 ppm from two ionic salts: magnesium chloride and magnesium sulfate	32
Figure 2.6 (a) Tetrahedral geometry of silicon dioxide (b) 3D Arrangement of amorphous silicon dioxide nanoparticles (c) The negative surface of silicon dioxide nanoparticles.....	33
Figure 2.7 The electrical double layer formed around the negative surface charged particle, such as silicon dioxide nanoparticles, in a continuous medium (Mehta et al., 2008)	34

Figure 2.8 The particle size measurements and pH (taken within one hour of sample preparation) of nanofluids prepared in three different methods at hydrochloric acid to silicon dioxide nanoparticle ratios ranging from 0.02 to 0.60.....	37
Figure 2.9 The particle size measurements silicon dioxide nanofluid across a range of hydrochloric acid and silicon dioxide ratio in the presence of 0.001 wt% and 0.003 wt% hydrochloric acid	40
Figure 2.10 The 0.05 wt% silicon dioxide nanoparticle size measurements at room temperature, at HCl to SiO ₂ ratio ranging from 0.12 to 0.60.....	42
Figure 2.11 The 0.05 wt% silicon dioxide nanoparticle size measurements at 62°C, at HCl to SiO ₂ ratio ranging from 0.12 to 0.60	42
Figure 3.1 Offshore Canada oil & gas developments, including Hebron Field (Sivira et al. 2016)	52
Figure 3.2 Mineralogical composition of Lower Ben Nevis Formation and Berea sandstone	55
Figure 3.3 Schematic diagram of coreflood set-up	58
Figure 3.4 SiO ₂ nanoparticle contribution on interfacial tension alteration (After Sivira et al. 2016)	59
Figure 3.5 Contact angle measurements on Berea with SiO ₂ nanofluids (After Sivira et al. 2016)	60
Figure 3.6 Oil recovery using 0.01 wt% and 0.03 wt% SiO ₂ nanofluid	60
Figure 4.1. Location of the Hebron asset	70
Figure 4.2. Cross section of Hebron assets (Modified after CNLOPB, 2011).....	70
Figure 4.3. Mineralogical composition of core from Ben Nevis Formation and Berea sandstone	74
Figure 4.4. Composition of simulated oil by the carbon number.....	76
Figure 4.5. Schematic diagram of coreflood experiment setup.....	77
Figure 4.6 (a) Coreflood injection schemes (b) Summary of cores used and fluids injected	78

Figure 4.7. Coreflood run 1: oil recovery using 0.05 wt% SiO₂ nanofluids on Berea sandstone core..... 80

Figure 4.8. Coreflood run 2: oil recovery using 0.05 wt% SiO₂ nanofluid on Hebron core 81

Figure 4.9. Coreflood run 3: oil recovery using seawater + HCl mixture (0.00 wt% nanofluid) on Berea sandstone core..... 82

List of Abbreviations and Symbols

Abbreviation/Symbol	Description
(aq)	Aqueous State (Dissolved in Water)
Ca, Ca ²⁺	Calcium
CaCl ₂	Calcium Chloride
Cl	Chlorine
D	Diffusion Coefficient
d _H	Hydrodynamic Diameter
DLS	Dynamic Light Scattering
EOR	Enhanced Oil Recovery
H ₂ O	Water
HCl	Hydrochloric Acid
HCO ³⁻	Bicarbonate
He	Helium
ICP	Inductively Coupled Plasma Spectrometry
K	Permeability
k	Boltzmann's Constant
KCl	Potassium Chloride
M	Mega
Mg, Mg ²⁺	Magnesium
MgCl ₂	Magnesium Chloride

MLA	Mineral Liberation Analysis
n	nano
Na ₂ SO ₄	Sodium Sulfate
NaCl	Sodium Chloride
Ne	Neon
O	Oxygen
SEM	Scanning Electron Microscopy
Si	Silicon
SiO ₂	Silicon Dioxide
SO ₄ , SO ₄ ²⁻	Sulfate
T	Temperature

Greek Letters	Description
φ	Porosity
η	Viscosity

Notes on Units

Field units are often used instead of SI units in petroleum engineering fields. Although most values are represented in SI units throughout the manuscript, the following field units are also used:

Variable	Field Unit	Equivalent SI Unit
Density	°API	g/cm^3 or g/mL
Permeability	mD	m^2
Pressure	psi	Pa
Rate	ft/day	cm^3/s or mL/s
Temperature	°C	Kelvin
Time	days	seconds
Viscosity	cp	$\text{Pa}\cdot\text{s}$
Volume	bb1	m^3

The accepted SI unit for concentration is mol/L, however, other units have been used to represent concentrations:

Variable	Unit Used	Equivalent SI Unit
Salt solutions, Seawater	ppm	mol/L
Nanoparticles	wt%	mol/L
Hydrochloric Acid	wt%	mol/L

The unit, ppm (parts per million), is used for concentrations of salt solutions, and seawater because it is a common unit used to represent the salinity. The nanoparticle was purchased in wt% suspension in water, and their concentrations were kept in wt% upon dilution because accurate determination of molar concentrations for particle sizes less than 30 nm is inaccurate (Shang & Gao, 2014). The hydrochloric acid concentrations are also represented in wt% for the nanoparticle stability studies, since the interest was in determining the ideal ratios between the hydrochloric acid and nanoparticles, and the ratio would make the most sense if both components were in the same unit, wt%, to give unit-less ratio.

Note that in Chapter 2 and Chapter 3, the amounts of hydrochloric acid used are shown in mol/L, because the SI unit was the paper submission requirement. The hydrochloric acid to nanoparticle concentration ratios are still unit-less, since they were never the less calculated based on hydrochloric acid and nanoparticle concentrations in wt%.

List of Appendices

Appendix A. Standard Deviations of Silicon Dioxide Nanoparticle Particle Size Measurements	102
Appendix B. Visual Examination of 0.05 wt% Silicon Dioxide Nanoparticles, with Hydrochloric to Nanoparticle Ratios 0.12, 0.18, 0.24, 0.46, and 0.60, over 14-Day Period at Room Temperature and 62 °C	111
Appendix C. 0.03 wt% Silicon Dioxide Nanoparticle Size Measurements at Room Temperature and at 62 °C with Hydrochloric Acid to Silicon Dioxide Ratio Ranging from 0.12 to 0.60	113
Appendix D. Visual Examination of 0.03 wt% Silicon Dioxide Nanoparticles, with Hydrochloric to Nanoparticle Ratios 0.12, 0.18, 0.24, 0.46, and 0.60, over 14-Day Period at Room Temperature and 62 °C	114
Appendix E. Visual Examination of 0.01 wt% Silicon Dioxide Nanoparticles, with Hydrochloric to Nanoparticle Ratios 0.12, 0.18, 0.24, 0.46, and 0.60, over 14-Day Period at Room Temperature and 62 °C	116
Appendix F. Determination of Core Porosity	118
Appendix G. Sample Porosity Calculation using Berea core used for 0.01 wt% nanoparticle flooding	119
Appendix H. Sample Calculations to Generate Oil Recovery Graphs from the Coreflood Experiments	120
Appendix I. Coreflood Experiment Using 0.01 wt% Nanofluid on Berea Sandstone Raw Data	121
Appendix J. Coreflooding Oil Recovery Plot with Differential Pressures using 0.01 wt% Nanofluid	124

Appendix K. Coreflood Experiment Using 0.03 wt% Nanofluid on Berea Sandstone Raw Data	125
Appendix L. Coreflooding Oil Recovery Plot with Differential Pressures using 0.03 wt% Nanofluid	128
Appendix M. Coreflood Experiment Using 0.05 wt% Nanofluid on Berea Sandstone Raw Data	129
Appendix N. Coreflood Experiment Using 0.05 wt% Nanofluid on Hebron Core Raw Data....	132
Appendix O. Coreflood Experiment Using HCl/Seawater Mixture on Berea Sandstone Raw Data	136

Chapter 1. Introduction

1.1. Overview

The application of any enhanced oil recovery methods in offshore fields such as Hebron Field pose difficulties in transportation and quality control of the injectants (Kang, Lim, & Huh, 2016). The remote offshore location of Hebron Field, and the harsh surrounding environmental conditions makes it even more imperative that the enhanced oil recovery to be applied has a small footprint. The nanoparticles exhibit heightened properties because of their small sizes, and therefore, small quantity can have a significant impact, easing the burden of transportation offshore. The use of nanoparticles in Hebron Field, however presents an unique challenge: high salinity of seawater used for the waterflood. The seawater is used for the waterfloods in Hebron Field, since it is the most abundant water source offshore. Nanoparticle enhanced oil recovery offshore would also involve dispersing nanoparticle in the seawater. The seawater unfortunately compromises the stability of the silicon dioxide (SiO_2) nanoparticles (Metin, Lake, Miranda, & Nguyen, 2011). The nanoparticles are dispersed in the liquid medium uniformly in stable nanofluid, whereas the nanoparticles agglomerate to form gelatinous solid in unstable nanofluids. The unstable nanofluids are undesirable, as the surface-active properties of the nanoparticles are reduced.

A cost-effective hydrochloric acid is introduced to stabilize the nanoparticles in seawater to prevent nanoparticles from agglomeration. The optimal concentration of hydrochloric acid as a stabilizing agent was investigated via nanoparticle size measurements on

Malvern™ Zetasizer® Nano ZS. The agglomeration of the nanoparticles as the nanofluids become unstable translates to larger particle size measurements compared to the particle size measurements of the stable nanofluids. The optimal concentration was defined as a minimum concentration ratio between the hydrochloric acid to nanoparticles required for nanoparticle size measurements to remain constant over time, while contributing to the ease of transportation.

The coreflood experiments were performed to examine the effectiveness of the nanoparticles on the incremental oil recovery. The degree of the incremental oil recovery from nanoparticle enhanced oil recovery is important in determining the economic feasibility of implementing nanoparticle enhanced oil recovery technique in the Hebron Field. The preliminary coreflood experiments were conducted on the Berea sandstone standard cores to determine the nanoparticle concentration that gives the highest incremental oil recovery. A final coreflood experiment was conducted on the Hebron core.

1.2. Hebron Field Overview

The Hebron Field was discovered in 1980, 350 km offshore St. John's, Newfoundland and Labrador, Canada in the Jeanne d'Arc Basin (Figure 1.1). The gravity based structured platform was towed out to the field in April 2017, and the first oil was produced in November 2017.

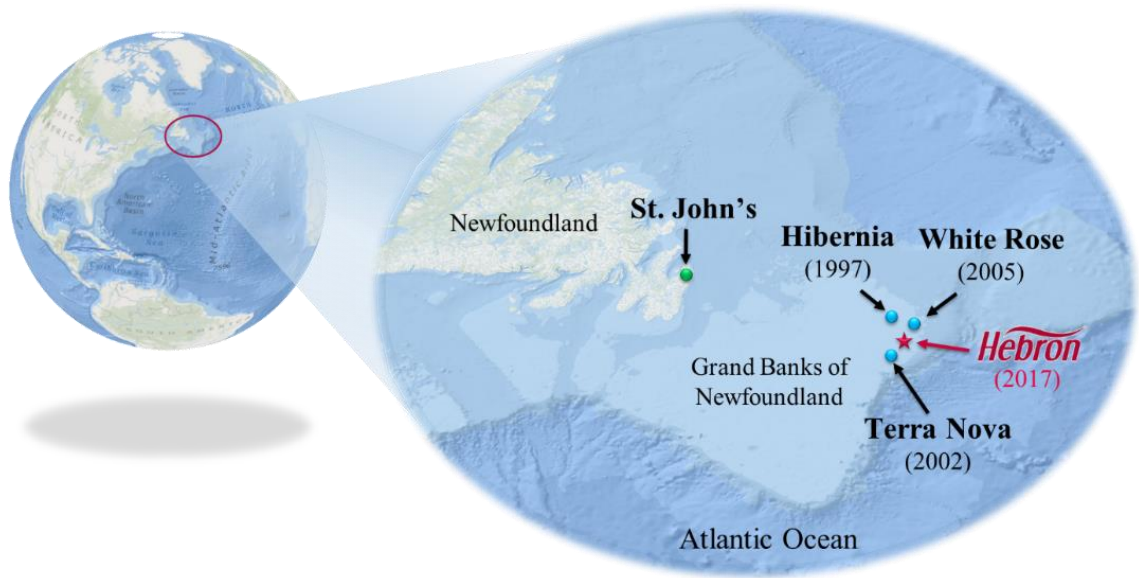


Figure 1.1 Hebron field location

The Hebron asset consists of Hebron Field, West Ben Nevis Field, and Ben Nevis Field (Figure 1.2). The development is focused on the Hebron Field, especially the Ben Nevis formation because it hosts the largest reservoir, Pool 1, and is anticipated to produce 70% of the Hebron Project’s crude oil.

The average depth of the reservoir (Pool 1) is 1900 m, with pressure of 19.0 MPa (2755 psia), and temperature of 62 °C. The oil gravity is 20.1°API, which is 10 to 20 times higher than water. The Ben Nevis Formation in Hebron Field is a “fine-grained sandstone with few shales that were deposited in a marine shoreface depositional environment”. The average permeability of Hebron Field at the Ben Nevis ranges from 50 to 400 mD, and average gross porosities range from 0.10 to 0.28 (CNLOPB, 2011).

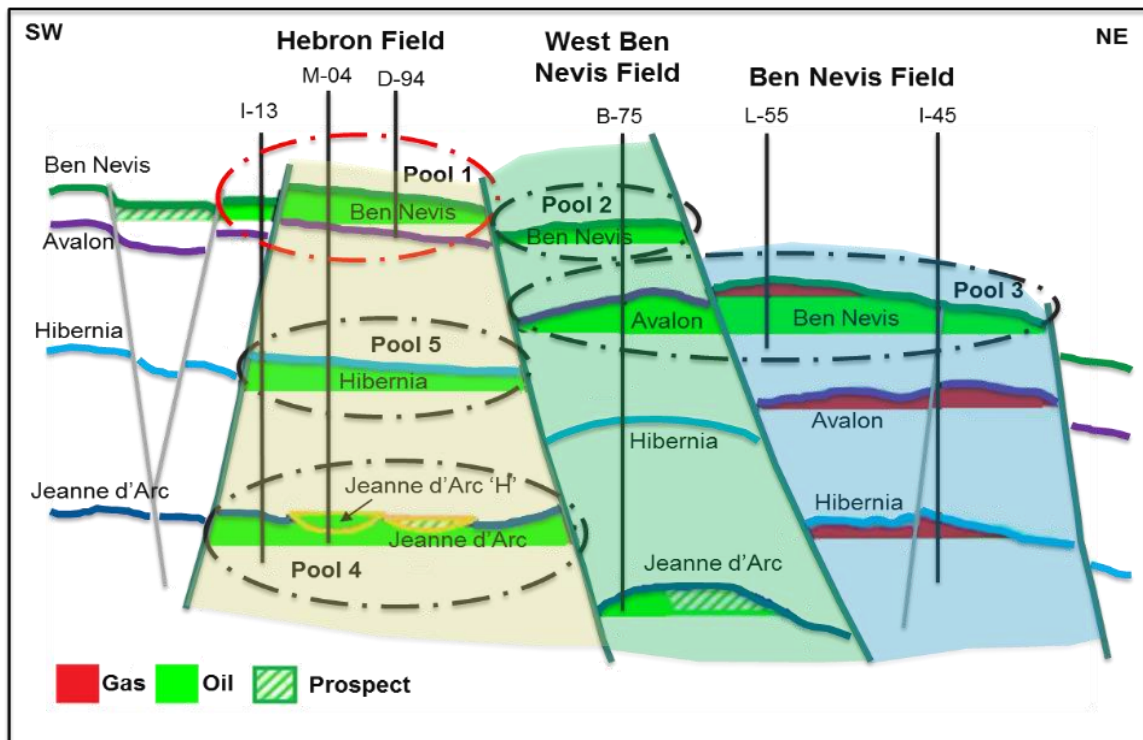


Figure 1.2 Cross-section of Hebron asset (CNLOPB, 2011)

1.3. Enhanced Oil Recovery

The primary recovery takes place in the early stage of production life, and relies on the natural drive energy. The natural drive energy sources include rock and fluid expansion, solution gas, water influx, gas cap, and gravity drainage (Stosur, Hite, Carnahan, & Miller, 2003). When the natural drive energy is depleted, an additional energy is applied to the reservoir, which is referred to as secondary recovery. The water and/or gas are commonly injected as an additional energy (Sheng, 2010). They mimic the natural process of water influx or gas expansion to maintain the reservoir pressure, and to increase volumetric sweep efficiency (Stosur et al., 2003). Enhanced Oil Recovery (EOR) is often applied as

tertiary recovery method, to recover oil that has not been produced by secondary recovery (Stosur et al., 2003). The enhanced oil recovery processes are characterized by injection of chemicals, miscible gases, and/or thermal energy (Sheng, 2010) to promote reservoir rock and oil system interaction (Green, 1998). These processes typically change the fundamental physics or chemistry to improve the oil recovery (N.R. Morrow & Heller, 1985), resulting in favourable conditions for oil recovery, such as interfacial tension reduction; oil swelling; oil viscosity reduction; wettability modification; or favourable phase behaviour (Green, 1998).

1.4. Nanoparticle Enhanced Oil Recovery

1.4.1. Advantages

The use of nanoparticles as a water additive is relatively new, and it is hoped to give alternative solutions for the challenges of traditional enhanced oil recovery processes (Ayatollahi, 2012). For example, the injection of carbon dioxide gas can be inefficient since injected gas can bypass large sections of the reservoir due to high mobility ratio. The chemical methods such as polymer flooding can damage the formation, and alkaline flooding can be expensive since excess amount has to be injected (Sun, Zhang, Chen, & Gai, 2017).

The nanoparticles are between 1 to 100 nanometers, which are much smaller than the typical diameters of the pores in reservoirs, 1 micrometer (equivalent to 1000 nanometers) (Ayatollahi, 2012). The nanoparticles can therefore easily move through the porous rocks,

without affecting the permeability (Ahmadi, Habibi, Pourafshry, & Ayatollahi, 2011). They are also believed to penetrate the pore spaces, due to their small sizes, that conventional recovery techniques cannot reach (Engeset, 2012). Another advantage of the small size is the high surface to the volume ratio. The increased surface area leads to increased number of reactions at its surface (El-diasty & Aly, 2015).

The nanoparticle is also cost effective, and environmentally friendly, especially the silicon dioxide nanoparticles (Sun et al., 2017). The starting material for silicon dioxide nanoparticle synthesis is widely available, since the silicon dioxide is one of the most common components on earth (Society for Mining, Metallurgy, 1998), contributing to the low cost. The silicon dioxide nanoparticles are also environmentally friendly because silicon dioxide is major components of the sand and sandstone.

1.4.2. Nanofluid Coreflood Experiments

Coreflood experiments are conducted to evaluate the effectiveness of the injecting fluid on enhancing the oil recovery in the laboratory scale. The nanofluid flooding experiments found in the literature mostly studied the effectiveness as a tertiary recovery method (Sun et al., 2017). That is, the nanoparticles added to water is injected after the core has been flooded with water until no more oil is produced. The selected coreflood experiments using silicon dioxide nanofluid (Table 1.1) all showed positive impact of nanofluids on the incremental oil recovery.

Despite the successes of the nanoparticle flooding experiments in the literature, further nanoparticle flooding studies are needed to apply the nanoparticle enhanced oil recovery

in the offshore fields. The coreflood experiments shown in Table 1.1 dispersed the nanoparticles in fluids with 0% salinity, or in a simple salt solution prepared from sodium chloride. The dispersing medium for nanoparticles in the offshore will likely be the surrounding seawater, which contains sodium and chloride ions, but also other ions such as magnesium, calcium, selenium, sulfate, and bicarbonate. The effect of salinity and the composition of seawater on the nanoparticle flooding must be investigated, as divalent cations in the seawater, such as magnesium and calcium ions are found to destabilize the nanoparticles (Metin et al., 2011).

The incremental oil recovery obtained from the coreflood experiments are also dependant on the reservoir conditions (namely pressure and temperature), reservoir properties (permeabilities and porosity), reservoir mineralogy, as well as properties of oil. The effect of nanofluid on the oil recovery specifically for the Hebron Field must then be evaluated with coreflood experiment set-up that emulates the Hebron Field conditions.

Table 1.1 Selected coreflood experiments using silicon dioxide nanofluid

References	SiO ₂ concentration	Dispersion medium	Porous media	Pore volume injected	Incremental recovery
Nazari Moghaddam, Bahramian, Fakhroueian, Karimi, & Arya, 2015	5 wt%	Paraffin/heptane, mixture of ethylene glycol, and lauryl alcohol	Type: Carbonate Φ*: 13.2% K**: 0.24 mD	1. Brine, 5 PV 2. Nanofluid, 2 PV 3. Brine	7.7%
Hendraningrat & Torsæter, 2014	0.05 wt%	3 wt% NaCl brine with PVP (Polyvinylpyrrolidone)	Type: Water-wet Berea Φ: 14.99% K: 119 mD	1. Brine, 5 PV 2. Nanofluid, 5 PV 3. Brine, 5 PV	21.4%
Aurand, Dahle, & Torsæter, 2014	0.05 wt%	Diluted to 2 wt% nanofluid with deionized water, then diluted further to 0.05 wt% with 3.53% salinity synthetic brine	Type: Water-wet Berea Φ: 18.1% K: 394 mD	1. Brine, 2 PV 2. Nanofluid, 2 PV	20.0% (Large fumed nanofluid)
Joonaki & Ghanaatian, 2014	Not given	Propanol	Type: Sandstone Φ: 17.34% K: 108.21 mD	1. Brine, 3 PV 2. Nanofluid, 3 PV	22.5%
Hendraningrat, Li, & Torsæter, 2013	0.01 wt%	3 wt% NaCl brine	Type: Berea Φ: 23.20% K: 392 mD	1. Brine, 3.7 PV 2. Nanofluid, 2.8 PV	9.6%
	0.05 wt%	3 wt% NaCl brine	Type: Berea Φ: 23.04% K: 302 mD	1. Brine, 3.2 PV 2. Nanofluid, 3.1 PV	13.0%
	0.1 wt%	3 wt% NaCl brine	Type: Berea Φ: 22.93% K: 354 mD	1. Brine, 3.1 PV 2. Nanofluid, 3.5 PV	8.6%
Roustaeei, Moghadasi, Jamshid Bagherzadeh, & Shahrabadi, 2012	5 g/L	Weak or non-polar solvent	Type: Sandstone Φ: 17% K: 186 mD	1. Brine, 2 PV 2. Nanofluid, 3 PV 3. Brine, 2 PV	28.6% (NWP) [§] 32.2% (HLP) ^{§§}

*Φ: Porosity, **K: Permeability, §NWP: Naturally Wet Polysilicon §§HLP: Hydrophobic and Lipophilic Polysilicon

1.5. Silicon Dioxide Nanoparticle

1.5.1. Structure and Surface Chemistry

Silicon dioxide exists as $[\text{SiO}_4]$ with four oxygens attached the central atom, silicon. It bears a tetrahedral structure (Bergna, 2005), contradictory to its name, which suggests linear structure (Figure 1.3).

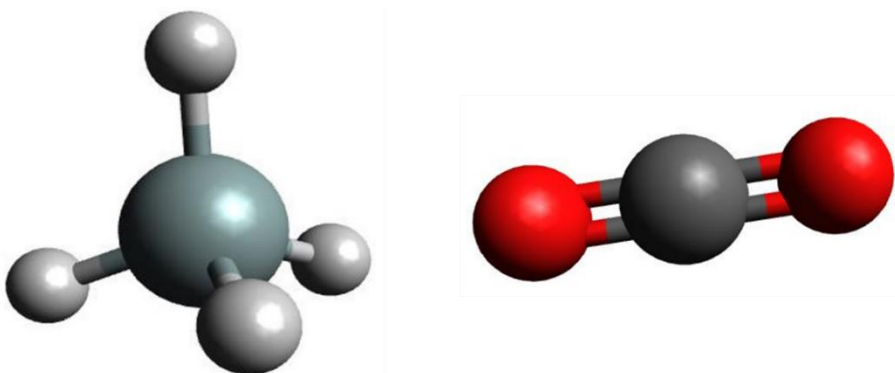


Figure 1.3 Tetrahedral geometry (left) and linear geometry (right)

The double bond between the silicon and oxygen does not form because the size of the silicon atom does not allow sufficient overlap between the p-orbitals (P. W. Atkins & Atkins, 2006). The $[\text{SiO}_4]$ tetrahedral structure can form pairs, rings, one-dimensional chains, two-dimensional sheets, or three-dimensional networks through Silicon-Oxygen-Silicon linkage (Salh, 2011). The amorphous silicon dioxide nanoparticles have a three-dimensional arrangement as shown in Figure 1.4.

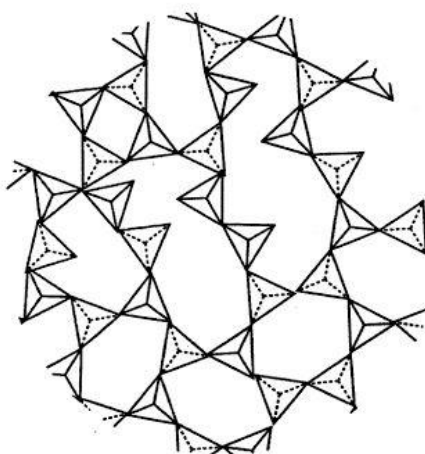


Figure 1.4 Three-dimensional arrangement of amorphous silicon dioxide nanoparticles (Bergna, 2005)

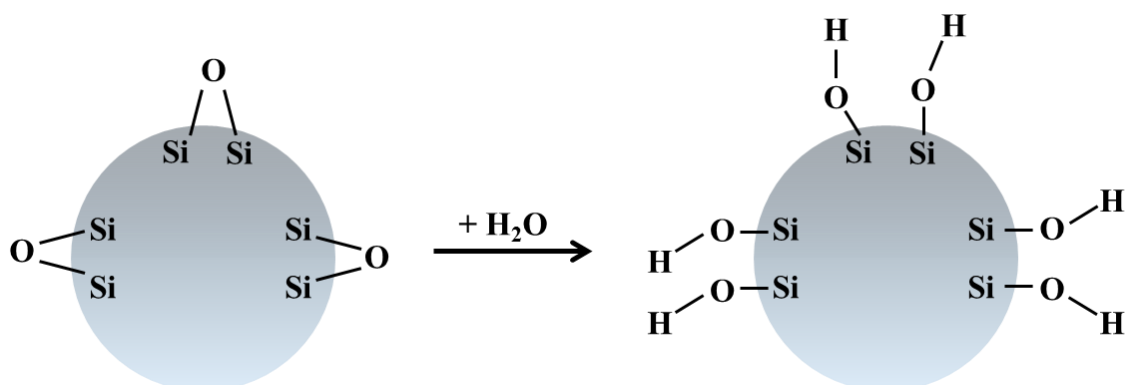


Figure 1.5 Formation of silanol group via rehydroxylation process (Modified after Comas-Vives, 2016)

The pure silicon dioxide nanoparticle surface is most commonly characterized by the siloxane links (Si–O–Si) and the silanol groups (Si–OH) (Rimola, Costa, Sodupe, & Ugliengo, 2013). Further formation of silanol group can occur via rehydroxylation

process when silicon dioxide is treated with water or aqueous solution, as free valence from the oxygen in the siloxane gains hydrogen (Zhuravlev, 2000), as shown in Figure 1.5.

The different types of silanol groups on the surface of amorphous silicon dioxide: isolated, germinal, vicinal, interacting, and internal (Comas-Vives, 2016; Zhuravlev, 2000) are depicted in Figure 1.6. The silanol groups can interact with other molecules via hydrogen bonding (electrostatic attraction between the molecules when hydrogen atom is bonded to strongly electronegative atom such as oxygen), thereby giving hydrophilic character of the silicon dioxide (Papirer, 2000).

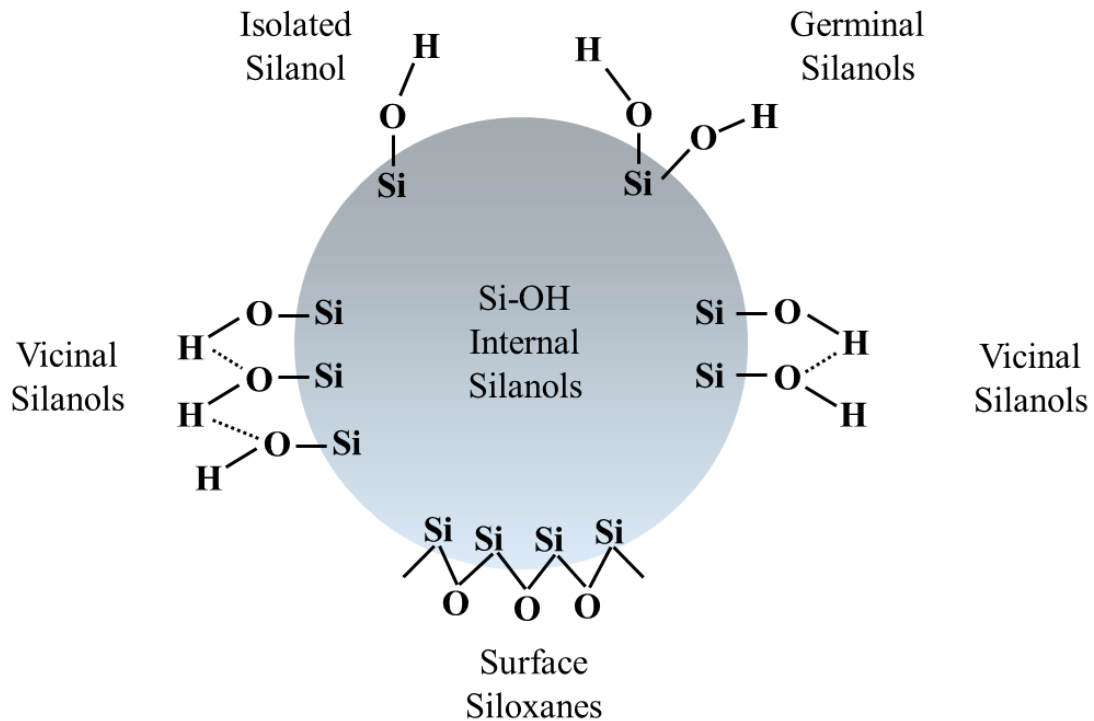


Figure 1.6 The surface of amorphous silicon dioxide (Modified after Comas-Vives, 2016)

These hydroxylated silanol groups can further be protonated by gaining a hydrogen, or lose a hydrogen to become deprotonated, and expose O^- on the nanoparticle surface (Hunter, 1981). The surface charge of silicon dioxide nanoparticles dispersed in water is dependant on the degree of protonation and deprotonation (Agzamkhodzhaev, Zhuravlev, Kiselev, & Shengeliya, 1969). At high pH, the surface is negatively charged because it becomes deprotonated. At low pH, the surface is mostly protonated, and is neutral (Sulpizi, Gaigeot, & Sprik, 2012).

1.5.2. Stability

The nanoparticles dispersed in water or aqueous solution, often called nanofluid, is a colloidal system. Colloidal system is a multi-phase system, consisting of the solid phase (i.e. nanoparticles), and a dispersing, continuous medium (i.e. water or aqueous solution) (Birdi, 2008). It is also an energetically high system because the surface free energy is high, resulting from the high surface area. As a result, the nanoparticles tend to aggregate to reduce the surface energy (Mehta, Somasundaran, Yu, & Krishnakumar, 2008), unless there are other energetic barriers (Birdi, 2008). The aggregation of nanoparticle is a sign of unstable colloidal system, as a stable colloidal system would exhibit constant number of particles in a unit volume of dispersing medium over time (Kissa, 1999). The unstable nanofluid in the context of enhanced oil recovery is highly undesirable, since the aggregation of nanoparticles to larger sizes may prevent nanoparticles from flowing through the pores, which are measured in microns. The aggregated nanoparticles may also

block the pores, decreasing the permeability of the rocks (Miranda, Lara, & Tonetto, 2012).

The colloidal stability is often described in terms of DLVO (Derjaguin-Verway-Landau and Overbeek) theory, which states that the colloidal system stability depends on the sum of van der Waals and electrical double layer interactions (Derjaguin & Landau, 1941; Verwey, 1947). The nature of van der Waals interaction is an attractive force, which exist between all atoms, ions, and molecules. The electrical double layer interaction arises from the structure of surfaces and adsorption of ions, and is repulsive. When attractive forces dominate, the particles will aggregate, and the dispersion destabilizes. When repulsive forces dominate, the system will remain in dispersed state (Kralchevsky, Danov, & Denkov, 2008). The silicon dioxides, however, is found not to conform to the DLVO theory (Bergna, 2005). Other surface forces, such as steric interaction, and hydration/solvation interaction must be taken into an account to correctly predict the silicon dioxide dispersions (Mehta et al., 2008).

The nanoparticles are constantly in motion in the dispersing medium. The rate of aggregation consequently depends on the nature of the surface interactions between the particles during these collisions; probability of collision between the particles; and the total number of particles in the system (Mehta et al., 2008). Other factors that affect the stability of nanofluids include pH, particle morphology, chemical structure of the particles, dispersing medium, and nanofluid preparation methods (Devendiran & Amirtham, 2016; Hwang et al., 2007).

1.6. Stability Evaluation Method

The nanofluid stability can be evaluated via visual examination paired with particle size measurement. In a stable colloidal system, the silicon dioxide (SiO₂) nanoparticles are uniformly dispersed in a liquid medium, characterized by the transparent and colourless appearance. In an unstable system, SiO₂ nanoparticles agglomerates, forming white gelatinous solid. The size of the nanoparticles in an unstable system grows because of the agglomeration. The instability of the system can then be spotted by the increasing nanoparticle size monitored over time, as illustrated in Figure 1.7.

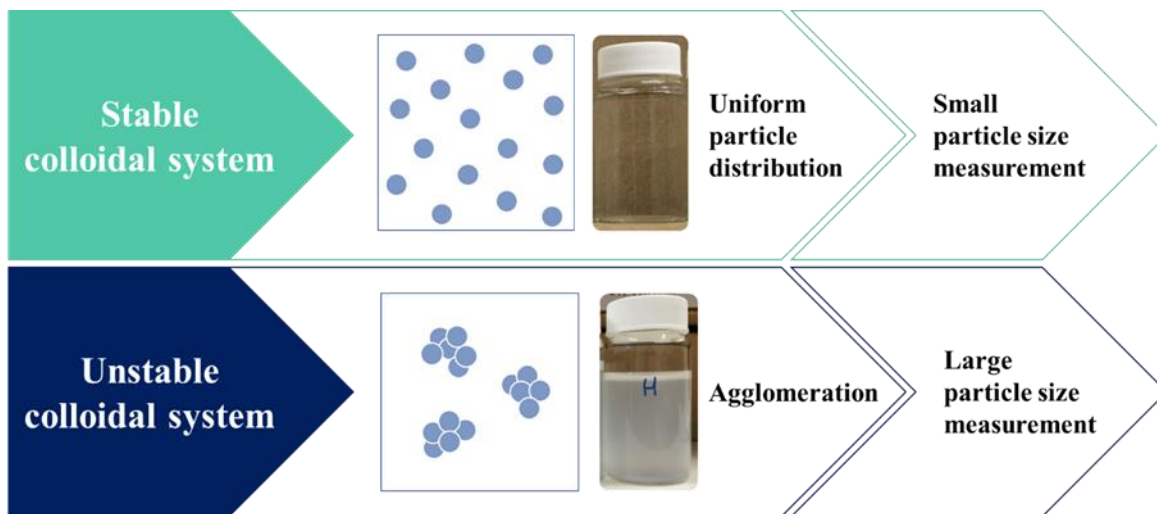


Figure 1.7 Stability of Colloidal System Evaluation via Particle Size Measurements

The particle sizes are measured by the Dynamic Light Scattering (DLS) method. The particles in suspension is in constant and random thermal motion by Brownian motion. The dynamic light scattering measures the speed of these particles. The smaller particles move fast, causing the scattered light intensity to fluctuate more rapidly compared to the larger particles that move slower. The translational diffusion coefficient is determined

from the velocity of the Brownian motion, which is in turn used to calculate the particle size by the Stokes-Einstein relationship (Shang & Gao, 2014):

$$d_H = \frac{kT}{3\pi\eta D} \quad (2)$$

Where:

- d_H = Hydrodynamic diameter
- k = Boltzmann's constant
- T = Temperature in Kelvin
- η = Viscosity
- D = Diffusion coefficient

1.7. Thesis Organization

This thesis is part of the bigger nanoparticle enhanced oil recovery project at the Hibernia EOR Laboratory; and fulfills the objectives of: identifying and tackling the challenges of implementing nanoparticle enhanced oil recovery in the Hebron Field; and evaluating the effectiveness of the nanoparticles on the incremental oil recovery as a tertiary recovery method at Hebron Field conditions.

The thesis is written in a manuscript format. In **Chapter 1**, the scope of the experimental work completed for the thesis is presented, as well as Hebron Field information. The literature review on the definition of the enhanced oil recovery; nanoparticles enhanced oil recovery technique; silicon dioxide nanoparticles; and the nanoparticle stability evaluation methods can also be found.

Chapter 2 is titled “Stability of Hydrophilic Silicon Dioxide Nanoparticles Dispersed in Seawater for the Enhanced Oil Recovery Application in the Offshore Reservoirs”. It examines why the silicon dioxide nanoparticles become unstable in seawater, and how the hydrochloric acid can be used to stabilize the nanoparticles in seawater. The optimal hydrochloric acid to silicon dioxide nanoparticle ratios to maintain nanoparticle stability to carry out coreflood experiments in Chapter 3 and 4 are also established. The content in Chapter 2 has not been published.

Chapter 3 was prepared for the EAGE 19th European Symposium on Improved Oil Recovery held in Stavanger, Norway, April 24-27, 2017. It is published as a conference proceeding, with the title: “Experimental Investigation of Enhanced Oil Recovery by

Injecting SiO₂ Nanoparticles as Water Additive with Application to the Hebron Field”. The coreflood experimental results on Berea standard cores using 0.01 wt% and 0.03 wt% nanofluids are presented.

Chapter 4 is “A Coreflood Study of Injecting Silicon Dioxide (SiO₂) Nanoparticles as a Water Additive for the Enhanced Oil Recovery on the Hebron field Cores”. It presents coreflood experiments conducted post-EAGE conference paper presented in Chapter 3. The coreflood experimental results on Berea standard core using 0.05 wt% nanofluid and coreflood results on Hebron core using 0.05 wt% nanofluid are included. The effect of the stabilizer, hydrochloric acid, on the incremental oil recovery on Berea standard core is also examined. The content in Chapter 4 has not been published.

Chapter 5 provides summary of all the experimental work. The recommendations for future work based on lessons learned can also be found.

Co-authorship Statement

The thesis author was responsible for the literature review; designing and executing the experimental work; data analysis; and preparation of the manuscripts.

Daniel Sivira helped with developing the experimental design; provided support conducting experiments as well as image processing; and reviewed the manuscripts.

Dr. Lesley James identified the scope of the project; provided guidance with the design of experiments; reviewed and approved the experiments; and provided her insight in interpreting the data. She also reviewed and suggested edits for the manuscripts.

Dr. Yahui Zhang provided his insight in the data analysis, especially with the stability analysis of the nanoparticles; and reviewed and suggested edits for the manuscripts.

Edison Sripal restored the core samples to the reservoir conditions for the coreflood experiments.

Chapter 2. Stability of Hydrophilic Silicon Dioxide Nanoparticles Dispersed in Seawater for the Enhanced Oil Recovery Application in the Offshore Reservoirs

Authors

Jenny Kim, Daniel J. Sivira, Lesley A. James, Yahui Zhang

Unpublished Manuscript

2.1. Abstract

The use of silicon dioxide nanoparticles is a novel enhanced oil recovery (EOR) technique. A major challenge to its use in EOR processes in offshore reservoirs is the nanoparticles stability in a high salinity environment. Though previous researches have proven the silicon dioxide nanoparticles performance as a water additive for EOR in either deionized water or sodium chloride solutions, they fail to emulate the offshore reservoir conditions since seawater is used for the nanoparticle injection. In this study, silicon dioxide nanoparticle stability in seawater is investigated via visual examination, followed by the particle size measurements. The effectiveness of the hydrochloric (HCl) acid as a silicon dioxide nanoparticle stabilizer in seawater is also examined by monitoring the appearance and the particle size over time. The experimental results show that the divalent cation, Mg^{2+} , in seawater compromises the silicon dioxide nanoparticles stability, causing them to agglomerate. It is also found that hydrochloric acid effectively stabilizes silicon dioxide nanoparticles possibly by shielding the nanoparticle surface from Mg^{2+} . The best way to prepare nanoparticle suspension in seawater is to mix the nanoparticle and the HCl first, then to add seawater last for the HCl to effectively protect

nanoparticle surface from cations in seawater. The amount of the HCl required to stabilize silicon dioxide nanoparticles in seawater is dependant on the nanoparticle concentration. This is because with increasing nanoparticle concentration, there is a larger nanoparticle surface area, and therefore more hydrochloric acid is required to protect their surfaces from the cations. A higher hydrochloric acid concentration is also required to stabilize the nanoparticles in seawater at 62 °C, compared to the room temperature.

2.2. Introduction

Enhanced Oil Recovery (EOR) entails an extraction of post-production oil residing in a reservoir after water or gas has been injected (Stosur et al., 2003). The use of nanoparticles is a novel method of chemically enhancing the oil recovery, though nanotechnology is not new in the oil and gas industry. For example, the application of the nanotechnology has allowed the development of more durable drilling equipment and construction of improved corrosion resistant offshore platforms (Mokhatab, Fresky, & Islam, 2006). In the recent years, there has been a growing research interest in using silicon dioxide (SiO₂) nanoparticles for EOR applications, and they have proven to be a promising water additive for EOR. The coreflooding experiments using hydrophilic SiO₂ nanoparticles are found to increase the oil recovery (Hendraningrat et al., 2012). The exact mechanisms of how SiO₂ nanoparticles improves the oil recovery is not very well understood. It has been proposed that it could be a result of the reduction in the interfacial

tension, and the oil-water-rock contact angle (Hendraningrat & Shidong, 2012; D. Wasan, Nikolov, & Kondiparty, 2011).

The challenges of introducing the SiO₂ nanoparticle EOR offshore is their instability in a high salinity and high temperature (62 °C) environment. The nanoparticles are well dispersed in the continuous medium (i.e. liquids, such as water) when stable, however, unstable nanoparticles will agglomerate, and form white gel-like solid in severe cases. The agglomeration of the nanoparticles is undesirable because their ability to decrease the interfacial tension is reduced, and could potentially block the pores of the rock. The previous laboratory studies (Hendraningrat et al., 2012; Hendraningrat & Shidong, 2012; D. Wasan et al., 2011), disperse the SiO₂ nanoparticles in either deionized water or sodium chloride solution, and lacks to address the challenges of nanoparticle instability in seawater. It is crucial to obtain stable nanoparticles in seawater for offshore production since seawater is the water source to disperse the nanoparticles.

This study investigates and identifies the ions in the seawater that successfully destabilizes the nanoparticles. Then, hydrochloric acid (HCl) is proposed as the nanoparticle stabilizer in seawater, which can counteract the ions in the seawater. The mechanism for SiO₂ stabilization in seawater using HCl is proposed, as well as the effect of HCl concentration on the SiO₂ stability. The effectiveness of HCl on stabilizing SiO₂ nanoparticles at 62 °C over 14-day period is also investigated. The SiO₂ stability is assessed with visual examination and particle size measurements in all the experiments.

2.3. Experimental Methodology

2.3.1. Experiment Overview

This paper presents four sets of experiments, and are organized in Figure 2.1 for the ease of conceptualization.

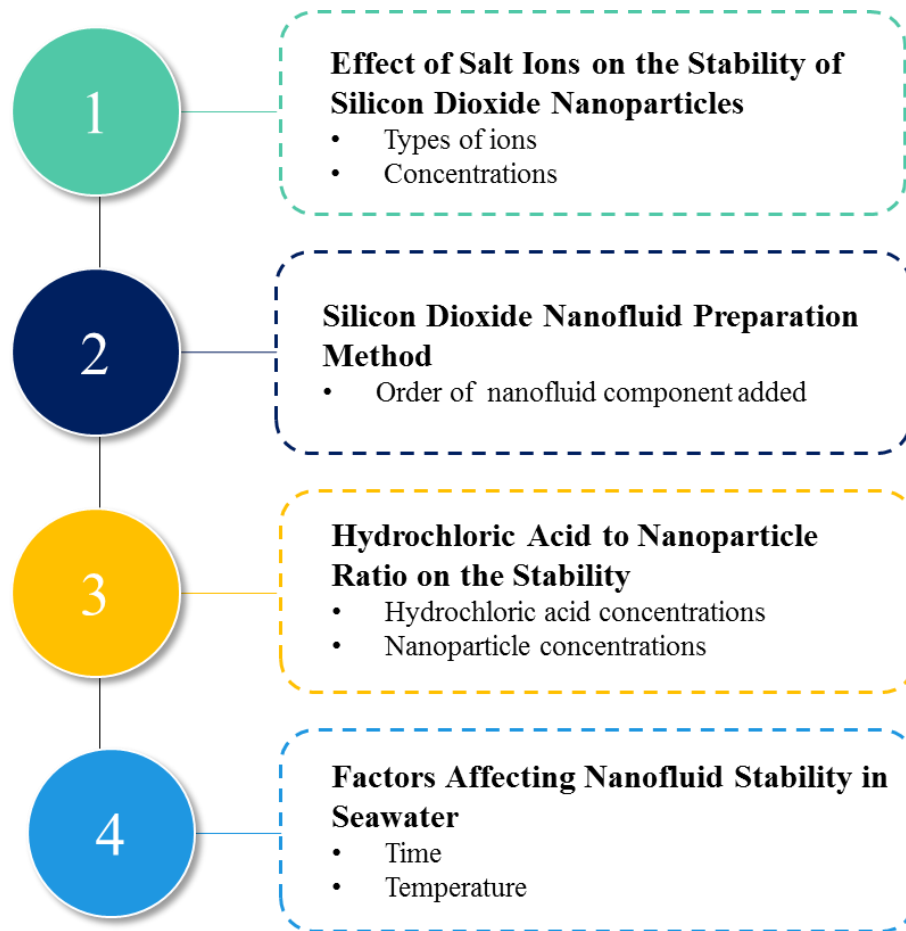


Figure 2.1 The experimental design

The experiments were designed to identify the ions in the seawater that affects the stability of the silicon dioxide (SiO_2) nanoparticles; then understand the effect of hydrochloric acid (HCl) on stabilizing SiO_2 nanoparticles in seawater. The nanoparticles dispersed in seawater were prepared in three different ways, to study whether the order of components added affects the SiO_2 stability. The HCl to SiO_2 ratio on the SiO_2 stability was also studied to find the optimal amount of HCl required to stabilize SiO_2 nanoparticles. Finally, the SiO_2 stability over time at room temperature as well as at $62\text{ }^\circ\text{C}$ was monitored to examine the effectiveness of HCl as a stabilizer at higher temperatures. $62\text{ }^\circ\text{C}$ was chosen because it is the temperature of the reservoir of interest for further SiO_2 nanoparticle enhanced oil recovery studies.

The analysis of SiO_2 nanoparticle stability was based upon the nanoparticle size measurements. The nanoparticles do not dissolve in a liquid or solution (such as seawater), rather, it becomes a colloidal system, in which nanoparticle (solid phase) suspends uniformly in the dispersing medium (continuous phase) (Birdi, 2008). The colloidal system is deemed “stable” when the number of particles in a unit volume of liquid or solution is constant over time (Kissa, 1999). This means that the nanoparticles are well dispersed in the continuous medium in a stable system, and therefore the nanoparticle size remains constant over time. In contrast, unstable system gives high nanoparticle size measurements compared to its original size, because of the agglomeration (Figure 2.2).

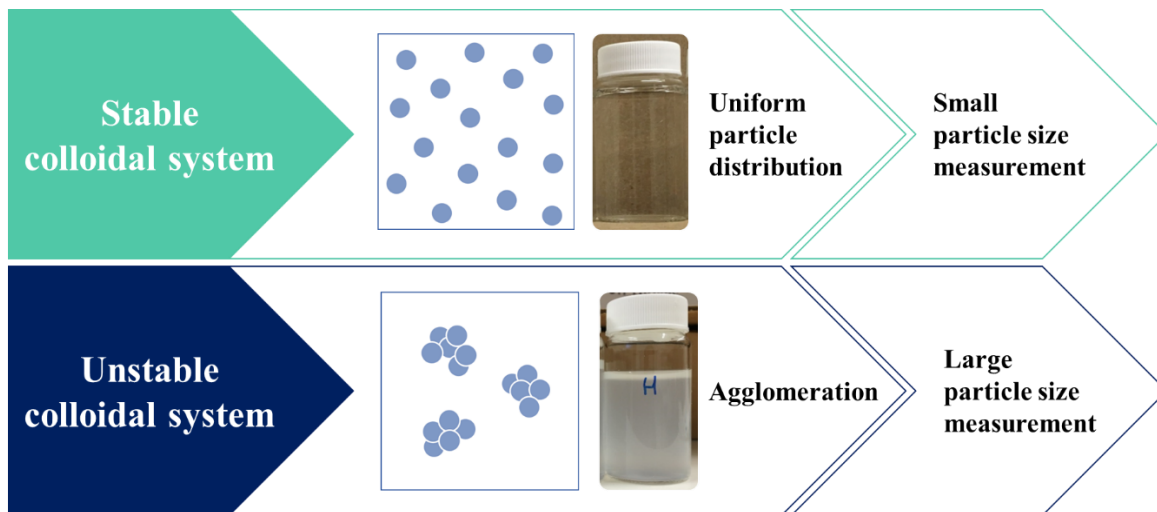


Figure 2.2 The relationship between the stability of colloidal system and the particle size measurements

The average SiO₂ nanoparticle size dispersed in deionized water from three measurements was 19.02 ± 0.22 nm, which falls in the manufacturer's particle size measurements of 5-35 nm. 19.02 nm was used as a reference particle size, and particle sizes ± 15 nm is considered "stable". In some cases, instability of nanoparticles was obvious via visual examination, as agglomerated nanoparticles produced white gelatinous solids. Not all the agglomeration of nanoparticles was observable via visual examinations, however, could be verified upon particle size measurements. The nanoparticles sized above 15 nm from the reference particle size falls outside of the manufactured particle size, which would mean the nanoparticles have started agglomerating, and therefore, were considered "unstable". The particle size measurement software also generates a quality report for every measurement (Malvern instruments, 2004). If the data did not meet the built-in quality criteria test, the nanoparticles were also deemed "unstable".

2.3.2. Materials

Silicon dioxide (SiO₂) nanoparticles (99.99%, amorphous, 5-35 nm diameter, from US Research Nanomaterials, Inc.) were purchased in a 25 wt% suspension in water. There was no further modification to the nanoparticles other than dilution. The ionic salts used to study SiO₂ nanoparticle stability in salt solutions are: sodium chloride ($\geq 99\%$, Sigma-Aldrich), magnesium chloride hexahydrate ($\geq 99\%$, Fisher), sodium sulfate (≥ 99.0 , Sigma-Aldrich), and magnesium sulfate (97%, Acros). These salts were dissolved in deionized water to prepare the salt solutions. The seawater collected from Grand Banks, offshore of Newfoundland, Canada was used for SiO₂ stability study in seawater. The density of the seawater is $1.04 \pm 0.01 \text{ g/cm}^3$ and its pH was 7.84 ± 0.12 at 25 °C. The composition of seawater is given in Table 2.1. Lastly, hydrochloric acid (HCl) (ACS reagent grade, 37%, Sigma-Aldrich) was used as a nanoparticle stabilizer.

Table 2.1 The composition of Grand Banks seawater (Valencia, James, & Azmy, 2017)

Ions	Concentration (ppm)
Na ⁺	10,887
Ca ²⁺	379
Mg ²⁺	1,323
SO ₄ ²⁻	3,248
Cl ⁻	20,186
HCO ³⁻	132
Total	35,987

2.3.3. Instruments for the Particle Size and pH Measurements

The particle sizes were measured with Malvern™ Zetasizer® Nano ZS, equipped with 633 nm He-Ne laser. Zetasizer® uses dynamic light scattering technique to report average hydrodynamic diameter, d_h , as particle sizes. All samples were measured at 25 °C and a scattering angle of 173°. For each sample, three measurements were made, each measurement consisting of 15 runs. The reported particle sizes are average of three measurements. The standard deviations of these measurements were miniscule, and could not be displayed properly in the plots of particle size measurements, and therefore are tabulated in Appendix A. The manufacturer claims $\pm 2\%$ accuracy and precision of the instrument based on the NIST Traceable Latex Standards.

The pH was measured with Corning Pinnacle 540 pH meter at room temperature. The pH meter was calibrated with buffer solutions with pH's of 4.00, 7.00, and 10.05 (Certified Grade, Fisher Chemical). This pH meter is accurate to ± 0.01 pH unit.

2.3.4. Experimental Procedures

2.3.4.1. Effect of Salt Ions on the Stability of Silicon Dioxide Nanoparticles

The most abundant ions in Grand Banks seawater are Na^+ , Mg^{2+} , Cl^- , and SO_4^{2-} , with concentrations of 10887, 1323, 20186, and 3248 ppm, respectively (Valencia et al., 2017).

The SiO_2 nanoparticles were added to the ionic salt solutions containing permutations of the cation and anion pairs of the notably abundant ions in Grand Banks seawater, to identify the utmost ion affecting the stability of the silicon nanoparticles. The resulting mixture was stirred with a magnetic stirrer for 15 minutes to ensure the homogeneity. The

ionic salts used to prepare the solutions, and the concentration range of the resulting salt solutions are summarized in Table 2.2.

Table 2.2 Ionic salt solution compositions and concentrations used to identify the ion affecting the stability of SiO₂ nanoparticles the most

Ionic Salt Solution Component	Cation Concentration Range (ppm)	Anion Concentration Range (ppm)
Sodium chloride (NaCl)	2500 - 50000	3855 - 77106
Sodium sulfate (Na ₂ SO ₄)	2500 - 50000	5223 - 104462
Magnesium sulfate (MgSO ₄)	500 - 5000	1459 - 3048
Magnesium chloride hexahydrate (MgCl ₂ ·6H ₂ O)	500 - 5000	1976 - 7905

Note that only the cation concentrations were controlled. The anion concentrations shown in Table 2.2 are resulting anion concentrations at a given cation concentrations. The reasons for the inconsistent cation concentration ranges across the selected ionic salts will be revealed in the results section. The final concentrations of SiO₂ nanoparticle were 0.05 wt% in all cases.

2.3.4.2. Silicon Dioxide Nanofluid Preparation Method

There are three potential ways of preparing the SiO₂ silicon dioxide nanofluid – nanoparticle suspension in seawater stabilized with HCl – as depicted in Figure 2.3. Method 1 is to mix SiO₂ and HCl, then adding seawater. Method 2 is to mix seawater and HCl, then adding SiO₂. Last method involves mixing SiO₂ and seawater first, then HCl the HCl. The 0.05 wt% SiO₂ nanoparticle suspension in seawater with hydrochloric acid

(HCl) was prepared in three different methods as outlined above, to investigate whether the order of components added affects the SiO₂ stability. The mixture was stirred with a stir bar for 5 minutes after the first and second components were combined, and the final mixture was mixed for 15 minutes with a stir bar.

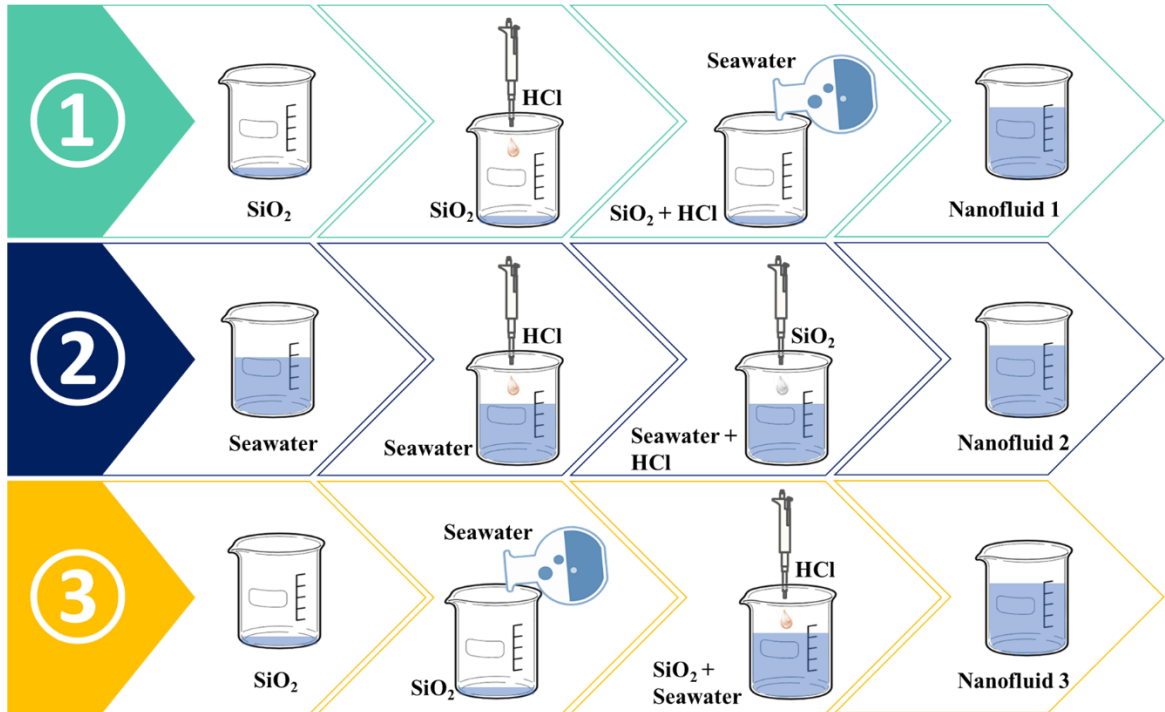


Figure 2.3 Three method of preparing silicon dioxide nanofluid

For each method, a range of HCl concentrations from 0.001 wt% to 0.03 wt% were used to determine the effect of HCl to SiO₂ ratio (Table 2.3) on the SiO₂ stability upon preparation. The final concentration of SiO₂ nanoparticles was 0.05 wt% in all the nanofluid prepared, regardless of the method and HCl concentration. The particle size and pH measurements were made within the first hour of the sample preparation.

Table 2.3 The HCl to SiO₂ ratio ranges prepared to study the effect of HCl

HCl Concentration (wt%)	SiO ₂ Concentration (wt%)	HCl to SiO ₂ Ratio
0.001	0.05	0.02
0.003	0.05	0.06
0.006	0.05	0.12
0.018	0.05	0.36
0.023	0.05	0.46
0.03	0.05	0.60

2.3.4.3. Hydrochloric Acid to Silicon Dioxide Nanoparticle Ratio on the Nanoparticle Stability

The stability of 0.001 wt% HCl mixed with 0.05 wt%, 0.15 wt%, and 0.30 wt% SiO₂ nanoparticles dispersed in seawater, and 0.003 wt% HCl mixed with the same three concentrations of SiO₂ dispersed in seawater were studied in this set of experiment. These six mixtures generate a range of HCl to SiO₂ ratio, enabling examination of the effect of the amount of HCl present compared to the amount of nanoparticles in seawater. The SiO₂ nanoparticles and HCl were mixed together first, then stirred for 5 minutes on the stir plate. Seawater was then added to the mixture, and stirred for another 15 minutes. The particle size and pH measurements were made within the first hour of the sample preparation.

2.3.4.4. Silicon Dioxide Nanoparticle Stability at Room Temperature and at 62 °C Over Time

This experiment was designed to investigate the effect of HCl on the SiO₂ nanoparticle stability over time and at temperature. The method for preparing nanofluid was identical

to experiment 3, in which SiO₂ nanoparticles and HCl were stirred together for 5 minutes on the stir plate, then another 15 minutes of stirring after seawater was added to the mixture. The stability analysis of 0.05 wt% SiO₂ nanoparticles in seawater were conducted at 1 hour, 1 day, 2, 3, 4, 6, 8, 10, 14, and 21 days that has been kept at room temperature. The concentrations of HCl was varied to have the following HCl to SiO₂ ratios: 0.12, 0.18, 0.24, 0.46 and 0.60. The same set of experiments were conducted for samples kept in the oven at 62 °C for comparison.

2.4. Experimental Results and Discussion

2.4.1. Aggregation Behaviour of Silicon Dioxide Nanoparticles in Ionic Salt Solutions

The 0.05 wt% SiO₂ particle sizes were measured in sodium chloride (NaCl) and sodium sulfate (Na₂SO₄) solutions at sodium (Na⁺) concentrations of 2500, 5000, 20000, 30000, and 50000 ppm (Figure 2.4). The particle size measurement at 0 ppm refers to the particle size of the 0.05 wt% SiO₂ nanoparticle suspension in deionized water. As can be seen in Figure 2.4, SiO₂ particle sizes are all within 19.02 ± 15 nm in NaCl(aq) and Na₂SO₄(aq) up to 50000 ppm Na⁺ concentrations. Therefore, it can be concluded that the SiO₂ nanoparticles do not present instability in the presence of Na⁺ even at high concentrations. The SiO₂ stability in solutions containing Na⁺ concentrations higher than 50000 ppm were not tested, because Na⁺ concentrations in Grand Banks seawater is 10669 ppm, and

the concentration up to 50000 ppm was sufficient to understand the effect of Na^+ in seawater on the SiO_2 stability.

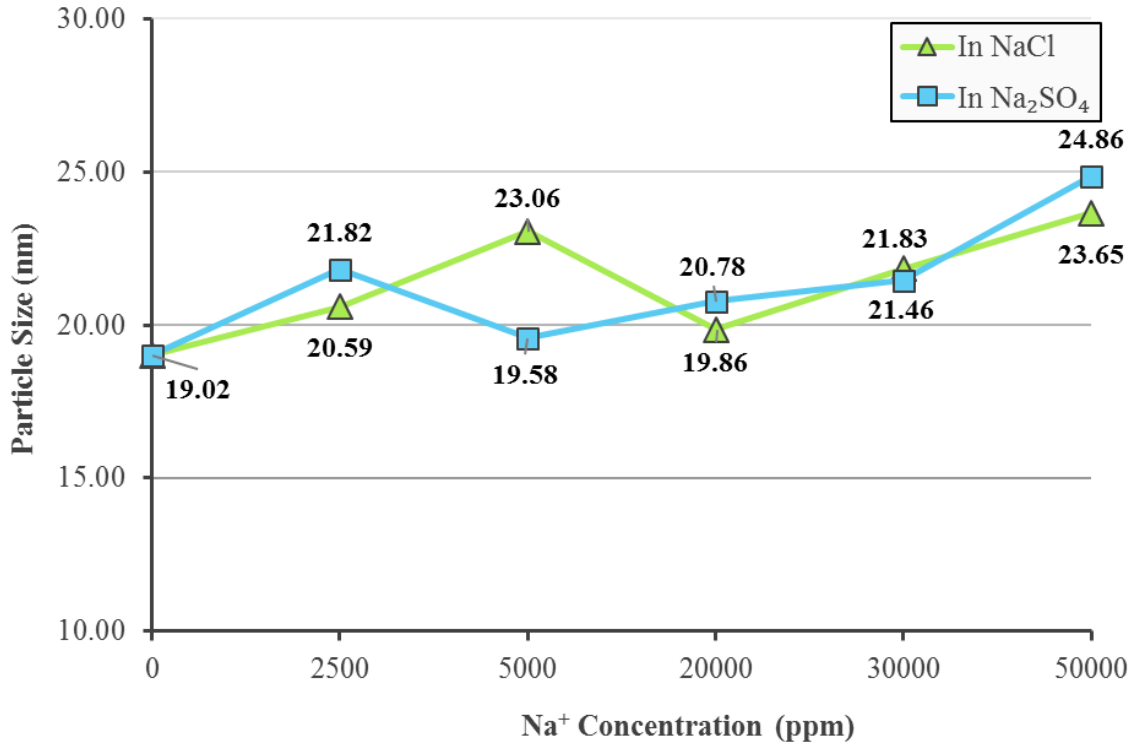


Figure 2.4 The particle size measurement at Na^+ concentrations of 0 ppm to 50000 ppm from two ionic salts: sodium chloride and sodium sulfate

Figure 2.5 shows the particle sizes of 0.05 wt% silicon dioxide nanoparticles in magnesium sulfate (MgSO_4) and magnesium chloride (MgCl_2) at magnesium (Mg^{2+}) concentration of 500 and 1000 ppm. In 500 ppm Mg^{2+} solutions, SiO_2 nanoparticle size slightly increased compared to the SiO_2 size in deionized water, but is still within 19.02 ± 15 nm, and therefore stable. There is a significant increase in the particle size from 500 ppm to 1000 ppm. In 1000 ppm Mg^{2+} solution from $\text{MgSO}_4(\text{aq})$, SiO_2 nanoparticle size is 120.60 nm, and in 1000 ppm Mg^{2+} solution from $\text{MgCl}_2(\text{aq})$, the particle size is 151.17

nm. They are unstable, since both measurements are significantly outside the 19.02 ± 15 nm range. The particle size at 2000 ppm Mg^{2+} and onwards in $MgSO_4(aq)$ and $MgCl_2(aq)$ could not be measured because severe SiO_2 agglomeration occurred immediately when SiO_2 nanoparticle was added to the 2000 ppm solutions, and are concluded unstable at Mg^{2+} concentrations higher than 2000 ppm.

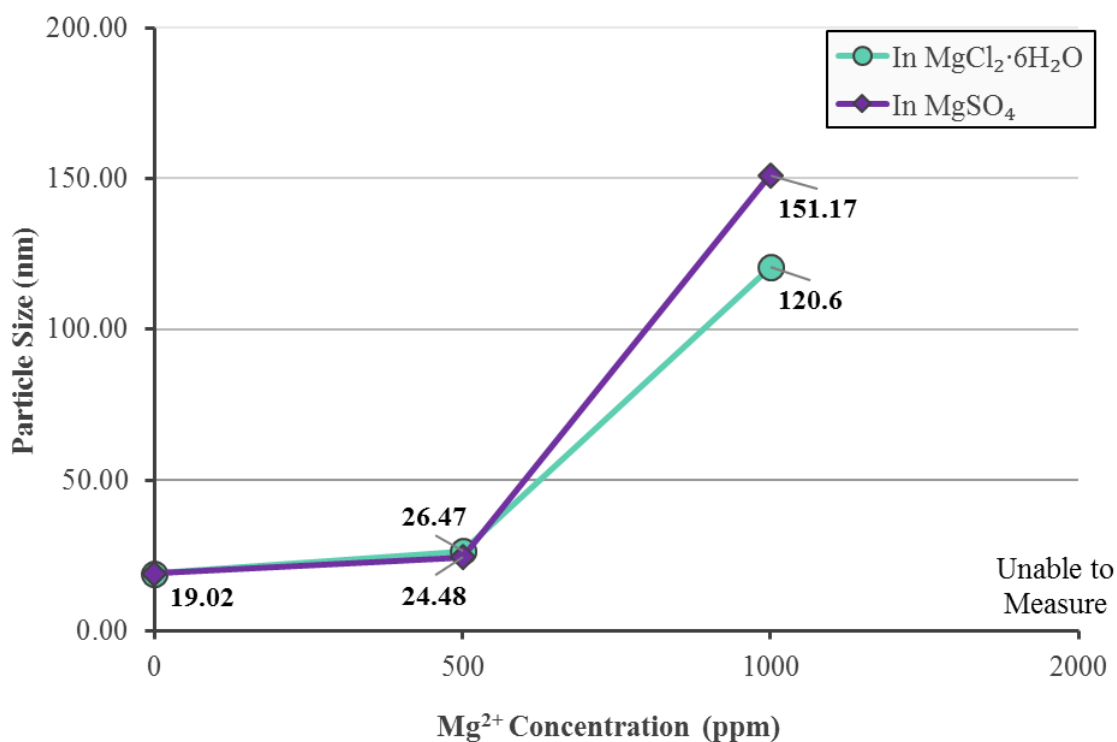


Figure 2.5 The particle size measurement at Mg^{2+} concentrations of 0 ppm to 2000 ppm from two ionic salts: magnesium chloride and magnesium sulfate

These results show that Na^+ does not affect the 0.05 wt% SiO_2 nanoparticle stability even at high concentrations, but the stability is highly compromised by Mg^{2+} ions even at lower concentrations. The effect of counter anions such as chloride (Cl^-) and sulfate (SO_4^{2-}) in the salt solutions seems to be minimal. The Cl^- concentration in 2500 ppm Na^+

solution prepared from NaCl is 3855 ppm, and the Cl^- concentration in 2000 ppm Mg^{2+} solution prepared from MgCl_2 is 3048 ppm. The Cl^- concentration prepared from MgCl_2 is lower than that of NaCl, however, the particle size could not be measured due to severe agglomeration. Similarly, the nanoparticle size was unmeasurable for 7905 ppm SO_4^{2-} solution prepared from MgSO_4 , but 10446 ppm and higher SO_4^{2-} solutions prepared from Na_2SO_4 were stable.

The effect of cations on the SiO_2 stability can be explained upon examining the SiO_2 structure, and its surface chemistry in the presence of water molecules and other ions. SiO_2 has a tetrahedral geometry (Figure 2.6 (a)), unlike carbon dioxide which is a linear molecule. This is because silicon atom is larger than carbon, which does not allow substantial overlap between the p-orbitals to form double bonds with oxygen (P. W. Atkins & Atkins, 2006). As a result, silicon only forms single bonds with oxygen, giving $[\text{SiO}_4]^{4-}$ arrangement. The amorphous SiO_2 is in fact a 3D structure, which is a result of random packing of $[\text{SiO}_4]^{4-}$ units (Bergna, 2005) (Figure 2.6 (b)). The SiO_2 nanoparticles therefore bears overall negative surface charge (Figure 2.6 (c)).

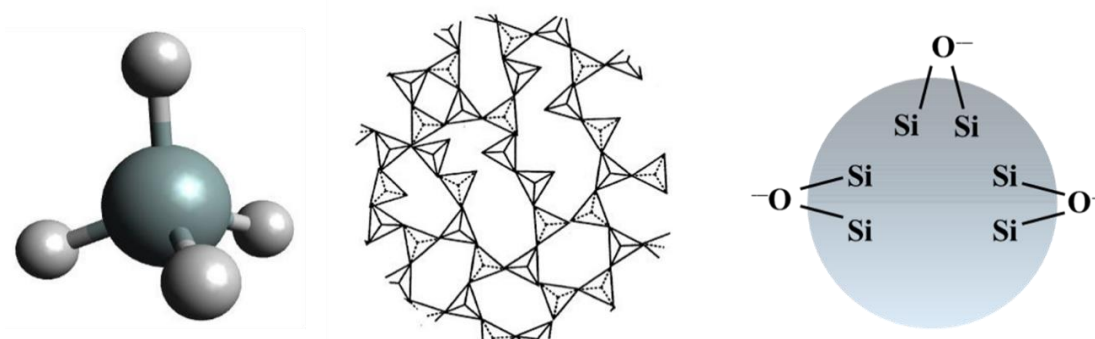


Figure 2.6 (a) Tetrahedral geometry of silicon dioxide (b) 3D Arrangement of amorphous silicon dioxide nanoparticles (c) The negative surface of silicon dioxide nanoparticles

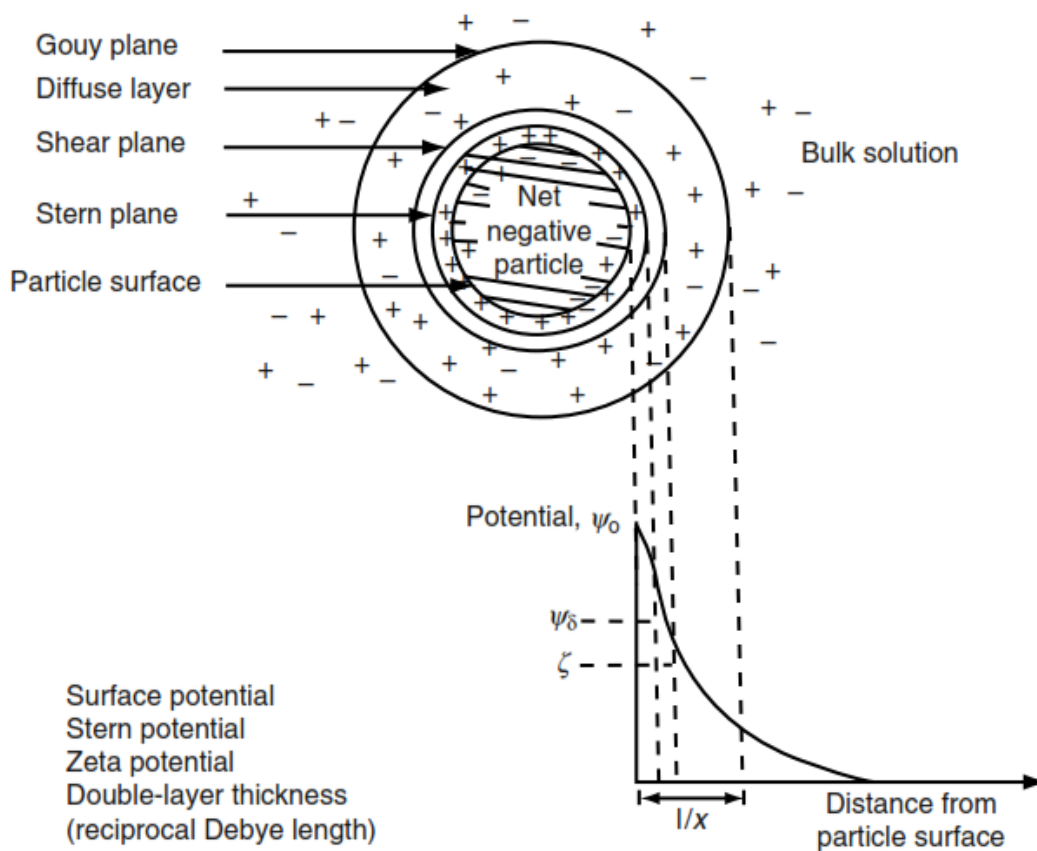


Figure 2.7 The electrical double layer formed around the negative surface charged particle, such as silicon dioxide nanoparticles, in a continuous medium (Mehta et al., 2008)

The electrical double layer is formed at the SiO₂ nanoparticle surface and liquid interface when nanoparticles are suspended in water, due to adsorption of ions (Figure 2.7). The electrical double layer consists of a stern plane and a diffuse layer, and affects the distribution of the ions around the nanoparticles (Williams, 1992). In case of SiO₂ nanoparticles, the negative surface charge attracts cations firmly to the surface while repelling anions away from the surface, forming a stern plane. At a short distance from the stern plane, a boundary between the diffuse layer exists, called a shear plane. Any remaining negative surface charges are compensated by the freely moving cations in the

diffused layer. The distribution of the cations and anions are balanced beyond the diffused layer. The thickness of the electrical double layer is reciprocal to the Debye length, and the nanoparticle stability increases in liquid phase as the thickness of the electrical double layer increases (Metin et al., 2011). It must be noted that the colloidal system is thermodynamically unstable (Birdi, 2008) because surface energy is high from the increased surface area of the suspended particles (Mehta et al., 2008). In attempts to lower the energy state, the particles tend to aggregate, unless other energy barriers are present such as electrostatic charge repulsions; steric; and hydration forces (Birdi, 2008). The thicker the electrical double layer, the higher the energy barrier, allowing nanoparticles to be stable.

When ions such as Na^+ and Mg^{2+} are present, the double layer is compressed, and the energy barrier decreases, leading to nanoparticle agglomeration (Brown, Goel, & Abbas, 2016; Mehta et al., 2008). Mg^{2+} ions attract stronger than Na^+ ions because it has a larger magnitude of positive charges, and is more effective in destabilizing the SiO_2 nanoparticles, as evident in the experimental results. The difference in the Na^+ and Mg^{2+} ion sizes are also a contributing factor. The ion size of Na^+ is 0.099 nm, and the ion size of Mg^{2+} is 0.049 nm (Shannon, 1976). The water molecules around the SiO_2 surface is known to favour small ions, allowing the ions to penetrate water layer easily (Torrie, Kusalik, & Patey, 1989). Mg^{2+} is a smaller ion compared to Na^+ , and therefore Mg^{2+} penetrates the water layer easier than Na^+ , and is consequently adsorbed onto the nanoparticle surface better than Na^+ .

The findings from this experiment prove that it is unrealistic to use NaCl solutions to investigate the effectiveness of SiO₂ nanoparticle as a water additive for enhanced oil recovery purposes. The use of stabilizer to produce stable SiO₂ suspension in seawater is unavoidable. Hydrochloric acid is proposed as such stabilizer in this paper, and its mechanisms and effectiveness is investigated in the following sections.

2.4.2. Optimization of Silicon Dioxide Nanofluid Preparation Method

The 0.05 wt% SiO₂ nanoparticle suspension in seawater with hydrochloric acid (nanofluid) was prepared using three different methods. The particle size measurements from each method are plotted against HCl to SiO₂ ratio (Figure 2.8). As can be seen in the figure, 0.05 wt% SiO₂ nanoparticle sizes vary significantly depending on how the nanofluid was prepared, even though they have the same HCl to SiO₂ ratio, and similar pH measurements. This is consistent across HCl to SiO₂ ratios from 0.02 to 0.60 tested in this study. The best way to prepare the nanofluid was Method 1 (SiO₂ nanoparticles and HCl are mixed first, and then the seawater is added) based on the particle size measurements, as nanoparticle sizes remained closest to the reference particle size, 19.02 nm. The nanoparticle sizes prepared as per Method 2 – seawater and HCl is mixed first, then SiO₂ last – increased up to 31.81 and 32.90 nm respectively, at the HCl to SiO₂ ratios of 0.02 and 0.06. As the HCl to SiO₂ ratio increases, the particle size tends to decrease to 23.57 nm, indicative of more stable dispersions. The worst way to prepare the nanofluid was Method 3 because the nanoparticle size increased up to approximately 30 nm at all HCl to SiO₂ ratios, indicating the nanofluids are not as stable as nanofluids prepared as per Method 1 or 2.

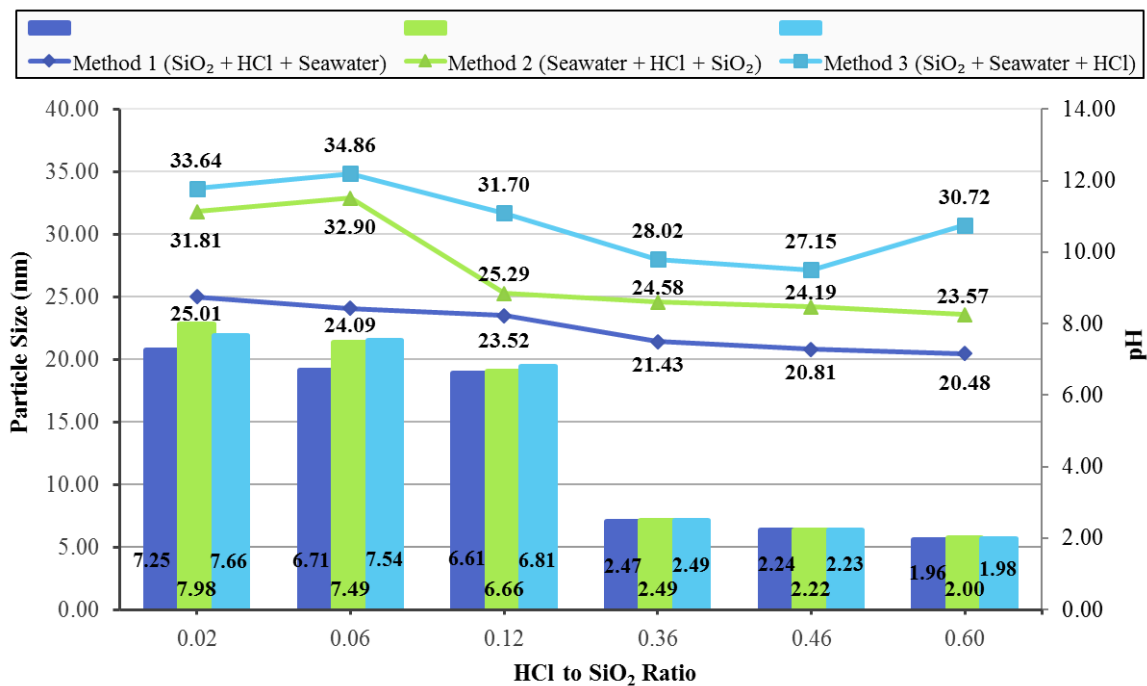


Figure 2.8 The particle size measurements and pH (taken within one hour of sample preparation) of nanofluids prepared in three different methods at hydrochloric acid to silicon dioxide nanoparticle ratios ranging from 0.02 to 0.60

The differences in the particle sizes at the same HCl to SiO₂ ratio and similar pH across the method is thought to be related to the mechanism HCl enables the SiO₂ nanoparticles to stay dispersed uniformly in seawater. The H⁺ ions from HCl seems to further encourage formation of the electrical double layer around the nanoparticle surface, when the nanoparticles are mixed with HCl first. Therefore, when seawater is added, the cations in the seawater would be repelled effectively from the nanoparticle surface, and the nanoparticles remain stable. Method 2 mixes seawater and HCl first, and the nanoparticle is added last. In seawater and HCl mixture, Na⁺, Mg²⁺ and H⁺ ions are all present. These ions would likely to compete to adsorb on the nanoparticle surface. There must be adsorption of all three cations on the nanoparticle surface, since the nanofluid from the

second method is not as stable as nanofluid prepared as per first method. H^+ ions must preferentially adsorb onto SiO_2 surface over Na^+ and Mg^{2+} , possibly because the ionic mobility of H^+ ion is $36.23 \cdot 10^{-8} m^2 s^{-1} V^{-1}$ in water at $25^\circ C$, which is approximately 6.5 – 7 times higher than that of Na^+ ($5.19 \cdot 10^{-8} m^2 s^{-1} V^{-1}$) and Mg^{2+} ($5.50 \cdot 10^{-8} m^2 s^{-1} V^{-1}$) (P. Atkins & Paula, 1907). The nanoparticles added to seawater first (Method 3) becomes unstable instantly, as it would experience shortened diffused layer immediately from the Mg^{2+} ions in the seawater. The addition of HCl after fact does not improve the stability, perhaps because Mg^{2+} ions have adsorbed onto the nanoparticle surface, and there is no room for H^+ ions to be adsorbed onto the nanoparticle surface to successfully restore the electrical double layer.

The trend in the three methods is that at lower HCl to SiO_2 ratio, the nanoparticle sizes are larger compared to the sizes at higher ratio, and thus less stable within the same methods. This observation indicates that there is a relationship between the amount of HCl relative to SiO_2 , in terms of determining the stability of SiO_2 nanoparticles. Hence the effect of HCl to SiO_2 is further investigated in the next section.

2.4.3. The Effect of Hydrochloric Acid Concentration on the Stability of Silicon Dioxide Nanofluid

Three SiO_2 nanofluids were prepared with varying nanoparticle concentrations at fixed hydrochloric acid (HCl) concentration of 0.001 wt%. Another three SiO_2 nanofluids were prepared with varying nanoparticle concentrations at fixed HCl concentration of 0.003 wt%, to investigate the effect of HCl concentrations on the SiO_2 stability in seawater.

Table 2.4 shows the final concentrations of HCl and SiO₂ of the nanofluids, corresponding HCl to SiO₂ ratio, as well as pH measurements. The nanofluids with HCl to SiO₂ ratio of 0.02 were prepared in both 0.001 and 0.003 wt% HCl, as bolded in Table 2.4 to confirm certain amount of HCl is required per SiO₂ for nanoparticles to be stable in seawater.

Table 2.4 The concentrations of hydrochloric acid and silicon dioxide to generate range of ratios between the two, and the pH measurements of resulting fluids

HCl Concentration (wt%)	SiO ₂ Concentration (wt%)	HCl to SiO ₂ Ratio	pH
0.001	0.05	0.02	7.25
0.001	0.15	0.007	7.85
0.001	0.30	0.003	7.99
0.003	0.05	0.06	6.71
0.003	0.15	0.02	7.28
0.003	0.30	0.01	7.53

Figure 2.9 shows the particle size measurements plotted against HCl to SiO₂ ratios. The particle size decreases with increasing HCl to SiO₂ ratio, indicating that increasing HCl concentration increases the stability of the nanoparticles in seawater. Only two points are plotted on Figure 2.9 for 0.001 wt% HCl because the concentration of HCl was insufficient to stabilize 0.30 wt% SiO₂ in seawater (equivalent to 0.003 HCl to SiO₂ ratio), and the particle size was unmeasurable due to visible agglomeration. 0.003 wt% HCl on the other hand could stabilize the 0.30 wt% SiO₂ (equivalent to 0.01 HCl to SiO₂ ratio), confirming that the higher concentration of HCl is required to stabilize higher

concentrations of SiO₂. The particle sizes and pH at HCl to SiO₂ ratio of 0.02, prepared from 0.001 and 0.003 wt% are essentially the same, as expected.

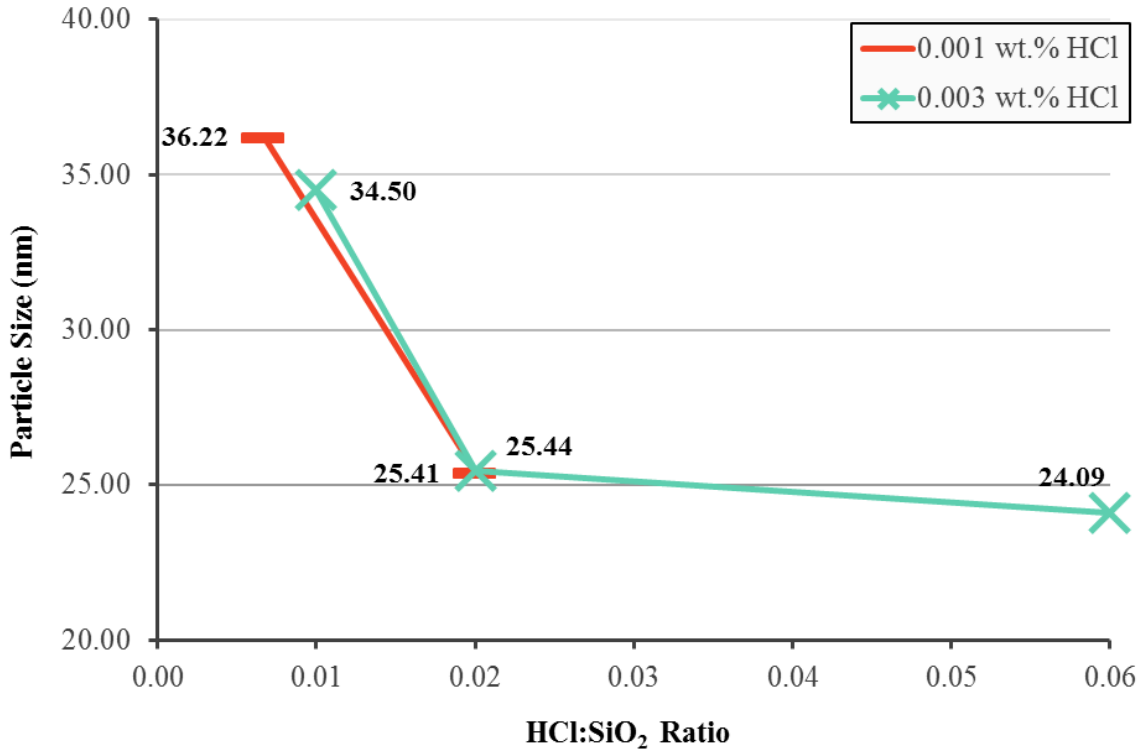


Figure 2.9 The particle size measurements silicon dioxide nanofluid across a range of hydrochloric acid and silicon dioxide ratio in the presence of 0.001 wt% and 0.003 wt% hydrochloric acid

The experimental results in this section shows that a certain amount of HCl must be present for a given number of nanoparticle suspension in seawater, to maintain the SiO₂ nanoparticle stability in seawater. This is because with increasing nanoparticle concentration, the more nanoparticles are present, meaning that there are increased nanoparticle surfaces that need to be protected from the cations in seawater. As a result, more HCl is needed at the higher nanoparticle concentrations.

2.4.4. The Effect of Hydrochloric Acid Concentration on the Stability of Silicon Dioxide Nanofluid over Time and Temperature

A set of 0.05 wt% SiO₂ nanoparticle in seawater was prepared at HCl to SiO₂ ratios of 0.12, 0.18, 0.24, 0.46 and 0.60. The ratios of 0.02 and 0.06 were also prepared, however, the results are not reported, since nanoparticle stability was compromised within an hour of sample preparation at 62 °C. As a result, accurate particle size measurements could not be carried out, and the meaningful comparison for temperature dependency could not be observed at 0.02 and 0.06 ratios.

The samples were kept at room temperature, and the particle sizes were measured at 1 hour, 1 day, 2, 3, 4, 6, 8, 10, and 14 days, as shown in Figure 2.10. The samples at 62 °C were also measured to observe the effect of temperature (Figure 2.11). The pictures taken for the visual examination for this set of experiment are presented in Appendix B. The same experiments were conducted on a set of 0.01 and 0.03 wt% SiO₂ nanofluids for the future SiO₂ nanoparticle enhanced oil recovery studies. Their results are presented in Appendix C to E, to keep the focus of discussion to 0.05 wt% SiO₂ nanofluids.

The particle size of nanofluid with 0.12 HCl to SiO₂ ratio at room temperature grows the quickest at room temperature. The agglomeration behaviour is clearly seen from 2 days, and severe agglomeration is continually observed from 3 days to 14 days. At the ratios higher than 0.12, there is not much difference in the particle sizes over the 14-day period, though the particle sizes at 0.18 and 0.24 HCl to SiO₂ ratio are slightly higher compared to the particle sizes at 0.46 and 0.60 HCl to SiO₂ ratio.

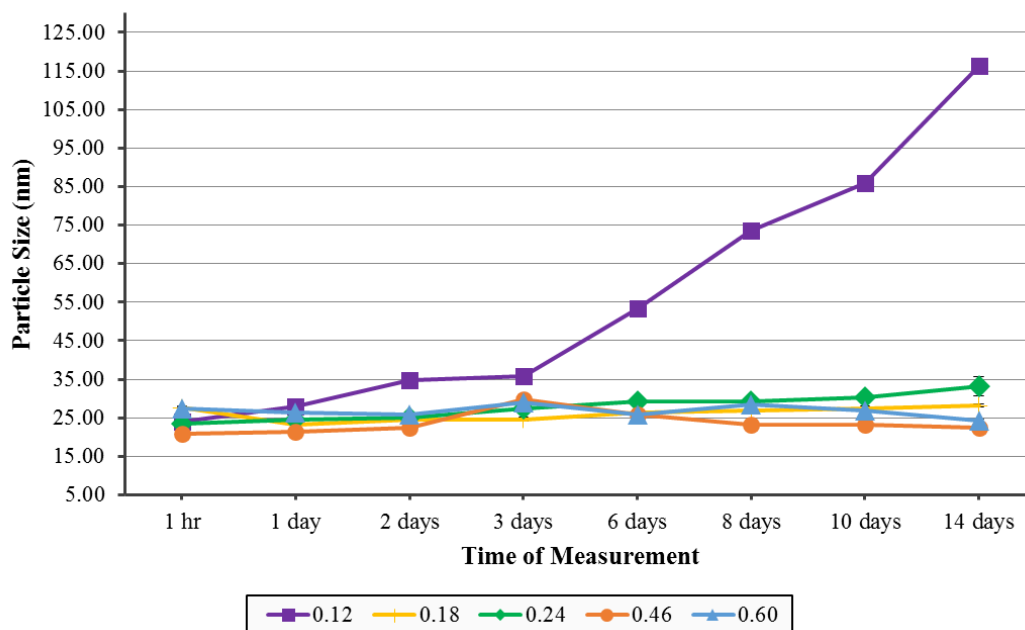


Figure 2.10 The 0.05 wt% silicon dioxide nanoparticle size measurements at room temperature, at HCl to SiO₂ ratio ranging from 0.12 to 0.60

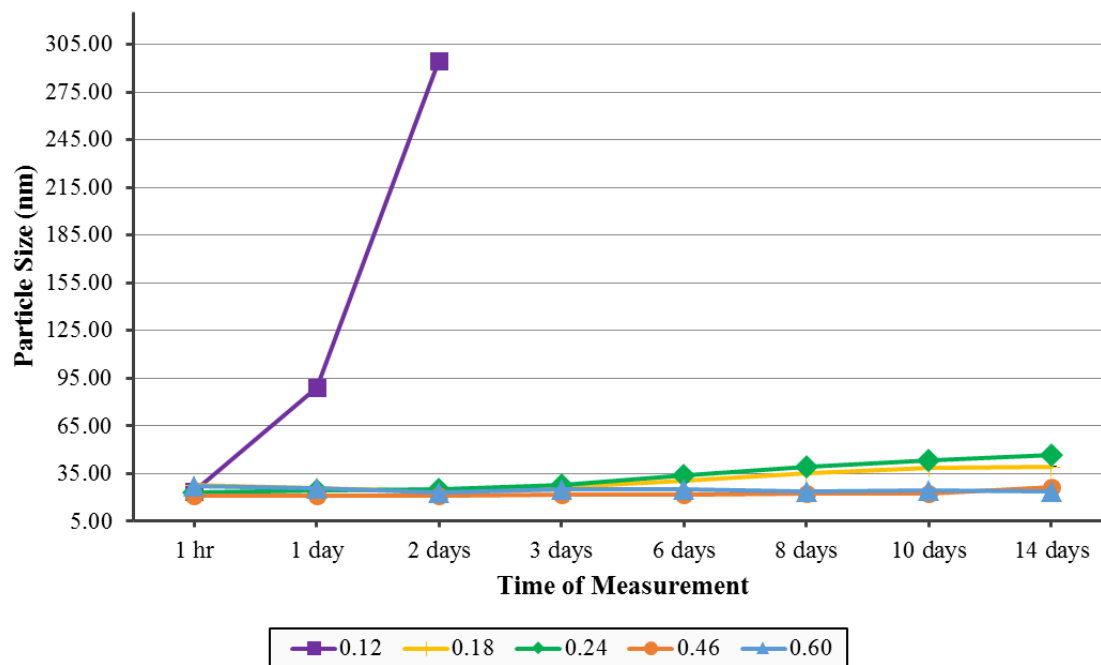


Figure 2.11 The 0.05 wt% silicon dioxide nanoparticle size measurements at 62°C, at HCl to SiO₂ ratio ranging from 0.12 to 0.60

The particle size of the nanoparticle grows rapidly after 1 day for the nanofluid with 0.12 HCl to SiO₂ ratio at 62 °C, which is also observed at room temperature. The difference is that the agglomeration is evident earlier on, and is more severe. The particle size grows to 294.40 nm only after the second day, and the particle size measurement after 2 days were not conducted because of visual agglomeration. With increasing HCl to SiO₂ ratio to 0.18 and 0.24, the nanoparticle size is relatively constant until 3 days, and remains stable. After 6 days, however, the particle size grows outside of the reference size range (19.02 ± 15 nm), indicating that they are no longer stable. The further increment of HCl to SiO₂ ratio to 0.46 and 0.60 successfully keeps the nanoparticle size constant up to 14 days. There is only a slight difference in the particle sizes between 0.46 and 0.60 HCl to SiO₂ ratio. There may be a critical HCl concentration, at which further addition of HCl no longer improves stability. If the measurements were continued for a longer period, there may be sign of instability, which is another possibility.

The comparison of the nanoparticle sizes of samples at room temperature and at 62 °C monitored over 14 days reveal that the stability of nanoparticles in seawater with same HCl to SiO₂ ratio is compromised earlier on at 62 °C. This is because the nanoparticles in a colloidal system moves constantly and randomly in the liquid phase (Birdi, 2008). The rate of aggregation increases with increasing probability of collision between particles (Mehta et al., 2008). With increasing temperature, the kinetic energy of the particles increases, and therefore the frequency of collisions between the particles increases (Petrucci, Harwood, Herring, & Madura, 2006), accelerating the agglomeration process. The interaction during the collisions between the particles also determine the rate of

aggregation. With increasing HCl concentration, the nanoparticle surfaces would form thicker protective layers. If the protective H^+ layer is not thick enough due to insufficient HCl, the nanoparticles will aggregate upon collisions, and destabilizes more readily.

2.5. Conclusions

The SiO_2 nanoparticle EOR is challenging in the offshore reservoir, since nanoparticles are unstable in high salinity. In this study, the stability of SiO_2 nanoparticles in seawater is examined through particle size measurements. The divalent cation, Mg^{2+} , in seawater is identified to highly compromise the stability of the 0.05 wt% SiO_2 nanoparticles, more so than a monovalent cation, Na^+ . The hydrochloric acid (HCl) is proposed as a SiO_2 stabilizer in seawater, and its effectiveness is evaluated. The best way to prepare the SiO_2 nanofluid in seawater using HCl is to mix nanoparticles and the stabilizer (HCl) first, then add the seawater last. The addition of H^+ to SiO_2 nanoparticles allows a protective layer to be formed on the nanoparticle surface, to prevent Mg^{2+} ions from affecting the stability. The HCl to SiO_2 ratio is crucial in preparing the stable SiO_2 nanoparticle in seawater because higher nanoparticle concentration requires higher concentration of HCl for SiO_2 nanoparticles to be stable in seawater. When there is insufficient HCl, the nanoparticles agglomerate quickly over time. A higher agglomeration rate is observed with nanofluids at $62^\circ C$ compared to the nanofluids at room temperature. These two sets had the same HCl to SiO_2 ratio, the only varying factor was the temperature. With increasing temperature, higher HCl to SiO_2 is required to maintain the stability of the nanoparticles,

to offset the increased kinetic energy of the nanoparticles, which leads to increased probability of successful collisions, and increased agglomeration rate.

Acknowledgements

The authors would like to thank Chevron Canada, Hibernia Management and Development Company (HMDC), Research and Development Corporation of Newfoundland and Labrador (RDC), Natural Sciences and Engineering Research Council of Canada (NSERC), and the Canadian Foundation for Innovation (CFI) for financial support. We thank our colleagues in the Hibernia EOR Research Group for technical support.

References

Atkins, P., & Paula, J. de. (1907). Elements of Physical Chemistry. Science (Vol. 26). <https://doi.org/10.1126/science.26.670.588-a>

Atkins, P. W., & Atkins, P. W. (2006). Shriver & Atkins inorganic chemistry. Oxford; New York; New York: Oxford University Press; W.H. Freeman and Co.

Bergna, H. (2005). Colloid Chemistry of Silica. In Colloidal Silica (pp. 9–35). CRC Press. <https://doi.org/doi:10.1201/9781420028706.ch3>

Birdi, K. S. (2008). Surface and Colloid Chemistry. In Handbook of Surface and Colloid Chemistry, Third Edition (pp. 1–43). CRC Press. <https://doi.org/doi:10.1201/9781420007206.ch1>

Brown, M. A., Goel, A., & Abbas, Z. (2016). Effect of Electrolyte Concentration on the Stern Layer Thickness at a Charged Interface. *Angewandte Chemie - International Edition*, 55(11), 3790–3794. <https://doi.org/10.1002/anie.201512025>

Hendraningrat, L., Engeset, B., Suwarno, S., & Torsæter, O. (2012). Improved oil recovery by nanofluids flooding: an experimental study. *SPE Kuwait International Petroleum Conference and Exhibition*, (2006), SPE 163335. <https://doi.org/10.2118/163335-MS>

Hendraningrat, L., & Shidong, L. (2012). A glass micromodel experimental study of hydrophilic nanoparticles retention for EOR project. *SPE Russian Oil and Gas Exploration*, (2010), SPE 159161. <https://doi.org/10.2118/159161-MS>

Kissa, E. (1999). *Dispersions : characterization, testing, and measurement*. M. Dekker. Retrieved from <https://www.crcpress.com/Dispersions-Characterization-Testing-and-Measurement/Kissa/p/book/9780824719944>

Malvern instruments. (2004). *Zetasizer Nano Series User Manual*. Department of Biochemistry Biophysics Facility, University of Chambridge, (2), 207. [https://doi.org/10.1016/S0294-3506\(99\)80105-7](https://doi.org/10.1016/S0294-3506(99)80105-7)

Mehta, S., Somasundaran, P., Yu, X., & Krishnakumar, S. (2008). Colloid Systems and Interfaces Stability of Dispersions through Polymer and Surfactant Adsorption. In *Handbook of Surface and Colloid Chemistry*, Third Edition (pp. 155–196). CRC Press. <https://doi.org/doi:10.1201/9781420007206.ch6>

Metin, C. O., Lake, L. W., Miranda, C. R., & Nguyen, Q. P. (2011). Stability of Aqueous Silica Nanoparticle Dispersions. *Journal of Nanoparticle Research*, 13(2), 839–850. <https://doi.org/10.1007/s11051-010-0085-1>

Mokhatab, S., Fresky, M. A., & Islam, M. R. (2006). Applications of Nanotechnology in Oil and Gas E&P. *Journal of Petroleum Technology*, 58(4), 48–51. <https://doi.org/10.2118/0406-0048-JPT>

Petrucci, R. H., Harwood, W. S., Herring, F. G., & Madura, J. D. (2006). *General Chemistry: Principles and Modern Application*. Pearson/Prentice Hall.

Shannon, R. D. (1976). Revised effective ionic radii and systematic studies of interatomic distances in halides and chalcogenides. *Acta Crystallographica Section A*, 32(5), 751–767. <https://doi.org/10.1107/S0567739476001551>

Stosur, G. J., Hite, J. R., Carnahan, N. F., & Miller, K. (2003). The Alphabet Soup of IOR, EOR and AOR: Effective Communication Requires a Definition of Terms. *SPE International Improved Oil Recovery Conference in Asia*, SPE 84908, 1–3. <https://doi.org/10.2118/84908-MS>

Torrie, G. M., Kusalik, P. G., & Patey, G. N. (1989). Theory of the electrical double layer: ion size effects in a molecular solvent. *Journal of Chemical Physics*, 91(10), 6367–6375. <https://doi.org/10.1063/1.457404>

Valencia, L., James, L. A., & Azmy, K. (2017). Implications of the Diagenetic History on Enhanced Oil Recovery (EOR) Performance for the Ben Nevis Formation, Hebron Field, Jeanne D'arc Basin, Offshore, Newfoundland, Canada. Memorial University.

Wasan, D., Nikolov, A., & Kondiparty, K. (2011). The wetting and spreading of nanofluids on solids: Role of the structural disjoining pressure. *Current Opinion in Colloid and Interface Science*, 16(4), 344–349. <https://doi.org/10.1016/j.cocis.2011.02.001>

Williams, R. A. (Richard A. (1992). *Colloid and surface engineering : applications in the process industries*. Oxford [England]; Butterworth-Heinemann. Retrieved from <https://searchworks.stanford.edu/view/2262789>

Chapter 3. Experimental Investigation of Enhanced Oil Recovery by Injecting SiO₂ Nanoparticles as Water Additive with Application to the Hebron Field

Authors

Jenny Kim, Daniel J. Sivira, Lesley A. James, Yahui Zhang

***Published as a Conference Proceeding** at EAGE 19th European Symposium on Improved Oil Recovery held in Stavanger, Norway, April 24-27, 2017*

3.1. Abstract

The use of silicon dioxide (SiO₂) nanoparticles for enhanced oil recovery is novel, and is attractive because of the cost effectiveness, considering low concentrations required for enhanced oil recovery technique, and its surface-active properties for both interfacial tension reduction, and possible wettability alterations. Previous laboratory scale investigations have demonstrated a potential of SiO₂ nanoparticles as water additive for enhanced oil recovery (EOR). In this study, the potential of injecting SiO₂ nanoparticles as water additive is experimentally investigated for EOR application in Ben Nevis Formation from Hebron Field, offshore Newfoundland and Labrador, Canada. Only 30% of its crude oil in Ben Nevis Formation from Hebron Field is projected to be recoverable. Therefore, the investigation of EOR method requires attention now, since first oil is expected in 2017. The experiments for this study are designed to be as realistic as possible. Unique from the previous laboratory investigations that used deionized water or simple synthetic brine as a medium to disperse nanoparticles, the SiO₂ nanoparticles are dispersed in seawater obtained from Grand Banks, offshore Newfoundland, of which

nanoparticles will be added to in the Hebron Field. Interfacial tension, contact angle, and coreflooding experiments are conducted at Hebron Field temperature and pressure (62 °C and 19.00 MPa). The results showed that the SiO₂ nanofluids decrease interfacial tension and contact angle, indicating positive impact on the oil recovery. Preliminary coreflooding experiments are conducted using 0.01 and 0.03 wt% SiO₂ nanofluid, with Berea standard cores, consisting of similar mineralogical composition as the lower facies of Ben Nevis Formation. The results show that 0.01 and 0.03 wt% SiO₂ nanoparticle flooding both increased additional recovery by 3.3% and 9.3%, respectively.

3.2. Introduction

The use of nanoparticles has broad applications because of their unique active surface properties. Nanoparticles have large surface areas, leading more reactions to occur at its surface (El-diasty and Aly 2015). They also have high surface energy, which allows them to defy gravity, and stay well dispersed in an aqueous medium (Miranda et al. 2012). Nanotechnology was introduced to the oil and gas industry more than 50 years ago (Matteo et al. 2012), and it has contributed to the development of more durable drilling equipment and the construction of improved corrosion resistant offshore platforms (Mokhatab et al. 2006). There are ongoing laboratory investigations to apply nanotechnology to enhance oil recovery of residual immobile oil post water or gas injection. Nanoparticles that alter the injected phase viscosity, interfacial tension of the

injected phase and oil, and possibly the wettability of the reservoir rock are ways in which nanoparticles may help address the challenge of increasing oil recovery.

Silicon dioxide (SiO₂) nanoparticles are the most popular nanoparticle studied as a water additive in enhanced oil recovery (EOR). Attractive features of silicon dioxide nanoparticles include low cost, and well understood physical-chemical properties at their surfaces (Miranda et al. 2012). They have been proven to reduce the interfacial tension and change the wettability of the rock surfaces to more water-wet (Sivira et al. 2016; Al-Ansari et al. 2016; Li et al. 2013; Maghzi et al. 2012). Incremental oil recovery has also been observed from coreflooding experiments (Nazari Moghaddam et al. 2015; Hendraningrat et al. 2014; Aurand et al. 2014; Joonaki and Ghanaatian, 2014; Hendraningrat et al. 2013; Roustaei et al. 2012) The summary of these coreflood studies in the literature are given in Table 3.1.

Table 3.1 Coreflood Experiments Using Silicon Dioxide Nanoparticles

References	SiO ₂ concentration	Dispersion medium	Porous media	Pore volume injected	Incremental recovery
Nazari Moghaddam, Bahramian, Fakhroueian, Karimi, & Arya, 2015	5 wt%	Paraffin/heptane, mixture of ethylene glycol, and lauryl alcohol	Type: Carbonate Φ*: 13.2% K**: 0.24 mD	1. Brine, 5 PV 2. Nanofluid, 2 PV 3. Brine	7.7%
Hendraningrat & Torsæter, 2014	0.05 wt%	3 wt% NaCl brine with PVP (Polyvinylpyrrolidone)	Type: Water-wet Berea Φ: 14.99% K: 119 mD	1. Brine, 5 PV 2. Nanofluid, 5 PV 3. Brine, 5 PV	21.4%
Aurand, Dahle, & Torsæter, 2014	0.05 wt%	Diluted to 2 wt% nanofluid with deionized water, then diluted further to 0.05 wt% with 3.53% salinity synthetic brine	Type: Water-wet Berea Φ: 18.1% K: 394 mD	1. Brine, 2 PV 2. Nanofluid, 2 PV	20.0% (Large fumed nanofluid)
Joonaki & Ghanaatian, 2014	Not given	Propanol	Type: Sandstone Φ: 17.34% K: 108.21 mD	1. Brine, 3 PV 2. Nanofluid, 3 PV	22.5%
Hendraningrat, Li, & Torsæter, 2013	0.01 wt%	3 wt% NaCl brine	Type: Berea Φ: 23.20% K: 392 mD	1. Brine, 3.7 PV 2. Nanofluid, 2.8 PV	9.6%
	0.05 wt%	3 wt% NaCl brine	Type: Berea Φ: 23.04% K: 302 mD	1. Brine, 3.2 PV 2. Nanofluid, 3.1 PV	13.0%
	0.1 wt%	3 wt% NaCl brine	Type: Berea Φ: 22.93% K: 354 mD	1. Brine, 3.1 PV 2. Nanofluid, 3.5 PV	8.6%
Roustaei, Moghadasi, Jamshid Bagherzadeh, & Shahrabadi, 2012	5 g/L	Weak or non-polar solvent	Type: Sandstone Φ: 17% K: 186 mD	1. Brine, 2 PV 2. Nanofluid, 3 PV 3. Brine, 2 PV	28.6% (NWP) [§] 32.2% (HLP) ^{§§}

* Φ: Porosity, **K: Permeability, § NWP: Naturally Wet Polysilicon §§: HLP: Hydrophobic and Lipophilic Polysilicon

This research focuses on the potential use of SiO₂ nanoparticles as a water additive for EOR in the Hebron Field. The Hebron Field is located about 350 km southeast of St. John's, Newfoundland and Labrador, Canada, and is Canada's fourth major offshore development Figure 3.1.

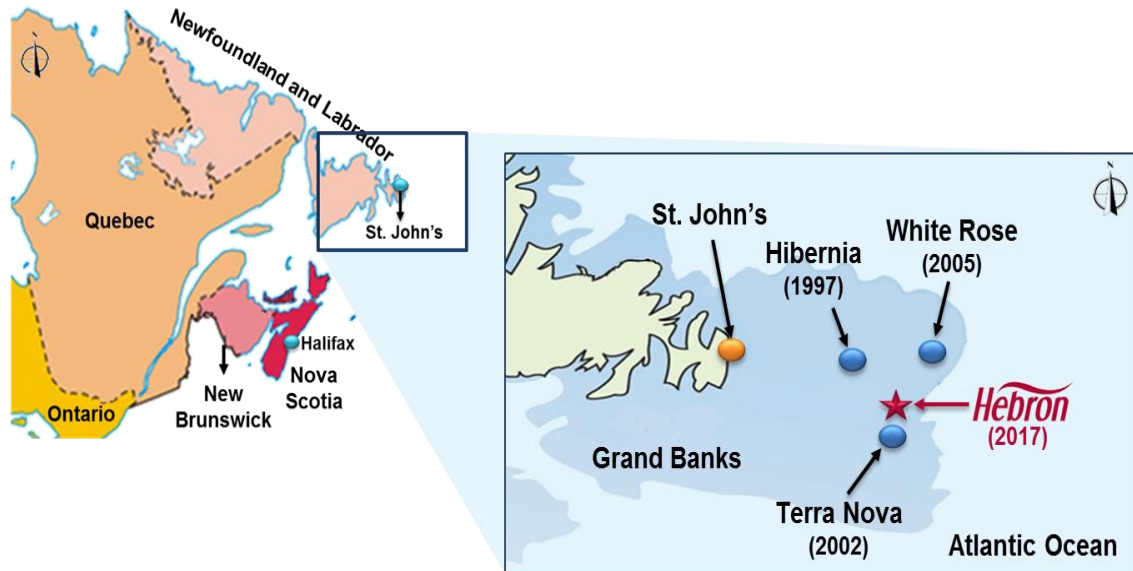


Figure 3.1 Offshore Canada oil & gas developments, including Hebron Field (Sivira et al. 2016)

Recoverable oil is expected to be 800 MMbbl out of 2620 MMbbl estimated original oil in place, with first oil expected in 2017 (CNLOPB 2011). Screening EOR methods requires attention now to maximize the production. The Hebron Field includes the Hibernia, Avalon, Jeanne d'Arc, and Ben Nevis formations where 70% of the recoverable oil is expected from the Ben Nevis Formation (CNLOPB 2011). Experiments were designed to mimic the Ben Nevis Formation including rock properties, temperature, and pressure. Seawater is the source for waterflooding offshore, and seawater will be the dispersant for chemical additives such as SiO₂ nanoparticles.

The literature summarized in Table 3.1 shows that brine used in laboratory tests consisted sodium chloride (NaCl) only, whereas SiO₂ nanoparticles are dispersed in seawater (collected from Grand Banks, the offshore development area) in this research, which includes magnesium and calcium divalent ions to best emulate the actual production conditions. Divalent ions such as magnesium and calcium ions are known to interact more with SiO₂ nanoparticles to cause agglomeration (Metin et al. 2011).

Applying EOR at approximately 350 km offshore requires overcoming logistical challenges: transportation and quality control of injectants to remote locations, water treatment and disposal, and installation of storage and processing facilities for the injectants on the platform (Kang et al. 2016). A fundamental understanding of the chemical additives used for enhanced oil recovery is vital to tackle these challenges. This includes but not limited to understanding the fluid-fluid interactions as well as fluid-rock interactions generated by the chemical additive being used, and also optimizing amount of chemical additives required to maximize the production at the lowest cost possible. The work presented in this paper explores recovery mechanism via SiO₂ nanoparticles through interfacial measurements and contact angle measurements. Coreflooding is performed at two different SiO₂ nanoparticle concentrations dispersed in seawater, all at Hebron reservoir temperature and pressure, to investigate effectiveness of SiO₂ nanoparticles on the incremental oil recovery.

3.3. Method

Amorphous hydrophilic silicon dioxide nanoparticles (99.99% purity, from US Research Nanomaterials, Inc.) are used for the coreflooding experiments. The nanoparticles were purchased as a 25 wt% aqueous dispersion, and no other modifications were made other than dilution.

Nanofluid is prepared by mixing silicon dioxide nanoparticles and hydrochloric acid solution (ACS Reagent, 37%, Sigma-Aldrich) with magnetic stir bar for 10 minutes, then the seawater (collected from Grand Banks, offshore Newfoundland and Labrador, Canada) was added to desired concentrations of silicon dioxide and hydrochloric acid (Table 3.2).

The addition of hydrochloric acid (HCl) to the nanofluid was to prevent nanoparticle agglomeration in the seawater. The Grand Banks seawater has a total dissolved solids (TDS) count of 35,987 ppm, as shown in Table 3.3 along with composition.

The standard Berea cores (From Berea Sandstone Petroleum Cores) were selected for contact angle measurements and coreflood experiments, since the Ben Nevis Formation is primarily composed of sandstones in the lower sections of the reservoir (CNLOPB 2011). The similarity in their mineralogical composition obtained from mineral liberation analysis (MLA 650 FEG by FEI) is shown in Figure 3.2. The upper facies of the Ben Nevis Formation increases to almost 20% carbonate and is currently under investigation.

Table 3.2 Nanofluid properties in seawater

	SiO ₂ concentration (wt%)	HCl concentration (mol/L)	pH	Density at 26 °C (g/cm ³)
Nanofluid 1	0.01	0.002	2.84	1.0227
Nanofluid 2	0.03	0.006	2.45	1.0233
Seawater	-	-	7.84	1.0230

Table 3.3 Grand Banks seawater composition (Valencia et al. 2017)

Ions	Concentration (ppm)
Na ⁺	10,887
Ca ²⁺	379
Mg ²⁺	1,323
SO ₄ ²⁻	3,248
Cl ⁻	20,186
HCO ₃ ³⁻	132
Total	35,987

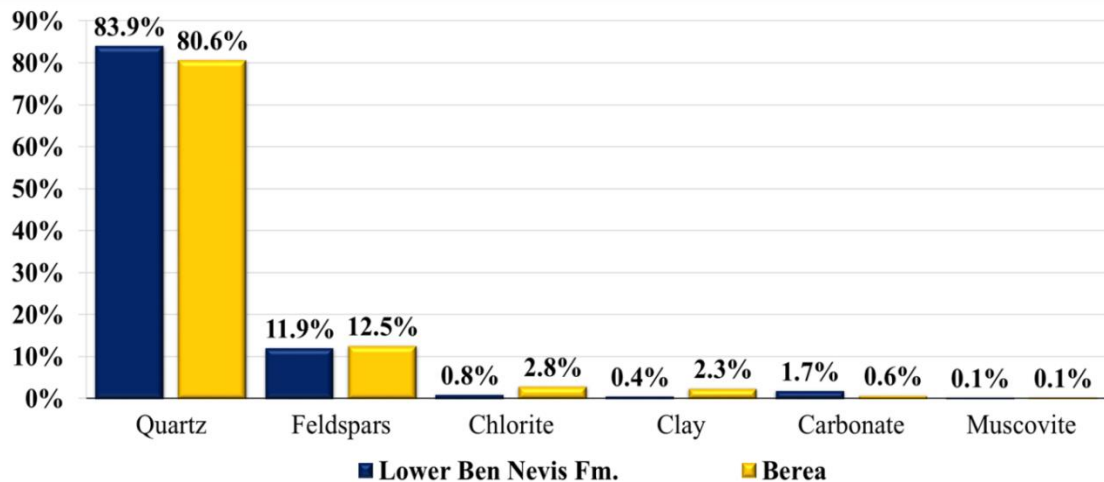


Figure 3.2 Mineralogical composition of Lower Ben Nevis Formation and Berea sandstone

The interfacial tension measurements between oil and each nanofluid were carried out using a pendant drop meter (IFT 700 by Vinci Technologies), at 62 °C and 19.00 MPa. The contact angles of the oil droplet on the Standard Berea core, surrounded by each nanofluid were also measured using the same equipment at the identical conditions. The measurements were collected by the drop shape method, for 15 minutes at 5 second intervals. The instrument was calibrated by measuring interfacial tension between deionized water and air; acetone and air; toluene and air, then comparing to the literature value, to ensure accuracy of the measurements. 20% of the measurements were replicated to ensure the accuracy of the results (Sivira et al., 2016).

The standard Berea cores were restored to reservoir conditions using the method as outlined by Sripal and James (2016) for the coreflood experiments. The specifications of standard Berea cores, and the synthetic brine used to produce connate water in the cores are organized in Table 3.4 and Table 3.5, respectively. Hebron crude oil was not available yet to run coreflood experiments, and therefore, oil was simulated by mixing crude oil from Hibernia (another offshore Newfoundland and Labrador field) with Athabasca bitumen, in a 14:1 proportion, to reach the Hebron crude oil viscosity of 10.9 mPa·s at 62 °C and 19.0 MPa, verified using a Cambridge PVT viscometer (Valencia et al. 2017).

Table 3.4 Standard Berea cores specifications for coreflood experiments

Run	SiO₂ Concentration (wt%)	Length (cm)	Pore Volume (mL)	Porosity
1	0.01	10.18	19.92	0.17
2	0.03	10.10	20.84	0.18

Table 3.5 Composition of synthetic formation water used to generate connate water

Composition	Concentration (ppm)	Concentration (mol/L)
NaCl ($\geq 99\%$, Sigma-Aldrich)	96,959	1.6590
CaCl ₂ ·2H ₂ O ($\geq 99\%$, Sigma-Aldrich)	14,158	0.096303
MgCl ₂ ·6H ₂ O ($\geq 99\%$, Fisher)	2966	0.01459
KCl (99.2%, Fisher)	461	0.00618
Na ₂ SO ₄ (≥ 99.0 , Sigma-Aldrich)	373	0.00263
Total	114,917	1.7787

The coreflood was setup as shown in Figure 3.3. Two accumulators were used, one filled with seawater, and the other with nanofluid. These fluids were injected into the core with Quizix pumps to allow injection at a constant flow rate. 20k Quizix pump injects deionized water at the bottom of the floating piston accumulator to allow 5000 Quizix pump to deliver fluids from the accumulator to the core. The second 20k Quizix pump injected silicon oil into the core holder to generate overburden pressure of 3500 psi.

To mimic the Hebron field conditions, the coreflood experiments were conducted at a temperature of 62 °C (335.15 K) and a pressure of 19.0 MPa. The seawater from Grand Banks was injected at a constant rate of 0.2 mL/min (0.0033 cm³/s) for 4 PV, followed by 2 PV of nanofluid at a constant flow rate of 0.2 mL/min (0.0033 cm³/s). This rate is equivalent to 1 ft/day. The set-up was then shut in for 6 hours to allow time for nanofluid to further interact with the minerals of the rock. Finally, the cores were flushed with seawater once again, at a constant flow rate of 0.2 mL/min (0.0033 cm³/s) for 4 PV.

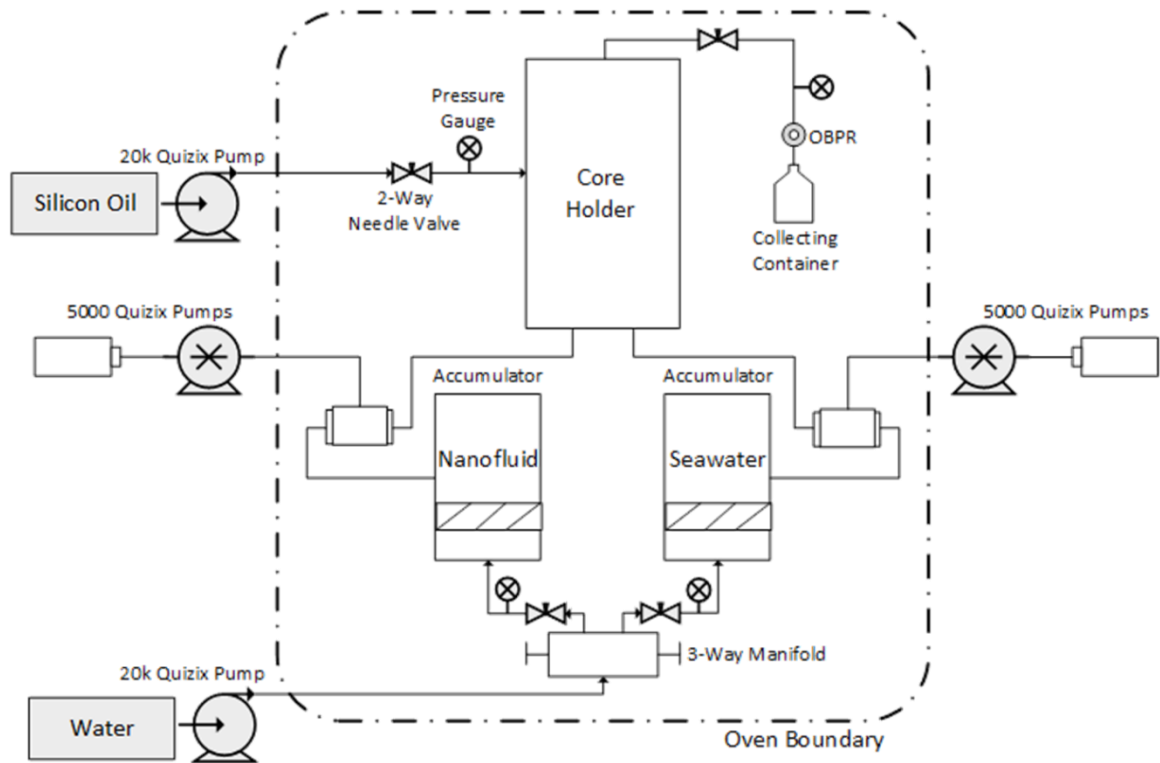


Figure 3.3 Schematic diagram of coreflood set-up

There are variations of coreflood experimental procedures in the literature. Joonaki and Ghanaatian (2014), Aurand et al. (2014), and Hendraningrat et al. (2013) injected brine, followed by nanofluid. Roustaei et al. (2012), Hendraningrat et al. 2014, and Nazari Moghaddam et al. (2015) injected brine, followed by nanofluid, then finished with second brine injection. Only Nazari Moghaddam et al. (2015) introduced shut-in period. They left the core plugs for 24 hours after injecting nanofluid to ensure adequate nanofluid treatment on the rock surface. This paper followed this approach, but with shut-in period of 6 hours. It was found that the maximum decrease in the contact angle, thereby indicating the greatest wettability alteration of the rock occurs when the cores were aged in nanofluid for 6 hours (Sivira et al. 2017). The core was injected with seawater after the

shut-in period, since the rock was considered to have become more water-wet during the 6-hour shut-in period, and additional oil recovery was deemed possible via sweeping with seawater.

3.4. Results and Discussion

The hydrophilic SiO₂ nanofluid at concentrations of 0.01 and 0.03 wt% decreases the interfacial tension, as well as the contact angle (Figure 3.4 and Figure 3.5). The decrease in interfacial tension and more water-wet condition evident from decreased contact angle values indicate that the SiO₂ nanofluids stabilized in hydrochloric acid solution should have positive impact on the incremental oil recovery. The coreflood experimental results with 0.01 as well as 0.03 wt % silicon dioxide nanofluids both confirm this prediction as shown in Figure 3.6.

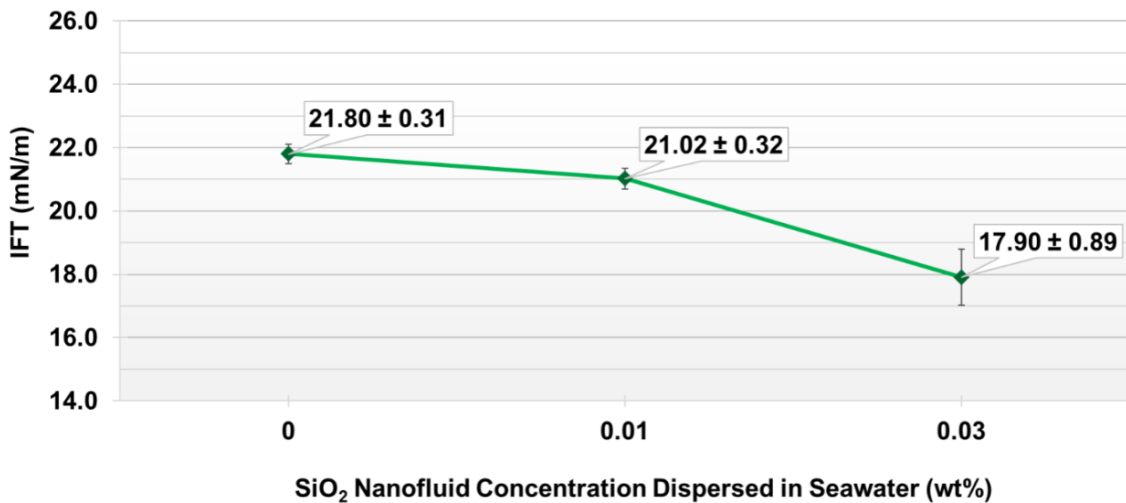


Figure 3.4 SiO₂ nanoparticle contribution on interfacial tension alteration (After Sivira et al. 2016)

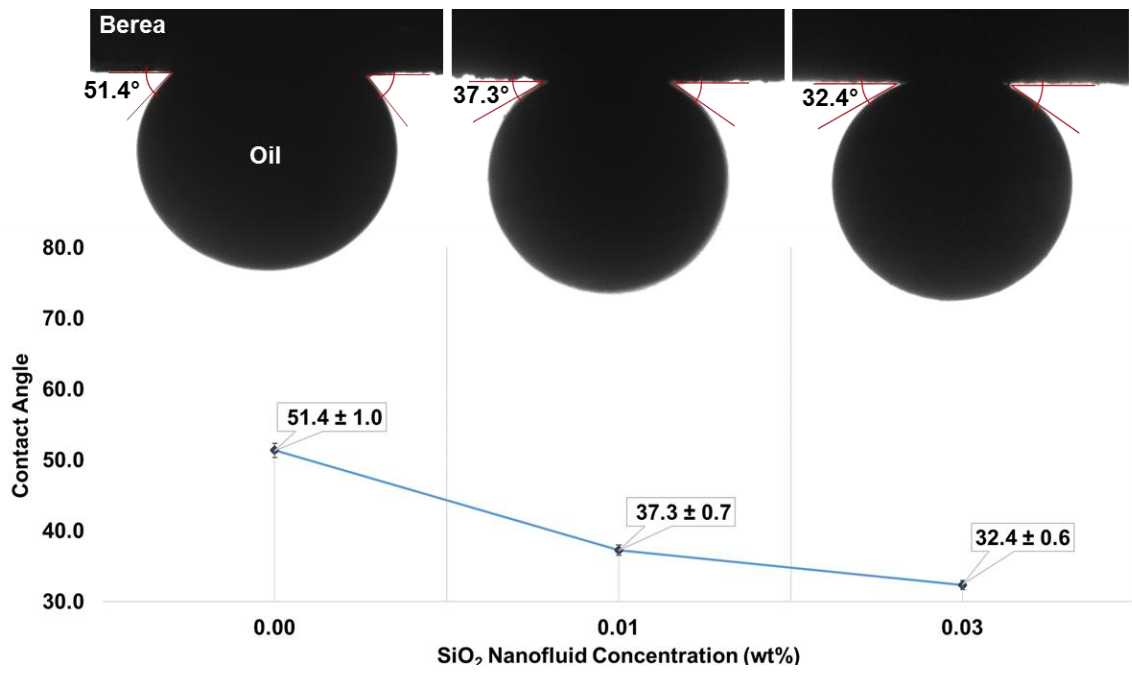


Figure 3.5 Contact angle measurements on Berea with SiO₂ nanofluids (After Sivira et al. 2016)

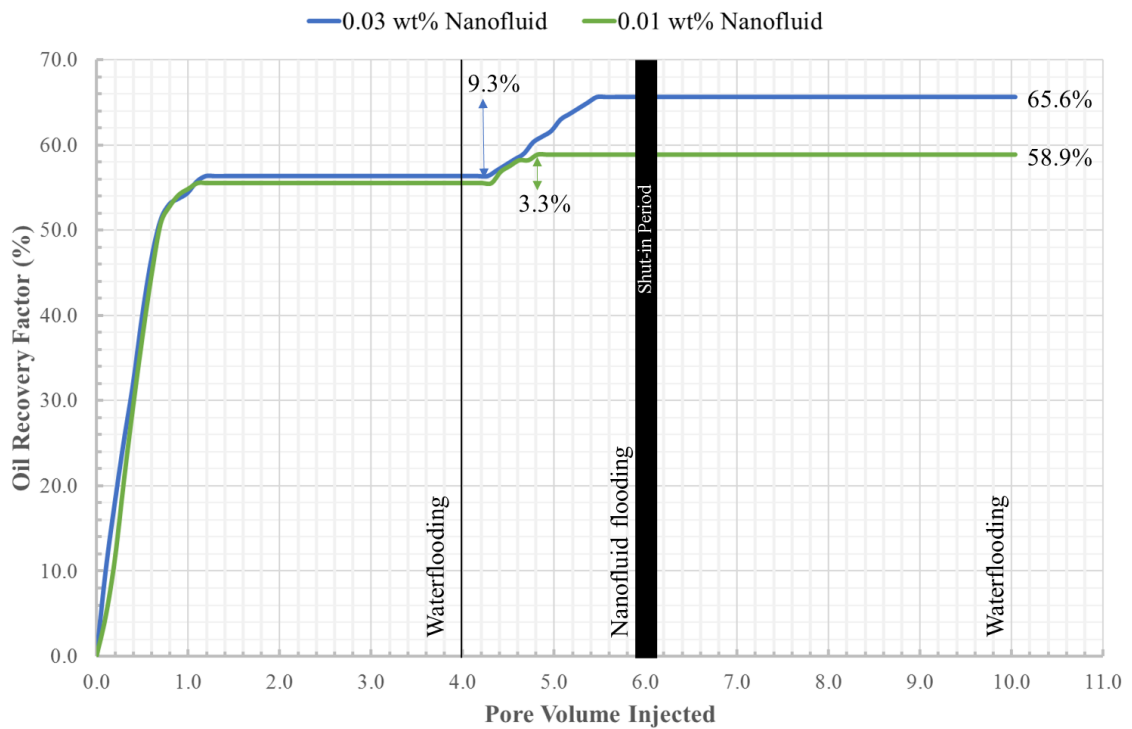


Figure 3.6 Oil recovery using 0.01 wt% and 0.03 wt% SiO₂ nanofluid

The oil recovery from the initial waterflood for 0.01 wt% SiO₂ coreflood experiment was 55.6%. The nanoparticle flooding increased oil recovery by 3.3%, thus resulting in 58.9% of total oil recovery, as shown in Figure 3.6. For 0.03 wt% SiO₂ coreflood experiment, the initial waterflood gave oil recovery of 56.3%, and nanoparticle flooding increased the oil recovery by 9.3%. 0.03 wt% SiO₂ nanoparticle flooding gave total oil recovery of 65.6%. These results show that the increasing nanoparticle concentrations improves oil displacement efficiency. Maghzi et al. (2012) suggests this is because increasing nanoparticle concentration increases the spreading of nanofluids on the rock surface. The spreading of nanoparticles on the rock surface are believed to form a wedge film between the oil and rock, and eventually detaching the oil drop (D. T. Wasan & Nikolov, 2003) to improve the oil recovery.

The purpose of the shut-in period after the nanoparticle flooding was to give the nanofluid more time to interact with the rock surface and alter the wettability. Previous wettability studies conducted at the Hebron field conditions showed that nanofluid stabilized with HCl decreases the contact angle between the rock and oil, making the rock more water wet (Sivira et al. 2016). It was also observed that the nanofluid decreases contact angle the most after 6 hours of aging, then the contact angle starts to increase again after 6 hours (Sivira et al. 2017). Since the rock surface reaches the most water-wet condition after 6 hours, it was hypothesized that the waterflooding after the 6 hours shut-in period would mobilize more residual oil. However, there was no further oil recovery upon second waterflooding in both coreflood experiments conducted in this study. The reason for this is to be further investigated, which would involve understanding of forces such as

Van der Waals, acid-base interaction, attractive and repulsive forces from electrical double layers, and hydrodynamics that affect adsorption and desorption of nanoparticles as well as the interactions of oil, nanofluid and rock in a complex system (Khilar & Fogler, 1998). Skauge, Hetland, Spildo, Skauge, & Cipr (2010) identified a production challenge with nanoparticles as nanoparticles adhering to the rock surface excessively, blocking the pore throats, and preventing further oil production. However, the blockage of nanoparticles is thought to be minimal in this study because nanofluid contains HCl, which would dissolve mineral content in the rock (Sivira et al. 2017), thereby increasing the pore space. The nanoparticle agglomeration has also been identified to block the pores of the rock in the literature. Hendraningrat et al. (2013b) have reported the problems of nanoparticle agglomeration which was visible at the inlet after coreflooding process with 0.03 wt% SiO₂ nanoparticles. There was no visible agglomeration at the inlet after coreflood experiment with both 0.01 and 0.03 wt% SiO₂ nanoparticles in this study, suggesting there was no agglomeration during the coreflooding. This shows that the hydrochloric acid successfully prevented nanoparticles agglomeration at reservoir temperature and pressure, even though some of HCl would have been used up from the reaction with the rock. Further study involving permeability measurements, pH measurements, SEM (Scanning Electron Microscopy), MLA (Mineral Liberation Analyzer), and ICP (Inductively Coupled Plasma Mass Spectrometry) are required to investigate the permeability, relative permeabilities, and material balances of the SiO₂ nanoparticles, salt ions, and HCl.

The dissolution of rock due to HCl raises a question whether it is HCl in the nanofluid that is responsible for the oil recovery, rather than the nanoparticle itself. Though it is possible that HCl contributes to higher recovery during the nanofluid flooding, two observations from the experiments suggest that the improved oil recovery is mainly because of the nanoparticles. Previous experiments showed that nanofluid without nanoparticles (i.e. HCl with seawater only) increases the interfacial tension between water and oil, and it is only when nanoparticles are present that interfacial tension decreases (Sivira et al. 2016). Secondly, if HCl increases oil recovery via dissolution of the minerals, more recovery should have been seen after the 6 hours shut-in period, as more dissolution would occur during that time. A coreflood experiment with HCl and seawater only is on the way to confirm that improved oil recovery is attributed to the nanoparticles.

3.5. Conclusions

The enhanced oil recovery efficiency of 0.01 and 0.03 wt% silicon dioxide nanofluids is studied through coreflood experiments, at conditions that emulated Hebron Field. The findings are listed as follows:

- The preliminary interfacial tension and contact angle measurements indicated positive impact on the oil recovery, and is confirmed by the coreflood experiments.
- 0.01 wt% nanofluid injection followed by waterflooding increased oil recovery by 3.3% in Berea cores.

- 0.03 wt% nanofluid injection followed by waterflooding increased oil recovery by 9.3% in Berea cores
- Higher nanoparticle concentration is more efficient in improving oil recovery.
- Under the employed conditions, additional time for nanofluid to interact with rock surface followed by waterflooding does not increase oil recovery. Explanation for this requires further investigation.

Acknowledgements

We would graciously like to thank the Hibernia Enhanced Oil Recovery lab staff and co-op students for their assistance with the experimental work. This research was made possible with a support of Hibernia Management Company (HMDC), Chevron Canada, Research and Development Corporation of Newfoundland and Labrador (RDC), and the Natural Sciences and Engineering Research Council of Canada (NSERC).

References

- Al-Anssari, S., Barifcani, A., Wang, S., Maxim, L., & Iglauer, S. (2016). Wettability Alteration of Oil-Wet Carbonate by Silica Nanofluid. *Journal of Colloid and Interface Science*, *461*, 435–442. <https://doi.org/10.1016/j.jcis.2015.09.051>
- Aurand, K. R., Dahle, G. S., & Torsæter, O. (2014). Comparison of Oil Recovery for Six Nanofluids in Berea Sandstone Cores. *International Symposium of the Society of Core Analysts*, 1–12.

CNLOPB. (2011). *Hebron Development Plan*. Retrieved from <http://www.cnlopb.ca/pdfs/conhebddevplan.pdf?lbisphpreq=1>

El-diasty, A. I., & Aly, A. M. (2015). Understanding the Mechanism of Nanoparticles Applications in Enhanced Applications of Nanoparticles in EOR. *Paper SPE 175806 - North Africa Technical Conference (Cairo / Egipto)*, 0, 1–19. <https://doi.org/10.2118/175806-MS>

Hendraningrat, L., Li, S., & Torsæter, O. (2013a). A Coreflood Investigation of Nanofluid Enhanced Oil Recovery. *Journal of Petroleum Science and Engineering*, 111, 128–138. <https://doi.org/10.1016/j.petrol.2013.07.003>

Hendraningrat, L., Li, S., & Torsæter, O. (2013b). Enhancing Oil Recovery of Low-Permeability Berea Sandstone through Optimized Nanofluids Concentration. *Society of Petroleum Engineers*, (2012).

Hendraningrat, L., & Torsæter, O. (2014). Unlocking the Potential of Metal Oxides Nanoparticles to Enhance the Oil Recovery, (2013). <https://doi.org/10.2118/24696-MS>

Joonaki, E., & Ghanaatian, S. (2014). The Application of Nanofluids for Enhanced Oil Recovery: Effects on Interfacial Tension and Coreflooding Process. *Petroleum Science and Technology*, 32(21), 2599–2607. <https://doi.org/10.1080/10916466.2013.855228>

Kang, P. S., Lim, J. S., & Huh, C. (2016). Screening Criteria and Considerations of Offshore Enhanced Oil Recovery. *Energies*, 9(1), 1–18. <https://doi.org/10.3390/en9010044>

Khilar, K. C., & Fogler, H. S. (1998). *Migrations of Fines in Porous Media*. Netherlands: Springer.

Li, S., Hendraningrat, L., & Torsæter, O. (2013). Improved Oil Recovery by Hydrophilic Silica Nanoparticles Suspension: 2-Phase Flow Experimental Studies, 1–15.

Maghzi, A., Mohammadi, S., Ghazanfari, M. H., Kharrat, R., & Masihi, M. (2012).

Monitoring Wettability Alteration by Silica Nanoparticles during Water Flooding to Heavy Oils in Five-Spot Systems: A Pore-Level Investigation. *Experimental Thermal and Fluid Science*, 40, 168–176. <https://doi.org/10.1016/j.expthermflusci.2012.03.004>

Matteo, C., Candido, P., Vera, R., Francesca, V., Duca, C., & Abruzzi, D. (2012). Current and Future Nanotech Applications in the Oil Industry. *American Journal of Applied Sciences*, 9(6), 784–793.

Metin, C. O., Lake, L. W., Miranda, C. R., & Nguyen, Q. P. (2011). Stability of Aqueous Silica Nanoparticle Dispersions. *Journal of Nanoparticle Research*, 13(2), 839–850. <https://doi.org/10.1007/s11051-010-0085-1>

Miranda, C. R., Lara, L. S. De, & Tonetto, B. C. (2012). Stability and Mobility of Functionalized Silica Nanoparticles for Enhanced Oil Recovery Applications. *SPE Oilfield Nanotechnology Conference*, SPE 157033. <https://doi.org/10.2118/157033-ms>

Mokhatab, S., Fresky, M. A., & Islam, M. R. (2006). Applications of Nanotechnology in Oil and Gas E&P. *Journal of Petroleum Technology*, 58(4), 48–51. <https://doi.org/10.2118/0406-0048-JPT>

Nazari Moghaddam, R., Bahramian, A., Fakhroueian, Z., Karimi, A., & Arya, S. (2015). Comparative Study of Using Nanoparticles for Enhanced Oil Recovery: Wettability Alteration of Carbonate Rocks. *Energy & Fuels*, 29(4), 2111–2119. <https://doi.org/10.1021/ef5024719>

Roustaei, A., Moghadasi, Jamshid Bagherzadeh, H., & Shahrabadi, A. (2012). An Experimental Investigation of Polysilicon Nanoparticles' Recovery Efficiencies Through Changes in Interfacial Tension and Wettability Alteration. *SPE International Oilfield Nanotechnology Conference, Noordwijk, Netherlands*, 200–206. <https://doi.org/10.2118/156976-MS>

Sivira, D., Kim, H. B., James, L., Johansen, T., & Zhang, Y. (2016). The Effectiveness of Silicon Dioxide SiO₂ Nanoparticle as an Enhanced Oil Recovery Agent in Ben Nevis

Formation, Hebron Field, Offshore Eastern Canada. *Society of Petroleum Engineers*.

Sivira, D., Kim, H. B., James, L., Wilton, D., & Zhang, Y. (2017). Fluid-Rock Interaction between Silicon Dioxide (SiO₂) Nanoparticle and Standard Cores Mimicking Hebron Field Conditions for Enhanced Oil Recovery Application. *EAGE 19th European Symposium on Improved Oil Recovery*.

Skauge, T., Hetland, S., Spildo, K., Skauge, A., & Cipr, U. (2010). Nano-Sized Particles for EOR. *SPE Improved Oil Recovery Symposium*, (April), 24–28. <https://doi.org/10.2118/129933-ms>

Sripal, E., & James, L. A. (2016). Application of an Optimization Method for Restoration of Core Samples for Scal Experiments. *Society of Core Analysts*, 1–12.

Valencia, L., James, L. A., & Azmy, K. (2017). *Implications of the Diagenetic History on Enhanced Oil Recovery (EOR) Performance for the Ben Nevis Formation, Hebron Field, Jeanne D'arc Basin, Offshore, Newfoundland, Canada*. Memorial University.

Wasan, D. T., & Nikolov, A. D. (2003). Spreading of Nanofluids on Solids. *Nature*, 423(6936), 156–159. <https://doi.org/10.1038/nature01591>

Chapter 4. A Coreflood Study of Injecting Silicon Dioxide (SiO₂) Nanoparticles as a Water Additive for the Enhanced Oil Recovery on the Hebron Field Cores

Authors

Jenny Kim, Daniel J. Sivira, Lesley A. James, Yahui Zhang, Edison Sripal

Unpublished Manuscript

4.1. Abstract

The first oil was pumped at the Hebron offshore platform, the fourth offshore development in Newfoundland and Labrador, Canada, in November 2017. The enhanced oil recovery methods to maximize the production at the Hebron Field must be investigated early on, as only 30% of the initial oil in place is recoverable. This experimental study focused on injecting silicon dioxide (SiO₂) nanofluid as a water additive for the enhanced oil recovery with application to the Hebron Field. The nanofluid consisted of silicon dioxide nanoparticles dispersed in seawater collected from Grand Banks, offshore of Newfoundland and Labrador, as well as the hydrochloric acid as a nanoparticle stabilizer, to prevent nanoparticles from agglomerating in seawater. The previous coreflood study (Kim, Sivira, James, & Zhang, 2017) on Berea standard cores at Hebron reservoir temperature and pressure (62 °C and 19.00 MPa, respectively) showed injecting 0.01 wt% SiO₂ contributes to 3.3% incremental oil recovery. The increase in the SiO₂ nanoparticle concentration to 0.03 wt% yielded 9.3% incremental oil recovery. The coreflood experiments presented in this paper is a continuation of Kim et al. (2017)'s coreflood study. The effect of increasing nanoparticle concentration to 0.05 wt% on the

oil recovery is investigated using Berea core, as well as Hebron core. The potential possibility of the nanoparticle stabilizer, hydrochloric acid, contributing to the oil recovery is also explored. The results showed that 0.05 wt% nanofluid injection on Berea core yields 14.9% oil recovery, showing it is the most efficient concentration in improving the oil recovery compared to 0.01 and 0.03 wt%. The injection of 0.05 wt% nanoparticle on Hebron core also had positive impact on the incremental oil recovery of 11.9%. The hydrochloric acid in the nanofluid was found to have minimal effect on the incremental oil recovery.

4.2. Introduction

The Hebron Project is the fourth offshore development in Newfoundland and Labrador (Eastern Canada), after Hibernia, Terra Nova, and White Rose. It is located 350 km offshore of St. John's, Newfoundland and Labrador as depicted in Figure 4.1.

The first oil was November 28, 2017, with a projected recovery of 30%. The largest reservoir, Pool 1 in Ben Nevis Formation (as shown in Figure 4.2), accounts for 70% of the recoverable oil, and this is where Hebron Field is currently producing. The secondary development will focus on Pool 3 in Ben Nevis Formation (CNLOPB, 2011).

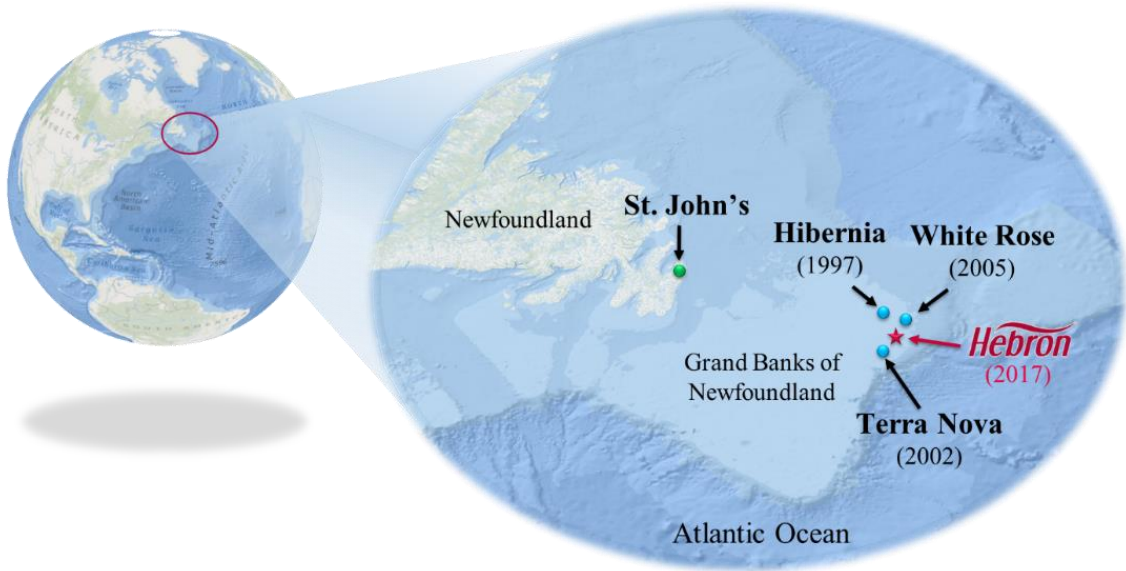


Figure 4.1. Location of the Hebron asset

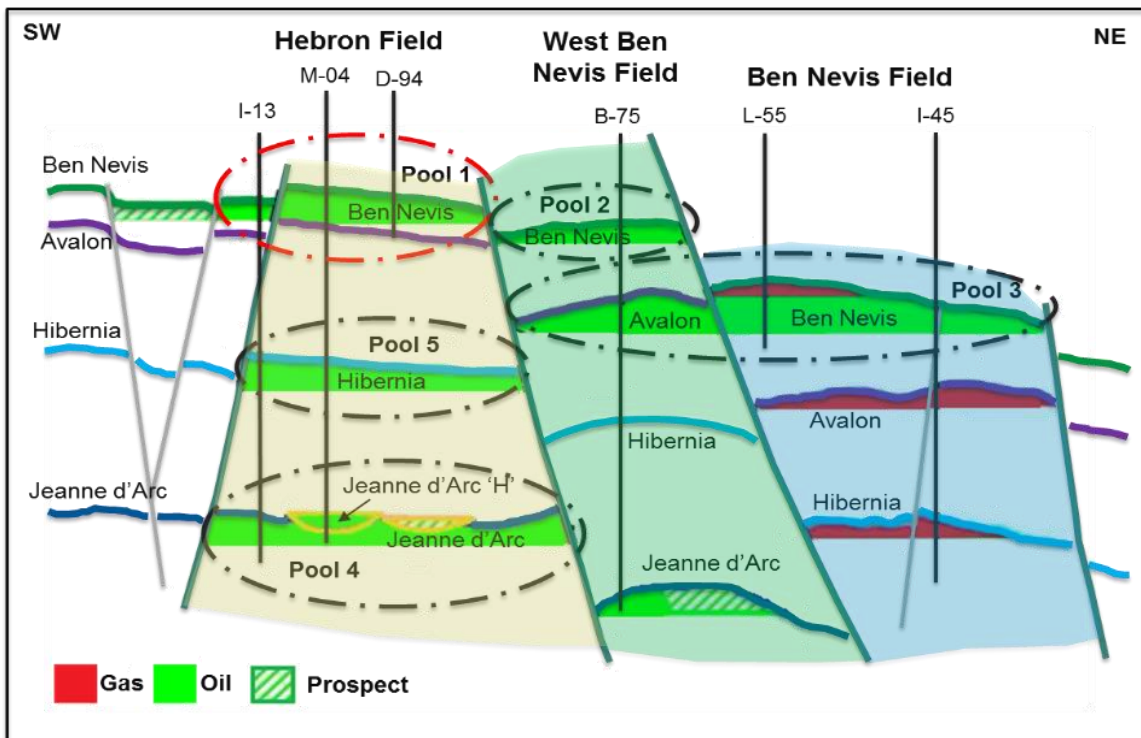


Figure 4.2. Cross section of Hebron assets (Modified after CNLOPB, 2011)

The enhanced oil recovery (EOR) entails extraction of oil residing in a reservoir after water or gas has been injected for a pressure support in the reservoir (Stosur et al., 2003). The EOR methods for Hebron asset must be investigated early on to improve the recovery factor from the projected 30%. This research investigates the effectiveness of 0.05 wt% silicon dioxide (SiO_2) nanoparticles as a water additive for EOR method with an application to the Hebron Field, through coreflood experiments.

The “nanofluid” injected in the coreflood experiments consisted of SiO_2 nanoparticles dispersed in seawater collected from Grand Banks, offshore of Newfoundland and Labrador, as well as the hydrochloric acid as a nanoparticle stabilizer. The nanoparticles were dispersed in seawater because the viable water source for Hebron offshore is the surrounding seawater. The SiO_2 nanoparticles become highly unstable in seawater because of the presence of divalent cations such as Ca^{2+} and Mg^{2+} (Metin et al. 2011), however, Jafari Daghlian Sofla, James, & Zhang (2018) have shown that the unmodified SiO_2 nanoparticles can be stabilized in seawater in the presence of hydrochloric acid (HCl). Chapter 2 of this manuscript also have shown that the SiO_2 nanoparticles remain stable for at least 14 days at Hebron Field temperature and pressure (62 °C and 19.00 MPa), when the ratio between wt% of HCl and wt% of SiO_2 nanoparticles is 0.46. This ratio was used to prepare 0.05 wt% SiO_2 nanofluid for the coreflood experiments in this paper.

Kim, Sivira, James, & Zhang (2017)’s coreflood experiments on Berea sandstone with 0.01 wt% and 0.03 wt% SiO_2 nanoparticles dispersed in the Grand Banks seawater have shown incremental oil recovery at Hebron Field conditions. This paper further

investigates the effectiveness of SiO₂ nanoparticles on oil recovery using 0.05 wt% nanoparticle dispersion in seawater at the same experimental conditions and set-up as Kim et al. (2017). A coreflood experiment on Hebron Field core is also performed, to further emulate Hebron reservoir conditions to study suitability of using SiO₂ in the field. Since there is a possibility of HCl (nanoparticle stabilizer) contributing to the incremental oil recovery, the effect of HCl on the coreflood experiment using cores predominantly made up of sandstone is also studied.

4.3. Experimental Methodology

The nanofluids prepared for the coreflood experiments consisted of three components: silicon dioxide (SiO₂) nanoparticles, hydrochloric acid (HCl), and seawater. The amorphous hydrophilic SiO₂ nanoparticle was purchased in 25 wt% aqueous dispersion from US research Nanomaterials. The 25 wt% aqueous nanoparticle dispersion was mixed with 3.0 mol/L hydrochloric acid (ACS Reagent, 37%, Sigma-Aldrich) with a magnetic stir bar for 10 minutes. The mixture was then diluted to 0.05 wt% dispersion by adding seawater from Grand Banks (Offshore Newfoundland and Labrador, Canada). Grand Banks seawater contains monovalent cation (Na⁺) and divalent ions (Ca²⁺ and Mg²⁺), with total dissolved solid count of approximately 36,000 ppm (Table 4.1). HCl is added as a nanoparticle stabilizer, to allow uniform dispersion of nanoparticles in seawater, preventing agglomeration. The final HCl concentration in the 0.05 wt% nanofluid was 0.010 M. The 0.05 wt% nanofluid had a resulting pH of 2.20, and a density of 1.024 g/cm³ at 26 °C.

Table 4.1. Grand Banks seawater composition (Valencia et al. 2017)

Ions	Concentration (ppm)
Na ⁺	10,887
Ca ²⁺	379
Mg ²⁺	1,323
SO ₄ ²⁻	3,248
Cl ⁻	20,186
HCO ³⁻	132
Total	35,987

The Berea standard core, as well as the core from the Ben Nevis Formation (Pool 3, Well L-55) was used for the coreflood experiments with 0.05 wt% SiO₂ nanofluid. The use of Berea standard core was to compare results from the coreflood experiments with 0.01 and 0.03 wt% SiO₂ nanofluids by Kim, Sivira, James, & Zhang (2017), and to select the most effective nanofluid to perform coreflood experiment on the Hebron core. Sivira, Kim, James, Wilton, & Zhang (2017) have reported that the use of HCl on Berea sandstone cores dissolves the carbonate content, and could wash the clay minerals away. This could potentially increase the porosity and permeability of the rock, increasing the oil recovery. Therefore, Berea standard core was used to run a coreflood experiment with the fluid that does not contain SiO₂ nanoparticles, but 0.010 M of HCl in Grand Banks seawater only, to verify that the significant incremental oil recovery is due to SiO₂ nanoparticles, not HCl.

The physical properties of the cores used are tabulated in Table 4.2. The Berea standard cores were chosen to be a surrogate for Hebron Field cores, because they bear similar

mineralogical composition as the Hebron core in the lower Ben Nevis Formation (Figure 4.3). They are both sandstones composed of mostly Quartz. The Berea sandstones are homogeneous according to the information provided by the suppliers (Kocurek Industries). Both Hebron and Berea cores are slightly water-wet.

Table 4.2. Physical properties of the cores used in coreflood experiments

Run	Core Type	Length (cm)	Pore Volume (mL)	Porosity	Permeability (mD)
1	Berea	9.91	19.71	17.4	400
2	Hebron	10.51	22.48	19.0	300 - 500
3	Berea	10.12	20.62	17.9	400

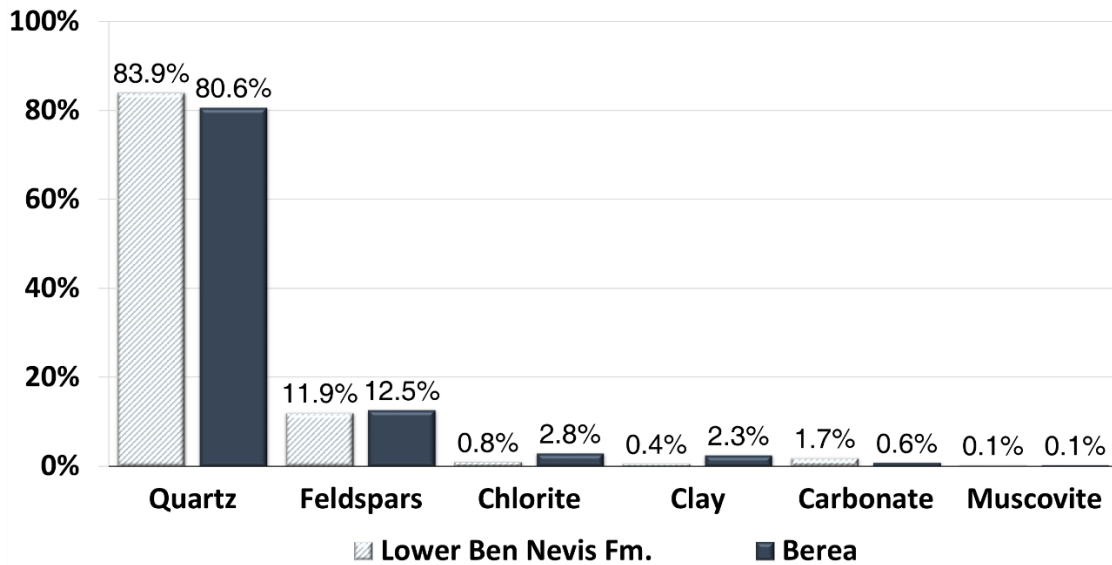


Figure 4.3. Mineralogical composition of core from Ben Nevis Formation and Berea sandstone

The cores were restored to the reservoir conditions as per Sripal & James (2016). This involved sonicating the cores for 45 minutes to remove any fines; saturating the cores in

synthetic formation brine (Table 4.3) to produce connate water; saturating the core with oil using centrifuge; then aging the cores at 90 °C and 20.7 MPa for 4 weeks.

Table 4.3. Composition of synthetic formation water used to generate connate water in Berea and Hebron Cores

Composition		Concentration (ppm)
NaCl	(≥99%, Sigma-Aldrich)	96,959
CaCl ₂ ·2H ₂ O	(≥99%, Sigma-Aldrich)	14,158
MgCl ₂ ·6H ₂ O	(≥99%, Fisher)	2966
KCl	(99.2%, Fisher)	461
Na ₂ SO ₄	(≥99.0, Sigma-Aldrich)	373
Total		114,917

Simulated oil was used to saturate the cores because sufficient Hebron crude oil to perform coreflood experiments was unavailable at the time of the experiment. The simulated oil was prepared to match the oil viscosity of Hebron field at Pool 1. The simulated oil prepared by mixing fourteen parts of Hibernia (another offshore Newfoundland and Labrador field) crude oil with one part of Athabasca bitumen, had a viscosity of 10.9 mPa·s at 62 °C and 19.0 MPa (Valencia et al., 2017). The viscosity was measured with a Cambridge PVT viscometer, which has an accuracy of ± 1%. The composition of the simulated oil (Valencia et al., 2017) by Agilent Technologies 7890A GC System is shown in Figure 4.4.

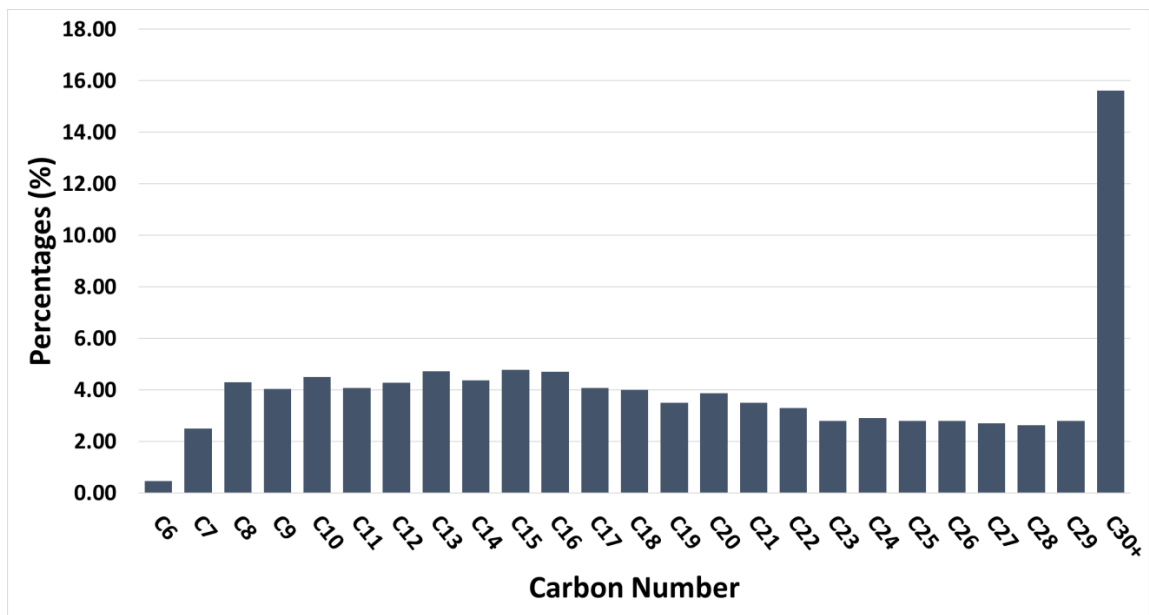


Figure 4.4. Composition of simulated oil by the carbon number

As can be seen in the schematic diagram of the coreflood experiment setup in Figure 4.5, the two accumulators were used, one filled with Grand Banks seawater for waterflooding, and the other with either 0.05 wt% nanofluid or seawater-HCl mixture, depending on the run. 20k Quizix pump injects deionized water at the bottom of the floating piston accumulator to allow two separates 5000 Quizix pumps to deliver seawater and injecting fluids from the accumulator to the core at a constant flowrate. The second 20k Quizix pump injected silicon oil into the core holder to generate overburden pressure of 24.1 MPa. The coreflood experiments were conducted at Hebron Field temperature and pressure of 62 °C and 19.0 MPa, respectively.

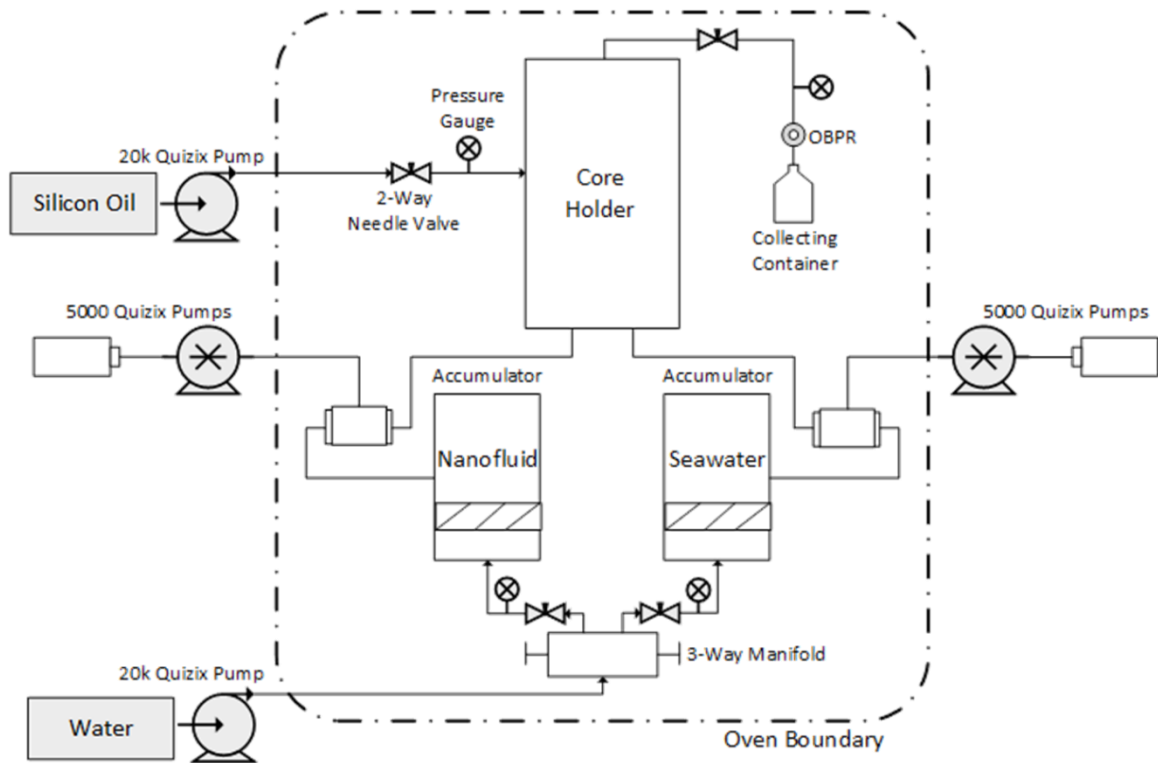
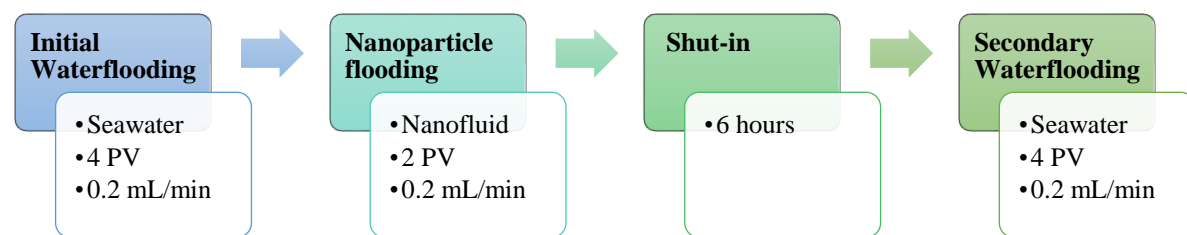


Figure 4.5. Schematic diagram of coreflood experiment setup

Figure 4.6 (a) shows coreflood injection scheme for three coreflood experiments conducted. The seawater from Grand Banks were used for both initial and secondary waterflooding. Though all the oil recoverable from the waterflood occurs within the injection of 1 to 2 pore volumes (PV) of water, 4 pore volumes of water was injected for initial waterfloods to ensure that there is absolutely no more recovery from the waterflooding, allowing effective evaluation of nanoparticle flooding as a tertiary recovery method.



Run	Core Type	SiO ₂ Concentration (wt %)	HCl Concentration (mol/L)	HCl:SiO ₂ Ratio (in wt %:wt %)
1	Berea	0.05	0.010	0.46
2	Hebron	0.05	0.010	0.46
3	Berea	0.00	0.010	N/A

Figure 4.6 (a) Coreflood injection schemes (b) Summary of cores used and fluids injected

The 2 PV of 0.05 wt% nanofluid flooding followed the waterflooding for Run 1 and 2, as labelled in Figure 4.6 (b). 0.05 wt% nanofluid was injected to the Hebron core in Run 2 because 0.05 wt% nanoparticle flooding was the most efficient in improving the incremental oil recovery out of 0.01, 0.03, and 0.05 wt% nanofluids on Berea standard cores. Run 3 is designed to quantify the contribution of HCl on the incremental oil recovery in sandstones, if any. Therefore, 2 PV of seawater and HCl mixture was injected for Run 3. The mixture contained the same concentration of HCl as in 0.05 wt% nanofluid.

The system was then shut-in for 6 hours to promote nanofluid to further interact with the core. Finally, the cores were injected with seawater once again for 4 PV to observe possibility of further oil recovery.

The fluids were always injected at a constant flowrate of 0.2 mL/min in all runs. This is equivalent to 1ft/day, which is the typical injection rate at the producing fields.

The effluents were collected in graduate cylinders to measure the volume of oil produced. The total volume of the content in the graduated cylinder, as well as volume of clear effluent were read directly from the graduated cylinder every 10 minutes. The difference between the two volumes gave the volume of oil produced. The raw data from coreflooding experiments can be found in Appendix, as well as sample calculation for oil recovery factor.

The effluent pH's were measured at the end of the initial waterflooding, nanoparticle flooding, and secondary waterflooding, and was compared to the pH's of the injectants. The pH's were measured with Corning Pinnacle 540 pH meter at room temperature. The pH meter was calibrated with buffer solutions with pH's of 4.00, 7.00, and 10.05 (Certified Grade, Fisher Chemical). The instrument measures accurately to ± 0.01 pH.

4.4. Results and Discussion

The oil recovery from the initial waterflood for 0.05 wt% SiO₂ coreflood experiment on Berea sandstone (Run 1) was 54.1%. The nanoparticle flooding increased the oil recovery by 14.9%. The second water flooding after the shut-in period did not further increase the oil recovery, which makes the total oil recovery to be 69.0% (Figure 4.7). It is evident that the higher nanoparticle concentration translates to a higher incremental oil recovery.

(As a reference, the incremental oil recovery using 0.01 and 0.03 wt% SiO₂ coreflood experiments on Berea sandstone performed by Kim et al. (2017) were 3.3%, and 9.3%, respectively).

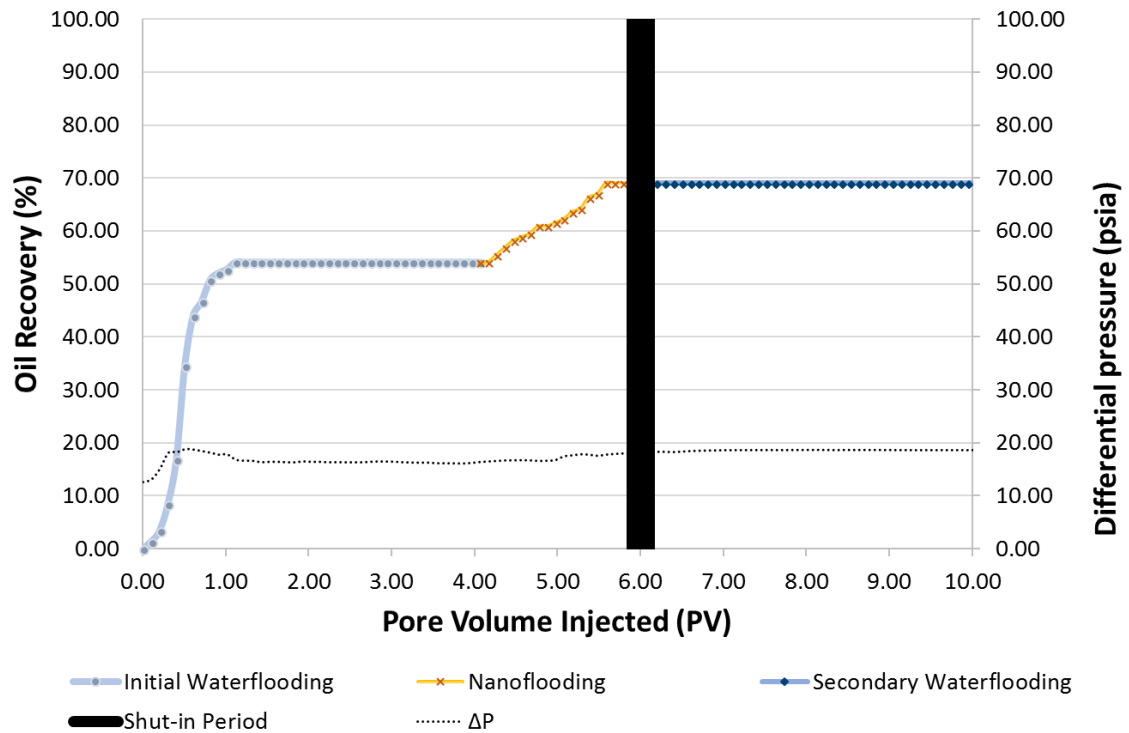


Figure 4.7. Coreflood run 1: oil recovery using 0.05 wt% SiO₂ nanofluids on Berea sandstone core

0.05 wt% nanofluid was used for the coreflood experiment on the Hebron Field core, because 0.05 wt% nanoparticle flooding gave the highest incremental oil recovery on Berea standard cores. As can be seen on Figure 4.8, 49.7% of oil was recovered from the initial waterflooding on the Hebron Field core. The nanoparticle flooding that followed waterflooding increased the oil recovery by 11.9%, totalling 61.6 % of oil recovery. The second 4 PV of waterflooding did not produce additional oil, which was the case in

coreflood experiments on the Berea sandstones, regardless of the concentrations of the nanofluids used. Therefore, the overall recovery obtained was 61.6%.

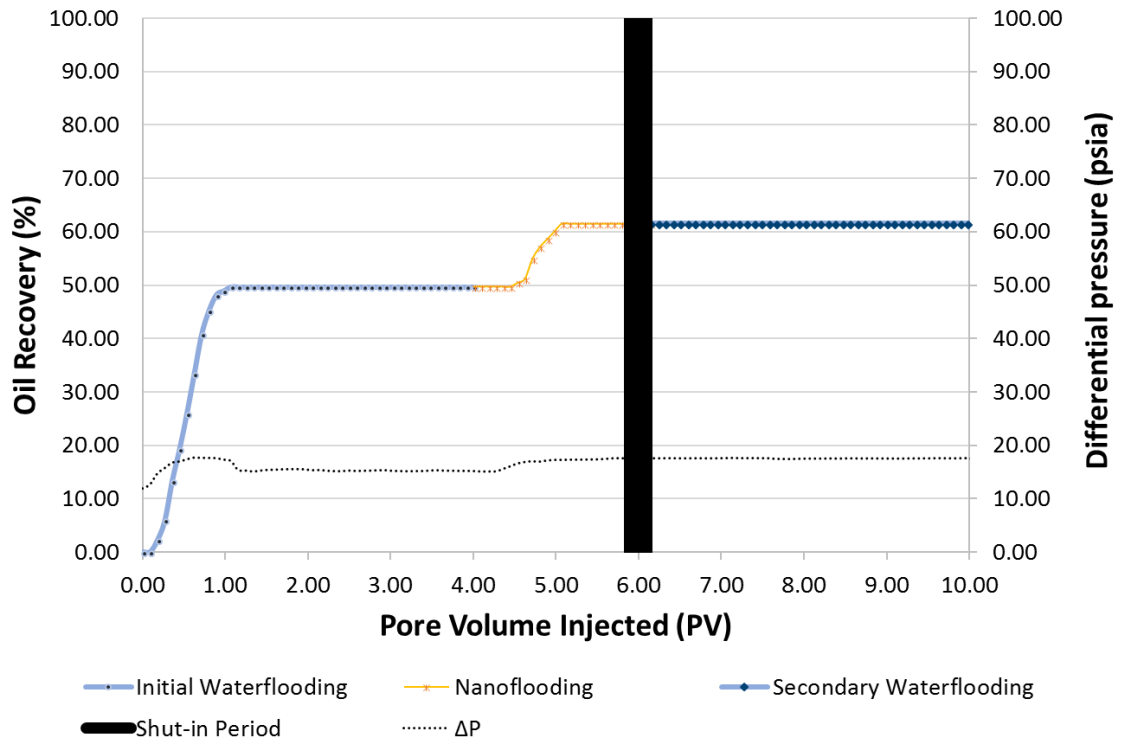


Figure 4.8. Coreflood run 2: oil recovery using 0.05 wt% SiO₂ nanofluid on Hebron core

The incremental oil recovery with 0.05 wt% nanofluid after the waterflooding on Berea standard core and Hebron core is expected to be similar, due to the similar mineralogical composition. In fact, the incremental oil recovery difference between the two are only 3.0%, demonstrating that the Berea standard core is a suitable surrogate for the Hebron core. The 3.0% difference in the incremental oil recovery between these two runs is most likely due to the differences in the mineral arrangements and morphology, despite the similarities in their compositions.

The purpose of adding hydrochloric acid in the nanofluid was to prevent SiO₂ nanoparticles from agglomerating in the seawater. There is a possibility that the hydrochloric acid could contribute to significant increase in the oil recovery, as HCl would dissolve carbonate content in the rocks, and wash away clay minerals (Sivira, Kim, James, Wilton, & Zhang, 2017), potentially increasing the porosity and permeability of the rocks. Berea has a minimal carbonate content (0.6%), however, the effect of HCl on the incremental oil recovery was examined through coreflood experiment (Figure 4.9).

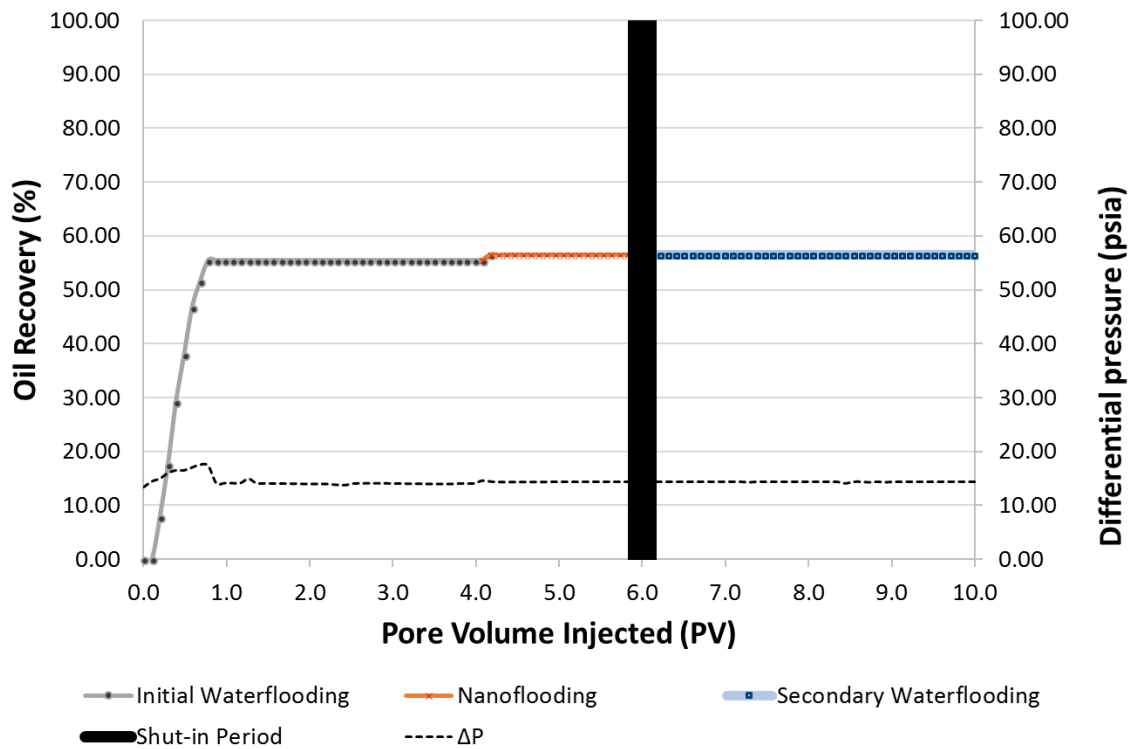


Figure 4.9. Coreflood run 3: oil recovery using seawater + HCl mixture (0.00 wt% nanofluid) on Berea sandstone core

The initial waterflooding gave 55.5% of recovery, and when seawater-HCl mixture is injected, a 1.0% of recovery is observed. The secondary waterflooding after the shut-in period did not increase the recovery, giving an overall recovery of 56.6%. The decrease in the carbonate and clay content from the HCl could have led to 1.0% incremental recovery observed during the seawater-HCl mixture flooding. Comparing the oil recovery curve from this run with Run 1 (0.05 wt% nanoparticle flooding on Berea standard core), which gave 14.9% incremental recovery during the nanoparticle flooding, it is evident that the nanoparticles contributes to a considerable additional oil recovery, not HCl.

The unusual spike in the differential pressure and/or continuous build-up of the pressures after nanoparticle flooding means that there may have been pore blocking due to nanoparticle agglomeration (Li & Torsæter, 2015). Such abnormalities in the differential pressures were not observed during any of the coreflood experiments, indicating no sign of nanoparticle agglomeration during the experiment.

The waterflooding 6-hour shut-in period did not improve oil recovery, as previously seen in Kim et al. (2017)'s results. This result is expected because SiO₂ nanoparticles changed the wettability of the core to more water-wet conditions as Sivira et al. (2017)'s results suggest. Increasing the injection rate for the second waterflooding may improve the oil recovery, however, was not experimentally examined in this study.

The pH's of the fluids initially injected, and the effluent collected at the end of each waterflooding, and nanoparticle flooding were measured. The measurements are tabulated as Table 4.4, 4.5 and 4.6 for three coreflood experiments conducted in the study.

Table 4.4 The summary of pH measurements from coreflood run 1

	Initial Waterflooding	Nanoparticle flooding	Secondary Waterflooding
Injectant	Grand Banks seawater	0.05 wt% nanofluid	Grand Banks seawater
Injectant pH	7.84	2.20	7.84
Effluent pH	6.84	7.04	7.04

Table 4.5 The summary of pH measurements from coreflood run 2

	Initial Waterflooding	Nanoparticle flooding	Secondary Waterflooding
Injectant	Grand Banks seawater	0.05 wt% nanofluid	Grand Banks seawater
Injectant pH	7.84	2.20	7.84
Effluent pH	7.82	7.96	7.97

Table 4.6 The summary of pH measurements from coreflood run 3

	Initial Waterflooding	Nanoparticle flooding	Secondary Waterflooding
Injectant	Grand Banks seawater	0.00 wt% nanofluid	Grand Banks seawater
Injectant pH	7.84	2.18	7.84
Effluent pH	6.85	6.87	7.06

The pH of the seawater injected for waterflooding was 7.84. The effluent pH collected after the initial waterflooding on Berea core was lower than the injected pH of 6.84 and 6.85. The pH after the first waterflood on Hebron core was 7.82, which has barely changed from the pH of the injected seawater. The pH of the effluent after the first waterflood seems to be affected by the type of the cores, since the effluent pH's from the Berea cores are relatively the same, but not the Hebron core. This may be attributed to the release of fines in Berea sandstone when seawater is injected (Kia, Fogler, & Reed, 1987), which would release acidic cations in the sandstone, such as Al^{3+} and Fe^{3+} . The SEM analysis and MLA is needed to find the exact composition of the Hebron core used, to explain why the pH of the effluent has not changed compared to the seawater injected. The pH of the 0.05 wt% SiO_2 nanofluid injected for nanoparticle flooding was 2.20. The pH of the seawater/HCl mixture containing the same HCl concentration as 0.05 wt% nanofluid, but without the nanoparticles was 2.18. The pH's of the effluents from the nanoparticle floodings and HCl flood were neutral, with pH ranging between 6.87 to 7.96, even though acidic fluids were injected. The likely reason for this is because acidic injectants became diluted with seawater that was previously injected. The pH's of the effluents after the second waterflooding that followed nanoparticle flooding on both Berea and Hebron cores remained constant. The effluent pH of the second waterflooding after seawater/HCl mixture was 7.06. This pH is slightly higher than the effluent pH from seawater/HCl flooding. This may be due to the ion exchange between the free H^+ ions with the clay minerals. The H^+ is known to readily adsorb onto the sandstone surfaces (Austad, Rezaeidoust, & Puntervold, 2010), which would in turn increase the pH because there are less H^+ in the solution. The effluent pH increase was not observed after 0.05 wt%

nanoparticle flooding, and this could be because of the presence of SiO₂ nanoparticles, preventing free H⁺ from adsorbing on to the rock surface. The detailed discussion for these differences would require further investigation, involving instrumentation, and understanding of the SiO₂ nanoparticle-oil-rock interaction in the nanoscale. It would also help to measure the pH of the effluent after every 1 PV injected, instead of measuring at the end of each flooding as performed here.

The nature of the coreflooding experiment makes it difficult to repeat the experiment on the same core. This is because enhanced oil recovery methods aim to change the properties of the fluid-rock and/or fluid-fluid interactions, and therefore the rock properties may have been irreversibly altered after running an experiment on a given core sample. Though coreflood experiments presented here cannot be duplicated, the validity of the results can be justified by comparing the initial waterflooding. All Berea sandstone cores used in this experiment, as well as the coreflooding presented in Kim et al. (2017)'s paper, were prepared the same way. The seawater used for the waterflooding were from the same batch, and the injection scheme was identical as well. Therefore, given the homogeneity of Berea sandstone cores, the oil recovery factor from the initial waterflooding would be expected to be similar, if not the same. The results from the initial waterflooding on Berea sandstone cores are agreeable across the coreflood experiments (including the ones presented in this paper and Kim et al. (2017)), with the maximum difference of 2.2%.

4.5. Conclusions

The coreflood experiments were conducted at Hebron Field pressure and temperature using 0.05 wt% silicon dioxide (SiO_2) nanofluid on Berea sandstone core and Hebron core. The effect of hydrochloric acid (HCl) in the nanofluid on the oil recovery is also studied. The summary of the findings is:

- Out of 0.01, 0.03, and 0.05 wt% SiO_2 nanofluid, the attained oil recovery was 58.9, 69.0, and 65.6%, respectively upon coreflood experiments on Berea sandstone cores. The highest concentration (0.05 wt% nanofluid) gave the highest oil recovery (65.6%).
- The coreflood experiment using 0.05 wt% nanofluid on Hebron field core gave total oil recovery of 61.6%, with 12.9% incremental oil recovery. This experiment emulated the offshore reservoir conditions as closely as possible – from the temperature, pressure, core, oil, injecting fluids, and nanoparticle dispersant. The positive impact of SiO_2 nanofluid at these conditions brings a step closer to implementing SiO_2 nanoparticles for enhanced oil recovery techniques.
- The HCl in the nanofluid has minimal effect on the oil recovery from the cores with low carbonate content, and the nanoparticle is a key player in increasing the oil recovery on cores mostly composed of quartz.

Acknowledgements

The authors would like to thank Chevron Canada, Hibernia Management and Development Company (HMDC), Research and Development Corporation of Newfoundland and Labrador (RDC), Natural Sciences and Engineering Research Council of Canada (NSERC), and the Canadian Foundation for Innovation (CFI) for financial support. We thank our colleagues in the Hibernia EOR Research Group for the technical support.

References

Aurand, K. R., Dahle, G. S., & Torsæter, O. (2014). Comparison of Oil Recovery for Six Nanofluids in Berea Sandstone Cores. *International Symposium of the Society of Core Analysts*, 1–12.

Austad, T., Rezaeidoust, A., & Puntervold, T. (2010). Chemical Mechanism of Low Salinity Water Flooding in Sandstone Reservoirs. *SPE*, 129767(September), 19–22. <https://doi.org/10.2118/129767-MS>

CNLOPB. (2011). *Hebron Development Plan*.

Retrieved from <http://www.cnlopb.ca/pdfs/conhebdevplan.pdf?lbisphpreq=1>

Kia, S. F., Fogler, H. S., & Reed, M. G. (1987). Effect of pH on Colloidally Induced Fines Migration. *Journal of Colloid and Interface Science* (Vol. 118). [https://doi.org/10.1016/0021-9797\(87\)90444-9](https://doi.org/10.1016/0021-9797(87)90444-9)

Kim, H., Sivira, D., James, L., & Zhang, Y. (2017). Experimental Investigation of EOR by Injecting SiO₂ Nanoparticles as Water Additive with Application to the Hebron Field. <https://doi.org/10.3997/2214-4609.201700234>

Li, S., & Torsæter, O. (2015). The impact of nanoparticles adsorption and transport on wettability alteration of water wet berea sandstone. *Society of Petroleum Engineers - SPE/IATMI Asia Pacific Oil and Gas Conference and Exhibition, APOGCE 2015*.

Metin, C. O., Lake, L. W., Miranda, C. R., & Nguyen, Q. P. (2011). Stability of Aqueous Silica Nanoparticle Dispersions. *Journal of Nanoparticle Research*, 13(2), 839–850. <https://doi.org/10.1007/s11051-010-0085-1>

Nazari Moghaddam, R., Bahramian, A., Fakhroueian, Z., Karimi, A., & Arya, S. (2015). Comparative Study of Using Nanoparticles for Enhanced Oil Recovery: Wettability Alteration of Carbonate Rocks. *Energy & Fuels*, 29(4), 2111–2119. <https://doi.org/10.1021/ef5024719>

Roustaei, A., Moghadasi, Jamshid Bagherzadeh, H., & Shahrabadi, A. (2012). An Experimental Investigation of Polysilicon Nanoparticles' Recovery Efficiencies Through Changes in Interfacial Tension and Wettability Alteration. *SPE International Oilfield Nanotechnology Conference, Noordwijk, Netherlands*, 200–206. <https://doi.org/10.2118/156976-MS>

Sivira, D., Kim, H. B., James, L., Johansen, T., & Zhang, Y. (2016). The Effectiveness of Silicon Dioxide SiO₂ Nanoparticle as an Enhanced Oil Recovery Agent in Ben Nevis Formation, Hebron Field, Offshore Eastern Canada. *Society of Petroleum Engineers*.

Sivira, D., Kim, H. B., James, L., Wilton, D., & Zhang, Y. (2017). Fluid-Rock Interaction between Silicon Dioxide (SiO₂) Nanoparticle and Standard Cores Mimicking Hebron Field Conditions for Enhanced Oil Recovery Application. *EAGE 19th European Symposium on Improved Oil Recovery*.

Sripal, E., & James, L. A. (2016). Application of an Optimization Method for Restoration of Core Samples for Scal Experiments. *Society of Core Analysts*, 1–12.

Stosur, G. J., Hite, J. R., Carnahan, N. F., & Miller, K. (2003). The Alphabet Soup of IOR, EOR and AOR: Effective Communication Requires a Definition of Terms. *SPE*

International Improved Oil Recovery Conference in Asia, SPE 84908, 1–3.
<https://doi.org/10.2118/84908-MS>

Valencia, L., James, L. A., & Azmy, K. (2017). *Implications of the Diagenetic History on Enhanced Oil Recovery (EOR) Performance for the Ben Nevis Formation, Hebron Field, Jeanne D'arc Basin, Offshore, Newfoundland, Canada.* Memorial University.

Chapter 5. Concluding Remarks

5.1. Summary

The enhanced oil recovery research using silicon dioxide nanoparticles has been growing in the laboratory scale because silicon dioxide nanoparticles are environmentally friendly; and have positive impact on the oil recovery. The nanoparticle enhanced oil recovery method in the offshore Hebron Field faces a major challenge, which is stabilizing nanoparticles in the seawater. The silicon dioxide nanoparticles are highly susceptible to magnesium ions (Mg^{2+}), and the nanoparticles agglomerate immediately when added to the seawater. The agglomerated nanoparticles could potentially block the pores of the rock, impairing permeability. There was a need to evaluate the effectiveness of silicon dioxide nanoparticles dispersed in seawater on the oil recovery, as previous laboratory coreflood studies found in the literature (Aurand et al., 2014; Hendraningrat & Li, 2013; Nazari Moghaddam et al., 2015) had dispersed nanoparticles in a simple sodium chloride solution.

The hydrochloric acid was suggested as a silicon dioxide nanoparticle stabilizer because it is widely available, and is cost-effective. The best method to prepare nanoparticle suspension in seawater using hydrochloric acid was to mix nanoparticles and hydrochloric acid first, then to add seawater. The higher hydrochloric acid to nanoparticle ratio was required with increasing concentrations of nanoparticles to stabilize the 0.05 wt% nanoparticle suspension in seawater. For example, a system with 0.003 ratio between hydrochloric acid to nanoparticle ratio was unstable, whereas the system with ratios of

0.02 and 0.06 were stable. The higher hydrochloric acid to nanoparticle ratio is also required to keep nanoparticles stable over time with increasing temperature. The 0.05 wt% nanofluid with HCl to nanoparticle ratio of 0.12 became unstable within a day at 62 °C, whereas the nanoparticles were stable up to 14-days for nanofluids with ratios higher than 0.46.

The coreflood experiments were performed with nanofluids that has HCl to nanoparticle ratio of 0.46 because nanoparticle stability study at 62 °C showed that the nanoparticles would remain stable at this ratio for longer than the duration of the experiment. The purpose of the coreflood experiment was to investigate whether the nanoparticles can increase the oil recovery when injected as a tertiary recovery method. The experiments were conducted at Hebron Field temperature (62 °C) and pressure (19.0 MPa). Table 5.1 below summarizes coreflood experiment results.

Table 5.1 Summary of coreflooding experiment results

Results Found in	Core Type	Nanofluid Conc.	Oil Recovery (%)			
			Initial Waterflooding	Nanoparticle flooding	Secondary Waterflooding	Total
Chapter 3	Berea	0.01 wt%	55.6	3.3	0.0	58.9
Chapter 3	Berea	0.03 wt%	56.3	9.3	0.0	65.6
Chapter 4	Berea	0.05 wt%	54.1	14.9	0.0	69.0
Chapter 4	Hebron	0.05 wt%	49.7	11.9	0.0	56.5
Chapter 4	Berea	0.00 wt%	55.5	1.0	0.0	61.6

Berea sandstone cores were used to investigate the effect of 0.01, 0.03 and 0.05 wt% silicon dioxide nanofluids on the oil recovery. The incremental oil recovery increased

with increasing nanoparticle concentration. The increments using 0.01, 0.03 and 0.05 wt% nanofluids were 3.3, 9.3, and 14.9%, respectively. The coreflood experiment on the Hebron core was also performed, and the incremental oil recovery was 11.9%. The 0.05 wt% nanofluid was used for Hebron core coreflood because 0.05 wt% nanofluid gave the highest recovery on the Berea coreflood experiments. All the coreflood experiments performed in this research proved the positive impact of silicon dioxide nanoparticles on the oil recovery. The hydrochloric acid in the nanofluid had minimal effect on the incremental oil recovery because using hydrochloric acid with seawater only (without the nanoparticles) merely achieved 1.0% of additional oil recovery.

5.2. Lessons Learned and Future Recommendations

5.2.1. SiO₂ Nanoparticle Stability

The Mg²⁺ cations are found to affect SiO₂ nanoparticle stability, and for the same reasons, Ca²⁺ cations in the seawater are likely to have similar effect on the stability. Although the Ca²⁺ concentration (379 ppm) in seawater is approximately 3.5 times lower than that of Mg²⁺ (1323 ppm), it would be interesting to compare the effect of Ca²⁺ to the effect of Mg²⁺ on the SiO₂ nanoparticle stability.

The duration of the nanoparticle stability in seawater will need to be in the scale of years, rather than days, for the real application of the nanoparticle enhanced oil recovery in the offshore field. The optimal hydrochloric acid concentration may need to be adjusted to achieve desired stability over the years. Further investigation on the nanoparticle stability,

such as looking into ways of modifying the surface of the nanoparticles; and searching new types of stabilizer could also be helpful.

5.2.2. Optimization of SiO₂ Nanoparticle Concentration

The nanoparticle concentration studied for the coreflood experiments were limited to 0.01, 0.03 and 0.05 wt%. This was based on the literature review earlier on in the project. The nanoparticle concentrations can be increased to see if it will result in a higher incremental oil recovery, without blocking the pores of the rocks impairing the permeability.

5.2.3. Coreflooding Experiments

To better emulate the Hebron Field conditions, coreflood experiments are recommended using Hebron crude oil, now that is more accessible. More coreflooding experiments should be run on Hebron cores, as it becomes available, to further evaluate suitability of nanoparticle enhanced oil recovery at Hebron Field.

The nanoparticle stabilizer, HCl had little effect on the oil recovery on the Berea sandstone core, however HCl may play a more significant role in the rocks with higher carbonate content. The effect of HCl on the standard cores with higher carbonate content is recommended.

The effluent pH measurements during the coreflooding experiments are recommended to be taken after every pore volume injected, to better understand the fluid-rock interactions.

This study focused on the use of nanoparticles as a tertiary recovery method. It would be interesting to run experiments as secondary recovery method, and compare the results.

5.2.4. Nanoparticle Retention due to Adsorption

The nanoparticles adsorption on the core is possible, and the degree of adsorption should be investigated for the economy of nanoparticle flooding. SEM/MLA on the core, as well as ICP-OES analysis on the effluent were performed in attempts to measure the retention of nanoparticles. However, it was extremely difficult to locate nanoparticles on a microscope given the size of the core. In addition, ICP instrument was unable to detect the nanoparticles due to the equipment limitation; as well as cross-contamination of the sample as silicon is abundantly present in glassware, and vials used to transport samples and to introduce to the ICP equipment. Alternatively, the output amount of the nanoparticle over time could be analyzed by injecting several pore volumes of nanofluid into a clean core by mass balance.

5.2.5. Nanoparticle Enhanced Oil Recovery Mechanisms

The coreflood experiments show that the SiO₂ nanofluids increase the oil recovery, however, it sheds very little light on “how”. The follow-up experiments that delves into understanding the mechanisms are needed. They can be (but not limited to) nanoparticle mass balance before/after coreflood; and SEM analysis to verify whether the nanoparticle preferentially adsorb onto the minerals in the rock.

Bibliography

Agzamkhodzhaev, A., Zhuravlev, L., Kiselev, A., & Shengeliya, K. (1969). Concentration of hydroxyl groups on the surface and in the volume of silicas. *Bulletin of the Academy of Sciences of the USSR, Division of Chemical Science*, 18(10), 1968–1973. <https://doi.org/10.1007/BF00906604>

Ahmadi, M., Habibi, A., Pourafshry, P., & Ayatollahi, S. (2011). Zeta Potential Investigation and Mathematical Modeling of Nanoparticles Deposited on the Rock Surface to Reduce Fine Migration. *Society of Petroleum Engineers*, pp.1-14. SPE-142633. <https://doi.org/10.2118/142633-ms>

Al-Anssari, S., Barifcani, A., Wang, S., Maxim, L., & Iglauer, S. (2016). Wettability Alteration of Oil-Wet Carbonate by Silica Nanofluid. *Journal of Colloid and Interface Science*, 461, 435–442. <https://doi.org/10.1016/j.jcis.2015.09.051>

Atkins, P. W., & Atkins, P. W. (2006). *Shriver & Atkins inorganic chemistry*. Oxford; New York; New York: Oxford University Press ; W.H. Freeman and Co.

Aurand, K. R., Dahle, G. S., & Torsæter, O. (2014). Comparison of Oil Recovery for Six Nanofluids in Berea Sandstone Cores. *International Symposium of the Society of Core Analysts*, 1–12.

Ayatollahi, S. (2012). Nanotechnology-Assisted EOR Techniques: New Solutions to Old Challenges, 12–14.

Bergna, H. (2005). Colloid Chemistry of Silica. In *Colloidal Silica* (pp. 9–35). CRC Press. <https://doi.org/doi:10.1201/9781420028706.ch3>

Birdi, K. S. (2008). Surface and Colloid Chemistry. In *Handbook of Surface and Colloid Chemistry, Third Edition* (pp. 1–43). CRC Press. <https://doi.org/doi:10.1201/9781420007206.ch1>

CNLOPB. (2011). *Hebron Development Plan*. Retrieved from <http://www.cnlopb.ca/pdfs/conhebddevplan.pdf?lbisphpreq=1>

Comas-Vives, A. (2016). Amorphous SiO₂ surface models: energetics of the dehydroxylation process, strain, ab initio atomistic thermodynamics and IR spectroscopic signatures. *Physical Chemistry Chemical Physics: PCCP*, 18(10), 7475–82. <https://doi.org/10.1039/c6cp00602g>

Derjaguin, B. V., & Landau, L. (1941). Colloidal stability of protein-polymer systems: A possible explanation by hydration forces. *Acta Physiocochim USSR*, 14, 663.

Devendiran, D. K., & Amirtham, V. A. (2016). A review on preparation, characterization, properties and applications of nanofluids. *Renewable and Sustainable Energy Reviews*, 60, 21–40. <https://doi.org/10.1016/j.rser.2016.01.055>

Donaldson, E. C., Chilingar, G. V., & Yen, T. F. (1985). *Enhanced oil recovery. I, Fundamentals and analysis*. Elsevier.

El-diasty, A. I., & Aly, A. M. (2015). Understanding the Mechanism of Nanoparticles Applications in Enhanced Applications of Nanoparticles in EOR. *Paper SPE 175806 - North Africa Technical Conference (Cairo / Egipto)*, 0, 1–19. <https://doi.org/10.2118/175806-MS>

Engeset, B. (2012). The Potential of Hydrophilic Silica Nanoparticles for EOR Purposes. *Norwegian University of Science and Technology*, (May).

Green, D. W. (1998). *Enhanced oil recovery*. (G. P. Willhite & P. (Firm), Eds.). Richardson, TX: Richardson, TX: Henry L. Doherty Memorial Fund of AIME, Society of Petroleum Engineers.

Hendraningrat, L., Engeset, B., Suwarno, S., & Torsæter, O. (2012). Improved Oil Recovery by Nanofluids Flooding: An Experimental Study. *SPE Kuwait International Petroleum Conference and Exhibition*, (2006), SPE 163335.

<https://doi.org/10.2118/163335-MS>

Hendraningrat, L., Li, S., & Torsæter, O. (2013). A Coreflood Investigation of Nanofluid Enhanced Oil Recovery. *Journal of Petroleum Science and Engineering*, *111*, 128–138. <https://doi.org/10.1016/j.petrol.2013.07.003>

Hendraningrat, L., & Torsæter, O. (2014). Understanding Fluid-Fluid and Fluid-Rock Interactions in the Presence of Hydrophilic Nanoparticles at Various Conditions. *SPE Asia Pacific Oil & Gas Conference and Exhibition*, (2011).

Hendraningrat, L., & Torsæter, O. (2014). Unlocking the Potential of Metal Oxides Nanoparticles to Enhance the Oil Recovery, (2013). <https://doi.org/10.2118/24696-MS>

Hwang, Y., Lee, J. K., Lee, C. H., Jung, Y. M., Cheong, S. I., Lee, C. G., ... Jang, S. P. (2007). Stability and thermal conductivity characteristics of nanofluids. *Thermochimica Acta*, *455*(1–2), 70–74. <https://doi.org/10.1016/j.tca.2006.11.036>

Joonaki, E., & Ghanaatian, S. (2014). The Application of Nanofluids for Enhanced Oil Recovery: Effects on Interfacial Tension and Coreflooding Process. *Petroleum Science and Technology*, *32*(21), 2599–2607. <https://doi.org/10.1080/10916466.2013.855228>

Kang, P. S., Lim, J. S., & Huh, C. (2016). Screening Criteria and Considerations of Offshore Enhanced Oil Recovery. *Energies*, *9*(1), 1–18. <https://doi.org/10.3390/en9010044>

Kissa, E. (1999). *Dispersions : characterization, testing, and measurement*. M. Dekker. Retrieved from <https://www.crcpress.com/Dispersions-Characterization-Testing-and-Measurement/Kissa/p/book/9780824719944>

Kralchevsky, P., Danov, K., & Denkov, N. (2008). Chemical Physics of Colloid Systems and Interfaces. In *Handbook of Surface and Colloid Chemistry, Third Edition* (pp. 197–377). CRC Press. <https://doi.org/doi:10.1201/9781420007206.ch7>

Mehta, S., Somasundaran, P., Yu, X., & Krishnakumar, S. (2008). Colloid Systems and

Interfaces Stability of Dispersions through Polymer and Surfactant Adsorption. In *Handbook of Surface and Colloid Chemistry, Third Edition* (pp. 155–196). CRC Press. <https://doi.org/doi:10.1201/9781420007206.ch6>

Metin, C. O., Lake, L. W., Miranda, C. R., & Nguyen, Q. P. (2011). Stability of Aqueous Silica Nanoparticle Dispersions. *Journal of Nanoparticle Research*, 13(2), 839–850. <https://doi.org/10.1007/s11051-010-0085-1>

Miranda, C. R., Lara, L. S. De, & Tonetto, B. C. (2012). Stability and Mobility of Functionalized Silica Nanoparticles for Enhanced Oil Recovery Applications. *SPE Oilfield Nanotechnology Conference*, SPE 157033. <https://doi.org/10.2118/157033-ms>

Morrow, N. R. (1990). Wettability and Its Effect on Oil Recovery. *Journal of Petroleum Technology*, 42(12), 1476–1484. <https://doi.org/10.2118/21621-PA>

Morrow, N. R., & Heller, J. P. (1985). Chapter 3 Fundamentals of Enhanced Recovery (pp. 47–74). [https://doi.org/10.1016/S0376-7361\(08\)70565-X](https://doi.org/10.1016/S0376-7361(08)70565-X)

Nazari Moghaddam, R., Bahramian, A., Fakhroueian, Z., Karimi, A., & Arya, S. (2015). Comparative Study of Using Nanoparticles for Enhanced Oil Recovery: Wettability Alteration of Carbonate Rocks. *Energy & Fuels*, 29(4), 2111–2119. <https://doi.org/10.1021/ef5024719>

Papirer, E. (2000). *Adsorption on silica surfaces*. Marcek Dekker.

Rimola, A., Costa, D., Sodupe, M., & Ugliengo, P. (2013). Silica Surface Features and Their Role in the Adsorption of Biomolecules.pdf. *Chemical Reviews*, 113, 4216–4313. <https://doi.org/10.1021/cr3003054>

Roustaei, A., Moghadasi, Jamshid Bagherzadeh, H., & Shahrabadi, A. (2012). An Experimental Investigation of Polysilicon Nanoparticles' Recovery Efficiencies Through Changes in Interfacial Tension and Wettability Alteration. *SPE International Oilfield Nanotechnology Conference, Noordwijk, Netherlands*, 200–206.

<https://doi.org/10.2118/156976-MS>

Salh, R. (2011). Defect Related Luminescence in Silicon Dioxide Network: A Review. In *Crystalline Silicon - Properties and Uses*. InTech. <https://doi.org/10.5772/22607>

Shang, J., & Gao, X. (2014). Nanoparticle counting: towards accurate determination of the molar concentration. *Chemical Society Reviews*, 43(21), 7267–7278. <https://doi.org/10.1039/c4cs00128a>

Sheng, J. (2010). *Modern Chemical Enhanced Oil Recovery: Theory and Practice*. Gulf Professional Publishing.

Sivira, D., Kim, H. B., James, L., Johansen, T., & Zhang, Y. (2016). The Effectiveness of Silicon Dioxide SiO₂ Nanoparticle as an Enhanced Oil Recovery Agent in Ben Nevis Formation, Hebron Field, Offshore Eastern Canada. *Society of Petroleum Engineers*.

Sivira, D., Kim, H. B., James, L., Wilton, D., & Zhang, Y. (2017). Fluid-Rock Interaction between Silicon Dioxide (SiO₂) Nanoparticle and Standard Cores Mimicking Hebron Field Conditions for Enhanced Oil Recovery Application. *EAGE 19th European Symposium on Improved Oil Recovery*.

Society for Mining, Metallurgy, and E. (1998). *Crystalline silica*. Society for Mining, Metallurgy, and Exploration.

Stosur, G. J., Hite, J. R., Carnahan, N. F., & Miller, K. (2003). The Alphabet Soup of IOR, EOR and AOR: Effective Communication Requires a Definition of Terms. *SPE International Improved Oil Recovery Conference in Asia*, SPE 84908, 1–3. <https://doi.org/10.2118/84908-MS>

Sulpizi, M., Gageot, M.-P., & Sprik, M. (2012). The Silica–Water Interface: How the Silanols Determine the Surface Acidity and Modulate the Water Properties. *Journal of Chemical Theory and Computation*, 8(3), 1037–1047. <https://doi.org/10.1021/ct2007154>

Sun, X., Zhang, Y., Chen, G., & Gai, Z. (2017). Application of nanoparticles in enhanced

oil recovery: A critical review of recent progress. *Energies*, 10(3).
<https://doi.org/10.3390/en10030345>

Valencia, L., James, L. A., & Azmy, K. (2017). *Implications of the Diagenetic History on Enhanced Oil Recovery (EOR) Performance for the Ben Nevis Formation, Hebron Field, Jeanne D'arc Basin, Offshore, Newfoundland, Canada*. Memorial University.

Verwey, E. J. W. (1947). Theory of the stability of lyophobic colloids. *The Journal of Physical and Colloid Chemistry*, 51(3), 631–636. <https://doi.org/10.1038/162315b0>

Zhuravlev, L. T. (2000). The surface chemistry of amorphous silica. Zhuravlev model. *Colloids and Surfaces A: Physicochemical and Engineering Aspects*, 173(1–3), 1–38.
[https://doi.org/10.1016/S0927-7757\(00\)00556-2](https://doi.org/10.1016/S0927-7757(00)00556-2)

Appendices

Appendix A. Standard Deviations of Silicon Dioxide Nanoparticle Particle Size Measurements

Experiment 1: Effect of Salt Ions on the Stability of Silicon Dioxide Nanoparticles

Sodium Chloride (NaCl)

Na ⁺ Concentration (ppm)	Particle Size (nm)	Standard Deviation (nm)
2500	20.59	0.10
5000	23.06	0.09
20000	19.86	0.22
30000	21.83	0.18
50000	23.65	0.13

Sodium Sulfate (Na₂SO₄)

Na ⁺ Concentration (ppm)	Particle Size (nm)	Standard Deviation (nm)
2500	21.82	0.08
5000	19.58	0.21
20000	20.78	0.21
30000	21.46	0.09
50000	24.86	0.03

Magnesium Chloride Hexahydrate (MgCl₂·6H₂O)

Na ⁺ Concentration (ppm)	Particle Size (nm)	Standard Deviation (nm)
500	26.47	0.10
1000	120.6	1.98

Magnesium Chloride Hexahydrate (MgCl₂·6H₂O)

Na ⁺ Concentration (ppm)	Particle Size (nm)	Standard Deviation (nm)
500	24.48	0.15
1000	151.17	17.48

Experiment 2: Silicon Dioxide Nanofluid Preparation Method

Method 1 (SiO₂ + HCl + Seawater)

HCl to SiO ₂ Ratio	Particle Size (nm)	Standard Deviation (nm)
0.02	25.01	0.05
0.06	24.09	0.19
0.12	23.52	0.12
0.36	21.43	0.29
0.46	20.81	0.12
0.60	20.48	0.14

Method 2 (Seawater + HCl + SiO₂)

HCl to SiO ₂ Ratio	Particle Size (nm)	Standard Deviation (nm)
0.02	33.64	0.18
0.06	34.86	0.18
0.12	31.70	0.14
0.36	28.02	0.31
0.46	27.15	0.14
0.60	30.72	0.17

Method 3 (SiO₂ + Seawater + HCl)

HCl to SiO ₂ Ratio	Particle Size (nm)	Standard Deviation (nm)
0.02	31.81	0.10
0.06	32.90	0.09
0.12	25.29	0.16
0.36	24.58	0.23
0.46	24.19	0.30
0.60	23.57	0.08

Experiment 3: Hydrochloric Acid to Silicon Dioxide Nanoparticle Ratio on the Nanoparticle Stability

HCl Concentration (wt%)	SiO ₂ Concentration (wt%)	HCl to SiO ₂ Ratio	Particle Size (nm)	Standard Deviation (nm)
0.001	0.05	0.02	25.41	0.05033
0.001	0.15	0.007	36.22	0.4102
0.001	0.30	0.003	*	*
0.003	0.05	0.06	24.09	0.1947
0.003	0.15	0.02	25.44	0.2427
0.003	0.30	0.01	34.50	0.4571

* Unmeasurable due to severe agglomeration

Experiment 4: Silicon Dioxide Nanoparticle Stability at Room Temperature

Room Temperature at 1 Hour

HCl to SiO ₂ Ratio	Particle Size (nm)	Standard Deviation (nm)
0.12	23.96	0.15
0.18	27.56	0.15
0.24	23.44	0.27
0.46	20.97	0.21
0.60	27.42	0.53

Room Temperature at 1 Day

HCl to SiO ₂ Ratio	Particle Size (nm)	Standard Deviation (nm)
0.12	27.84	0.29
0.18	23.26	0.03
0.24	24.65	0.44
0.46	21.50	0.28
0.60	26.31	0.42

Room Temperature at 2 Days

HCl to SiO ₂ Ratio	Particle Size (nm)	Standard Deviation (nm)
0.12	34.88	0.36
0.18	24.53	0.12
0.24	25.01	0.45
0.46	22.50	0.31
0.60	25.89	0.38

Room Temperature at 3 Days

HCl to SiO ₂ Ratio	Particle Size (nm)	Standard Deviation (nm)
0.12	35.90	0.50
0.18	24.61	0.48
0.24	27.48	0.20
0.46	29.70	1.42
0.60	29.02	0.59

Room Temperature at 6 Days

HCl to SiO ₂ Ratio	Particle Size (nm)	Standard Deviation (nm)
0.12	53.25	0.21
0.18	26.38	0.62
0.24	29.28	0.11
0.46	25.79	0.40
0.60	25.94	0.57

Room Temperature at 8 Days

HCl to SiO ₂ Ratio	Particle Size (nm)	Standard Deviation (nm)
0.12	73.49	1.19
0.18	26.91	0.90
0.24	29.11	0.51
0.46	23.31	0.41
0.60	28.56	0.29

Room Temperature at 10 Days

HCl to SiO ₂ Ratio	Particle Size (nm)	Standard Deviation (nm)
0.12	85.84	1.18
0.18	27.49	0.53
0.24	30.32	0.40
0.46	23.29	0.65
0.60	26.88	0.26

Room Temperature at 14 Days

HCl to SiO ₂ Ratio	Particle Size (nm)	Standard Deviation (nm)
0.12	116.30	1.01
0.18	28.19	0.46
0.24	33.17	2.40
0.46	22.53	0.19
0.60	24.33	0.30

Experiment 4: Silicon Dioxide Nanoparticle Stability at 60°C over time

At 1 Hour, 62 °C

HCl to SiO ₂ Ratio	Particle Size (nm)	Standard Deviation (nm)
0.12	23.96	0.15
0.18	27.56	0.15
0.24	23.44	0.27
0.46	20.97	0.21
0.60	27.42	0.53

1 Day at 62 °C

HCl to SiO ₂ Ratio	Particle Size (nm)	Standard Deviation (nm)
0.12	89.31	0.83
0.18	25.89	0.25
0.24	24.32	0.43
0.46	20.87	0.16
0.60	25.50	0.42

2 Days at 62 °C

HCl to SiO ₂ Ratio	Particle Size (nm)	Standard Deviation (nm)
0.12	294.4	1.37
0.18	23.53	0.42
0.24	25.28	1.12
0.46	20.98	0.35
0.60	22.90	0.23

3 Days at 62 °C

HCl to SiO ₂ Ratio	Particle Size (nm)	Standard Deviation (nm)
0.12	*	*
0.18	26.6	0.09
0.24	27.77	0.53
0.46	21.86	0.27
0.60	25.43	0.33

* Unmeasurable due to severe agglomeration

6 Days at 62 °C

HCl to SiO ₂ Ratio	Particle Size (nm)	Standard Deviation (nm)
0.12	*	*
0.18	30.45	0.69
0.24	34.05	0.62
0.46	22.09	0.55
0.60	25.12	0.42

* Unmeasurable due to severe agglomeration

8 Days at 62 °C

HCl to SiO ₂ Ratio	Particle Size (nm)	Standard Deviation (nm)
0.12	*	*
0.18	35.43	0.28
0.24	39.07	1.85
0.46	22.42	0.04
0.60	24.01	0.99

* Unmeasurable due to severe agglomeration

10 Days at 62 °C

HCl to SiO ₂ Ratio	Particle Size (nm)	Standard Deviation (nm)
0.12	*	*
0.18	38.69	0.39
0.24	43.66	2.03
0.46	22.41	0.08
0.60	24.28	1.92

* Unmeasurable due to severe agglomeration

14 Days at 62 °C

HCl to SiO ₂ Ratio	Particle Size (nm)	Standard Deviation (nm)
0.12	*	*
0.18	39.21	0.55
0.24	46.70	1.15
0.46	26.25	0.32
0.60	23.98	0.40

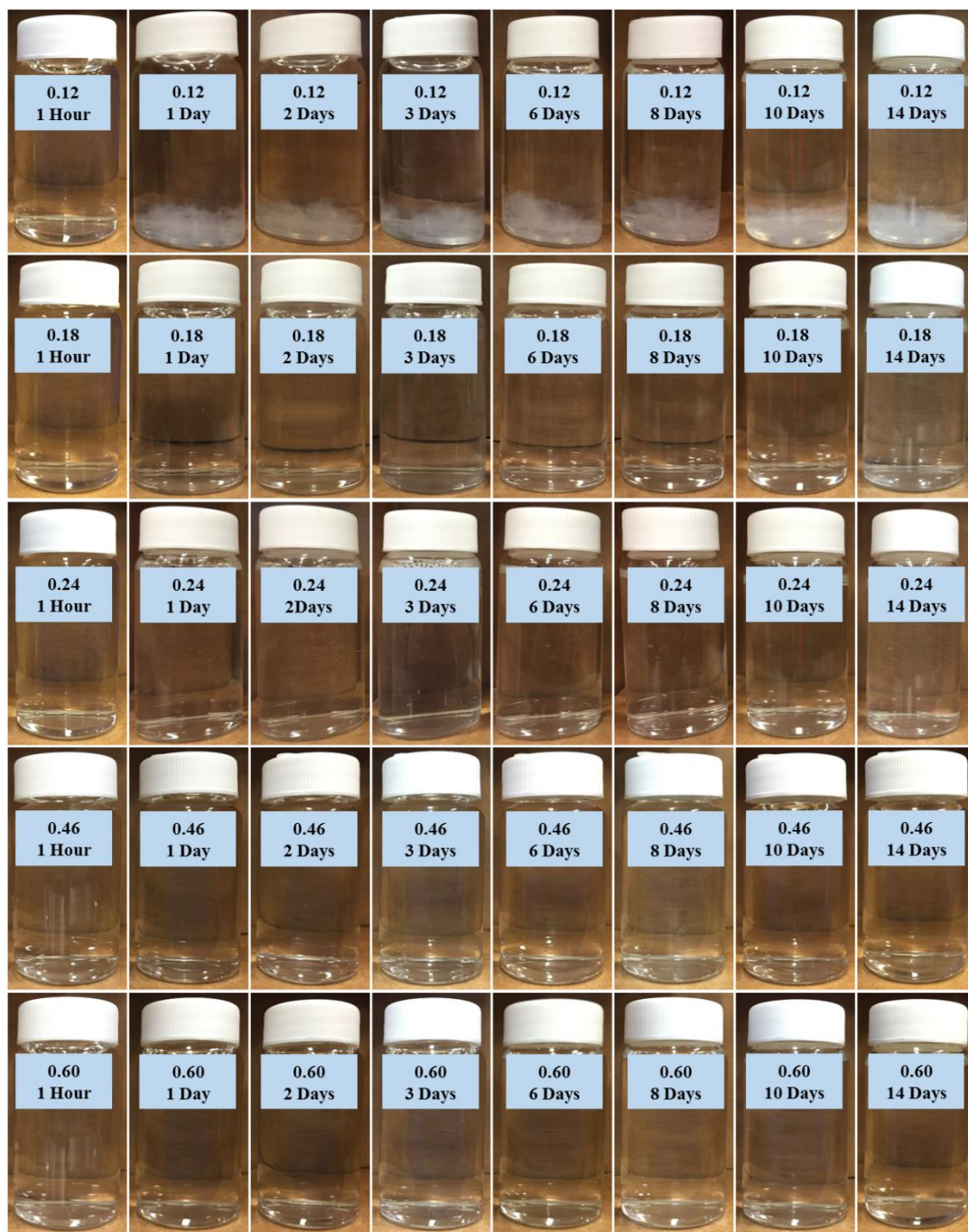
* Unmeasurable due to severe agglomeration

Appendix B. Visual Examination of 0.05 wt% Silicon Dioxide Nanoparticles, with Hydrochloric to Nanoparticle Ratios 0.12, 0.18, 0.24, 0.46, and 0.60, over 14-Day Period at Room Temperature and 62 °C

Room Temperature

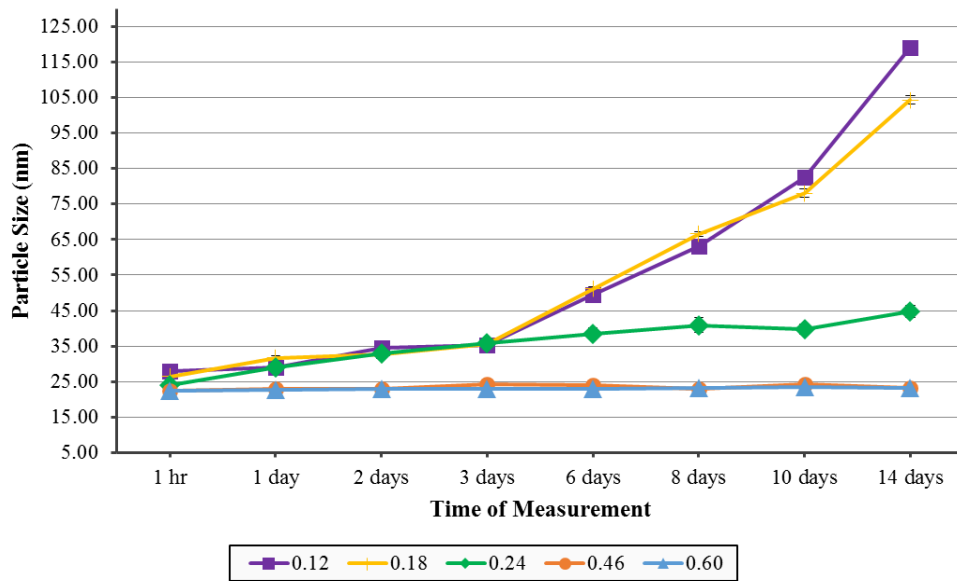


At 62 °C

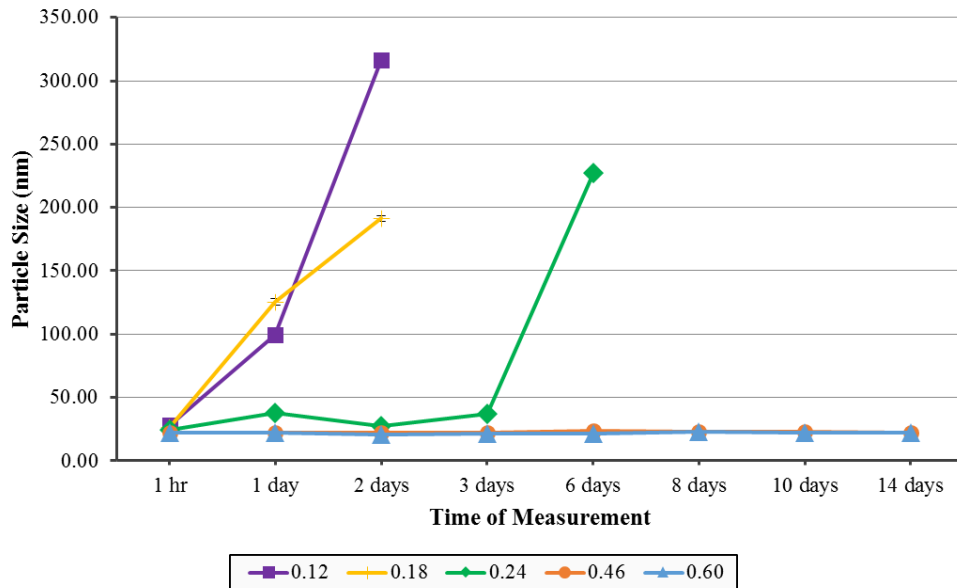


Appendix C. 0.03 wt% Silicon Dioxide Nanoparticle Size Measurements at Room Temperature and at 62 °C with Hydrochloric Acid to Silicon Dioxide Ratio Ranging from 0.12 to 0.60

Room Temperature



At 62 °C



Appendix D. Visual Examination of 0.03 wt% Silicon Dioxide Nanoparticles, with Hydrochloric to Nanoparticle Ratios 0.12, 0.18, 0.24, 0.46, and 0.60, over 14-Day Period at Room Temperature and 62 °C

Room Temperature



At 62 °C



Appendix E. Visual Examination of 0.01 wt% Silicon Dioxide Nanoparticles, with Hydrochloric to Nanoparticle Ratios 0.12, 0.18, 0.24, 0.46, and 0.60, over 14-Day Period at Room Temperature and 62 °C

Room Temperature



At 62 °C



* Note: The particle size measurements of 0.01 wt% silicon dioxide nanoparticles were inaccurate due to the equipment detection limit, hence only the visual examination pictures are presented.

Appendix F. Determination of Core Porosity

Description of Experiment	Type	Length	Diameter	Area of Cross Section	Dry Weight	Wet Weight	Pore Volume	Bulk Volume	Porosity
		(cm)	(cm)	(cm ²)	(g)	(g)	(cm ³ or mL)	(cm ³ or mL)	%
0.01 wt% nanoparticle flooding	Berea	10.18	3.81	11.4	245.769	265.690	19.92	116.06	0.172
0.03 wt% nanoparticle flooding	Berea	10.10	3.81	11.4	242.7371	263.582	20.84	115.15	0.181
0.05 wt% nanoparticle flooding	Berea	9.91	3.81	11.4	239.1125	258.824	19.71	112.98	0.174
HCl flooding	Berea	10.12	3.81	11.4	239.2621	259.881	20.62	115.38	0.179
0.05 wt% nanoparticle flooding	Hebron	10.51	3.79	11.2	244.3825	266.8579	22.48	118.57	0.190

Appendix G. Sample Porosity Calculation using Berea core used for 0.01 wt% nanoparticle flooding

$$\begin{aligned}\text{Area of Cross Section} &= \pi \times \left(\frac{\text{Diameter}}{2}\right)^2 = \pi \times \left(\frac{3.81\text{cm}}{2}\right)^2 \\ &= 11.4\end{aligned}$$

$$\begin{aligned}\text{Bulk Volume} &= \text{Length} \times \text{Area of Cross Section} = 11.18 \text{ cm} \times 11.4 \text{ cm}^2 \\ &= 116.06 \text{ cm}^3\end{aligned}$$

$$\begin{aligned}\text{Pore Volume} &= \frac{\text{Wet Weight} - \text{Dry Weight}}{\text{Density of Water}} = \frac{265.690\text{g} - 245.769 \text{ g}}{0.9982 \text{ g/cm}^3} \\ &= 19.92 \text{ cm}^3\end{aligned}$$

$$\begin{aligned}\text{Porosity} &= \frac{\text{Pore Volume}}{\text{Bulk Volume}} = \frac{19.92 \text{ cm}^3}{116.06 \text{ cm}^3} \\ &= 0.172\end{aligned}$$

Appendix H. Sample Calculations to Generate Oil Recovery Graphs from the Coreflood Experiments

Calculation shown for Berea core used for 0.01 wt% nanoparticle flooding

$$\begin{aligned}\text{Pore Volume Injected} &= \frac{\text{Cumulative Volume Injected}}{\text{Core Pore Volume}} = \frac{2.0 \text{ mL}}{19.92 \text{ mL}} \\ &= 0.10\end{aligned}$$

$$\begin{aligned}\% \text{ Oil Recovery} &= \frac{\text{Cumulative Oil Produced}}{(\text{Pore Volume} \times \text{Oil Saturation})} \times 100\% \\ &= \frac{0.7 \text{ mL}}{19.92 \text{ mL} \times 0.75} \times 100\% \\ &4.69\end{aligned}$$

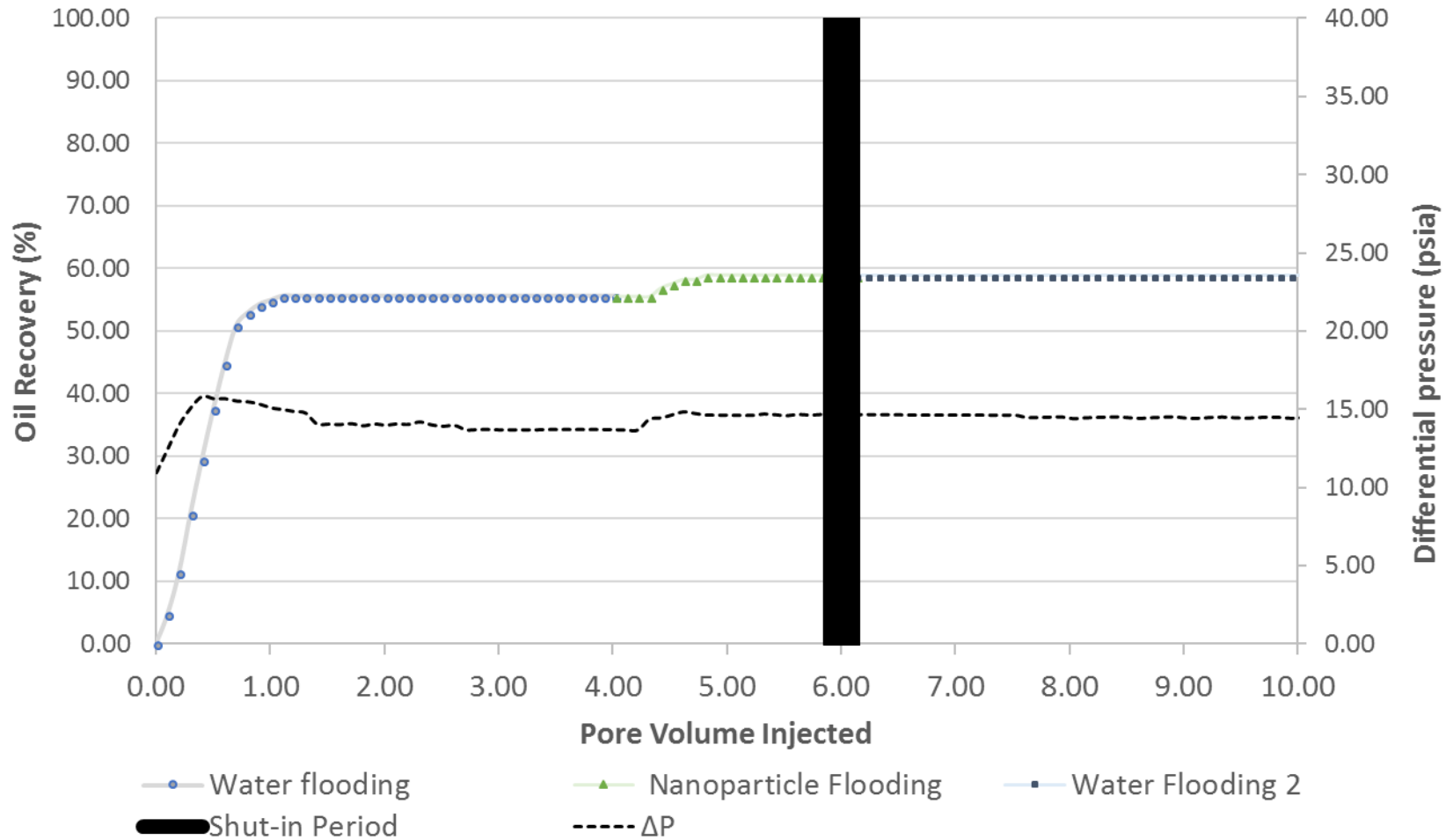
Appendix I. Coreflood Experiment Using 0.01 wt% Nanofluid on Berea Sandstone Raw Data

Injection Type	Volume Injected (per min) mL	Cumulative Volume injected mL	Pore Volume Injected mL	Total Pore Volume Injected	Cumulative Oil Produced mL	% Oil Recovery	ΔP psia
seawater	0.0	0.0	0.00	0.00	0.0	0.00	10.92
seawater	2.0	2.0	0.10	0.10	0.7	4.69	12.48
seawater	2.0	4.0	0.20	0.20	1.7	11.38	14.02
seawater	2.0	6.0	0.30	0.30	3.1	20.75	15.10
seawater	2.0	8.0	0.40	0.40	4.4	29.45	15.82
seawater	2.0	10.0	0.50	0.50	5.6	37.48	15.67
seawater	2.0	12.0	0.60	0.60	6.7	44.84	15.67
seawater	2.0	14.0	0.70	0.70	7.6	50.87	15.52
seawater	2.0	16.0	0.80	0.80	7.9	52.88	15.47
seawater	2.0	18.0	0.90	0.90	8.1	54.21	15.32
seawater	2.0	20.0	1.00	1.00	8.2	54.88	15.08
seawater	2.0	22.0	1.10	1.10	8.3	55.55	14.98
seawater	2.0	24.0	1.20	1.20	8.3	55.55	14.85
seawater	2.0	26.0	1.31	1.31	8.3	55.55	14.75
seawater	2.0	28.0	1.41	1.41	8.3	55.55	14.05
seawater	2.0	30.0	1.51	1.51	8.3	55.55	14.04
seawater	2.0	32.0	1.61	1.61	8.3	55.55	14.01
seawater	2.0	34.0	1.71	1.71	8.3	55.55	14.07
seawater	2.0	36.0	1.81	1.81	8.3	55.55	13.93
seawater	2.0	38.0	1.91	1.91	8.3	55.55	14.05
seawater	2.0	40.0	2.01	2.01	8.3	55.55	13.97
seawater	2.0	42.0	2.11	2.11	8.3	55.55	14.06
seawater	2.0	44.0	2.21	2.21	8.3	55.55	14.02
seawater	2.0	46.0	2.31	2.31	8.3	55.55	14.18
seawater	2.0	48.0	2.41	2.41	8.3	55.55	13.99
seawater	2.0	50.0	2.51	2.51	8.3	55.55	13.90
seawater	2.0	52.0	2.61	2.61	8.3	55.55	13.96
seawater	2.0	54.0	2.71	2.71	8.3	55.55	13.67
seawater	2.0	56.0	2.81	2.81	8.3	55.55	13.69
seawater	2.0	58.0	2.91	2.91	8.3	55.55	13.69
seawater	2.0	60.0	3.01	3.01	8.3	55.55	13.67

seawater	2.0	62.0	3.11	3.11	8.3	55.55	13.67
seawater	2.0	64.0	3.21	3.21	8.3	55.55	13.67
seawater	2.0	66.0	3.31	3.31	8.3	55.55	13.67
seawater	2.0	68.0	3.41	3.41	8.3	55.55	13.69
seawater	2.0	70.0	3.51	3.51	8.3	55.55	13.69
seawater	2.0	72.0	3.61	3.61	8.3	55.55	13.69
seawater	2.0	74.0	3.71	3.71	8.3	55.55	13.69
seawater	2.0	76.0	3.82	3.82	8.3	55.55	13.69
seawater	2.0	78.0	3.92	3.92	8.3	55.55	13.69
seawater	2.0	80.0	4.02	4.02	8.3	55.55	13.68
nanofluid	0.0	0.0	0.00	4.02	8.3	55.55	13.68
nanofluid	2.0	2.0	0.10	4.12	8.3	55.55	13.66
nanofluid	2.0	4.0	0.20	4.22	8.3	55.55	13.66
nanofluid	2.0	6.0	0.30	4.32	8.3	55.55	14.35
nanofluid	2.0	8.0	0.40	4.42	8.5	56.89	14.44
nanofluid	2.0	10.0	0.50	4.52	8.6	57.56	14.63
nanofluid	2.0	12.0	0.60	4.62	8.7	58.23	14.83
nanofluid	2.0	14.0	0.70	4.72	8.7	58.23	14.72
nanofluid	2.0	16.0	0.80	4.82	8.8	58.90	14.62
nanofluid	2.0	18.0	0.90	4.92	8.8	58.90	14.62
nanofluid	2.0	20.0	1.00	5.02	8.8	58.90	14.61
nanofluid	2.0	22.0	1.10	5.12	8.8	58.90	14.60
nanofluid	2.0	24.0	1.20	5.22	8.8	58.90	14.60
nanofluid	2.0	26.0	1.31	5.32	8.8	58.90	14.69
nanofluid	2.0	28.0	1.41	5.42	8.8	58.90	14.64
nanofluid	2.0	30.0	1.51	5.52	8.8	58.90	14.58
nanofluid	2.0	32.0	1.61	5.62	8.8	58.90	14.67
nanofluid	2.0	34.0	1.71	5.72	8.8	58.90	14.61
nanofluid	2.0	36.0	1.81	5.82	8.8	58.90	14.66
nanofluid	2.0	38.0	1.91	5.92	8.8	58.90	14.65
nanofluid	2.0	40.0	2.01	6.02	8.8	58.90	14.64
seawater	2.0	2.0	0.10	6.12	8.8	58.90	14.64
seawater	2.0	4.0	0.20	6.22	8.8	58.90	14.65
seawater	2.0	6.0	0.30	6.32	8.8	58.90	14.64
seawater	2.0	8.0	0.40	6.43	8.8	58.90	14.64
seawater	2.0	10.0	0.50	6.53	8.8	58.90	14.63
seawater	2.0	12.0	0.60	6.63	8.8	58.90	14.62
seawater	2.0	14.0	0.70	6.73	8.8	58.90	14.62
seawater	2.0	16.0	0.80	6.83	8.8	58.90	14.62

seawater	2.0	18.0	0.90	6.93	8.8	58.90	14.62
seawater	2.0	20.0	1.00	7.03	8.8	58.90	14.62
seawater	2.0	22.0	1.10	7.13	8.8	58.90	14.62
seawater	2.0	24.0	1.20	7.23	8.8	58.90	14.62
seawater	2.0	26.0	1.31	7.33	8.8	58.90	14.61
seawater	2.0	28.0	1.41	7.43	8.8	58.90	14.61
seawater	2.0	30.0	1.51	7.53	8.8	58.90	14.61
seawater	2.0	32.0	1.61	7.63	8.8	58.90	14.45
seawater	2.0	34.0	1.71	7.73	8.8	58.90	14.47
seawater	2.0	36.0	1.81	7.83	8.8	58.90	14.49
seawater	2.0	38.0	1.91	7.93	8.8	58.90	14.50
seawater	2.0	40.0	2.01	8.03	8.8	58.90	14.39
seawater	2.0	42.0	2.11	8.13	8.8	58.90	14.44
seawater	2.0	44.0	2.21	8.23	8.8	58.90	14.47
seawater	2.0	46.0	2.31	8.33	8.8	58.90	14.49
seawater	2.0	48.0	2.41	8.43	8.8	58.90	14.50
seawater	2.0	50.0	2.51	8.53	8.8	58.90	14.44
seawater	2.0	52.0	2.61	8.63	8.8	58.90	14.41
seawater	2.0	54.0	2.71	8.73	8.8	58.90	14.46
seawater	2.0	56.0	2.81	8.83	8.8	58.90	14.49
seawater	2.0	58.0	2.91	8.94	8.8	58.90	14.50
seawater	2.0	60.0	3.01	9.04	8.8	58.90	14.41
seawater	2.0	62.0	3.11	9.14	8.8	58.90	14.42
seawater	2.0	64.0	3.21	9.24	8.8	58.90	14.47
seawater	2.0	66.0	3.31	9.34	8.8	58.90	14.49
seawater	2.0	68.0	3.41	9.44	8.8	58.90	14.45
seawater	2.0	70.0	3.51	9.54	8.8	58.90	14.42
seawater	2.0	72.0	3.61	9.64	8.8	58.90	14.46
seawater	2.0	74.0	3.71	9.74	8.8	58.90	14.49
seawater	2.0	76.0	3.82	9.84	8.8	58.90	14.47
seawater	2.0	78.0	3.92	9.94	8.8	58.90	14.41
seawater	2.0	80.0	4.02	10.04	8.8	58.90	14.46

Appendix J. Coreflooding Oil Recovery Plot with Differential Pressures using 0.01 wt% Nanofluid



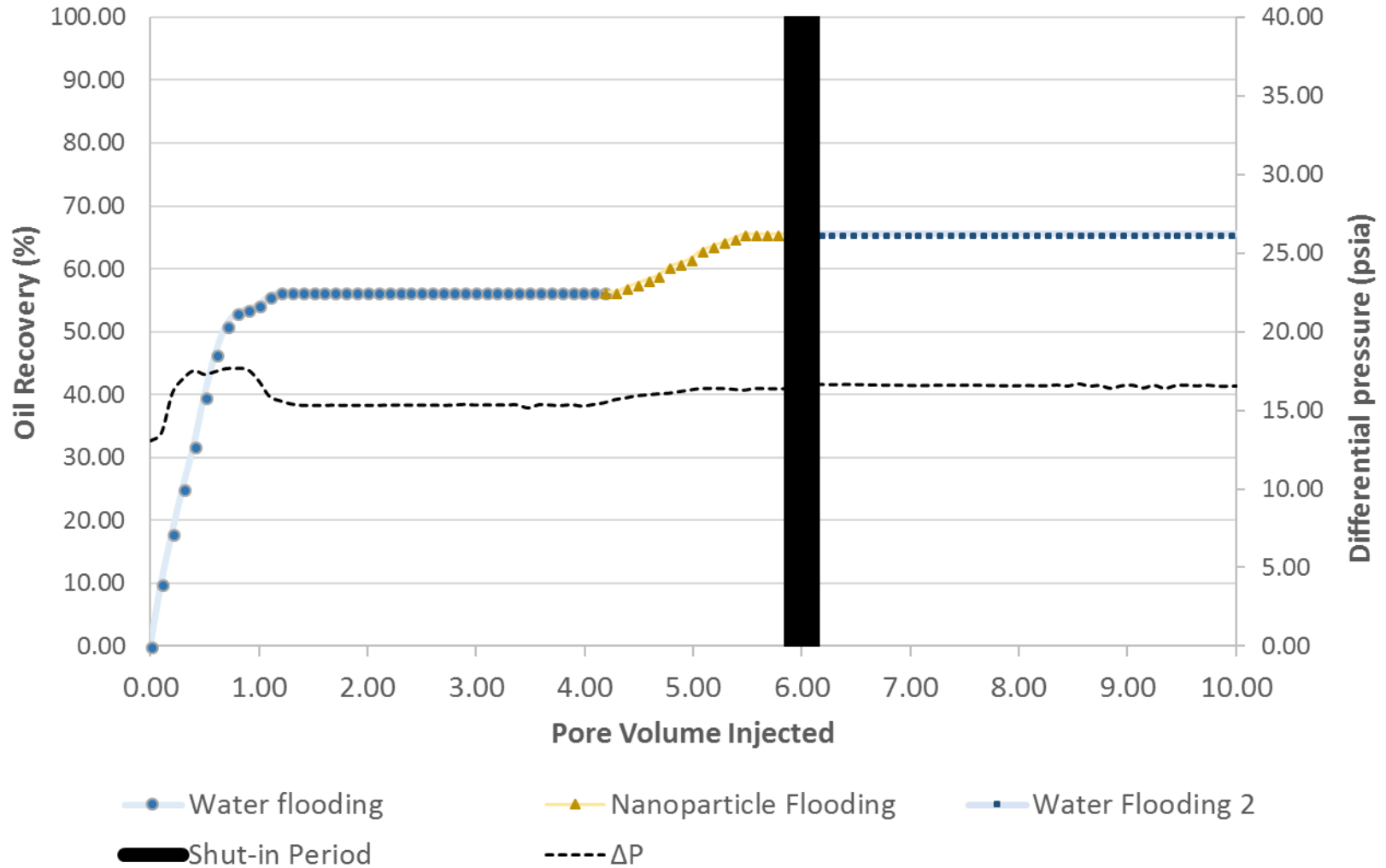
Appendix K. Coreflood Experiment Using 0.03 wt% Nanofluid on Berea Sandstone Raw Data

Injection Type	Volume Injected (per min) mL	Cumulative Volume injected mL	Pore Volume Injected mL	Total Pore Volume Injected	Cumulative Oil Produced mL	% Oil Recovery	ΔP
seawater	0.0	0.0	0.00	0.00	0.0	0.00	13.05
seawater	2.0	2.0	0.10	0.10	1.5	9.94	13.56
seawater	2.0	4.0	0.20	0.20	2.7	17.89	16.09
seawater	2.0	6.0	0.30	0.30	3.8	25.18	17.02
seawater	2.0	8.0	0.40	0.40	4.8	31.81	17.54
seawater	2.0	10.0	0.50	0.50	6.0	39.76	17.29
seawater	2.0	12.0	0.60	0.60	7.0	46.39	17.48
seawater	2.0	14.0	0.70	0.70	7.7	51.03	17.67
seawater	2.0	16.0	0.80	0.80	8.0	53.02	17.68
seawater	2.0	18.0	0.89	0.89	8.1	53.68	17.60
seawater	2.0	20.0	0.99	0.99	8.2	54.34	16.90
seawater	2.0	22.0	1.09	1.09	8.4	55.67	15.90
seawater	2.0	24.0	1.19	1.19	8.5	56.33	15.61
seawater	2.0	26.0	1.29	1.29	8.5	56.33	15.41
seawater	2.0	28.0	1.39	1.39	8.5	56.33	15.32
seawater	2.0	30.0	1.49	1.49	8.5	56.33	15.31
seawater	2.0	32.0	1.59	1.59	8.5	56.33	15.32
seawater	2.0	34.0	1.69	1.69	8.5	56.33	15.33
seawater	2.0	36.0	1.79	1.79	8.5	56.33	15.32
seawater	2.0	38.0	1.89	1.89	8.5	56.33	15.32
seawater	2.0	40.0	1.99	1.99	8.5	56.33	15.32
seawater	2.0	42.0	2.09	2.09	8.5	56.33	15.32
seawater	2.0	44.0	2.19	2.19	8.5	56.33	15.33
seawater	2.0	46.0	2.29	2.29	8.5	56.33	15.34
seawater	2.0	48.0	2.39	2.39	8.5	56.33	15.33
seawater	2.0	50.0	2.49	2.49	8.5	56.33	15.33
seawater	2.0	52.0	2.58	2.58	8.5	56.33	15.33
seawater	2.0	54.0	2.68	2.68	8.5	56.33	15.32
seawater	2.0	56.0	2.78	2.78	8.5	56.33	15.33
seawater	2.0	58.0	2.88	2.88	8.5	56.33	15.38
seawater	2.0	60.0	2.98	2.98	8.5	56.33	15.34

seawater	2.0	62.0	3.08	3.08	8.5	56.33	15.34
seawater	2.0	64.0	3.18	3.18	8.5	56.33	15.34
seawater	2.0	66.0	3.28	3.28	8.5	56.33	15.34
seawater	2.0	68.0	3.38	3.38	8.5	56.33	15.35
seawater	2.0	70.0	3.48	3.48	8.5	56.33	15.15
seawater	2.0	72.0	3.58	3.58	8.5	56.33	15.36
seawater	2.0	74.0	3.68	3.68	8.5	56.33	15.34
seawater	2.0	76.0	3.78	3.78	8.5	56.33	15.30
seawater	2.0	78.0	3.88	3.88	8.5	56.33	15.36
seawater	2.0	80.0	3.98	3.98	8.5	56.33	15.27
seawater	2.0	82.0	4.08	4.08	8.5	56.33	15.37
nanofluid	2.0	2.0	0.10	4.17	8.5	56.33	15.48
nanofluid	2.0	4.0	0.20	4.27	8.5	56.33	15.68
nanofluid	2.0	6.0	0.30	4.37	8.6	56.99	15.79
nanofluid	2.0	8.0	0.40	4.47	8.7	57.65	15.93
nanofluid	2.0	10.0	0.50	4.57	8.8	58.32	15.99
nanofluid	2.0	12.0	0.60	4.67	8.9	58.98	16.05
nanofluid	2.0	14.0	0.70	4.77	9.1	60.31	16.09
nanofluid	2.0	16.0	0.80	4.87	9.2	60.97	16.20
nanofluid	2.0	18.0	0.89	4.97	9.3	61.63	16.30
nanofluid	2.0	20.0	0.99	5.07	9.5	62.96	16.40
nanofluid	2.0	22.0	1.09	5.17	9.6	63.62	16.40
nanofluid	2.0	24.0	1.19	5.27	9.7	64.28	16.40
nanofluid	2.0	26.0	1.29	5.37	9.8	64.94	16.35
nanofluid	2.0	28.0	1.39	5.47	9.9	65.61	16.29
nanofluid	2.0	30.0	1.49	5.57	9.9	65.61	16.40
nanofluid	2.0	32.0	1.59	5.67	9.9	65.61	16.39
nanofluid	2.0	34.0	1.69	5.77	9.9	65.61	16.38
nanofluid	2.0	36.0	1.79	5.86	9.9	65.61	16.38
nanofluid	2.0	38.0	1.89	5.96	9.9	65.61	16.37
nanofluid	2.0	40.0	1.99	6.06	9.9	65.61	16.37
seawater	2.0	0.0	0.00	6.06	9.9	65.61	16.65
seawater	2.0	2.0	0.10	6.16	9.9	65.61	16.66
seawater	2.0	4.0	0.20	6.26	9.9	65.61	16.64
seawater	2.0	6.0	0.30	6.36	9.9	65.61	16.65
seawater	2.0	8.0	0.40	6.46	9.9	65.61	16.66
seawater	2.0	10.0	0.50	6.56	9.9	65.61	16.64
seawater	2.0	12.0	0.60	6.66	9.9	65.61	16.62
seawater	2.0	14.0	0.70	6.76	9.9	65.61	16.61

seawater	2.0	16.0	0.80	6.86	9.9	65.61	16.61
seawater	2.0	18.0	0.89	6.96	9.9	65.61	16.60
seawater	2.0	20.0	0.99	7.06	9.9	65.61	16.58
seawater	2.0	22.0	1.09	7.16	9.9	65.61	16.59
seawater	2.0	24.0	1.19	7.26	9.9	65.61	16.60
seawater	2.0	26.0	1.29	7.36	9.9	65.61	16.60
seawater	2.0	28.0	1.39	7.46	9.9	65.61	16.60
seawater	2.0	30.0	1.49	7.55	9.9	65.61	16.61
seawater	2.0	32.0	1.59	7.65	9.9	65.61	16.60
seawater	2.0	34.0	1.69	7.75	9.9	65.61	16.59
seawater	2.0	36.0	1.79	7.85	9.9	65.61	16.57
seawater	2.0	38.0	1.89	7.95	9.9	65.61	16.56
seawater	2.0	40.0	1.99	8.05	9.9	65.61	16.59
seawater	2.0	42.0	2.09	8.15	9.9	65.61	16.57
seawater	2.0	44.0	2.19	8.25	9.9	65.61	16.57
seawater	2.0	46.0	2.29	8.35	9.9	65.61	16.62
seawater	2.0	48.0	2.39	8.45	9.9	65.61	16.55
seawater	2.0	50.0	2.49	8.55	9.9	65.61	16.70
seawater	2.0	52.0	2.58	8.65	9.9	65.61	16.55
seawater	2.0	54.0	2.68	8.75	9.9	65.61	16.59
seawater	2.0	56.0	2.78	8.85	9.9	65.61	16.41
seawater	2.0	58.0	2.88	8.95	9.9	65.61	16.57
seawater	2.0	60.0	2.98	9.05	9.9	65.61	16.61
seawater	2.0	62.0	3.08	9.15	9.9	65.61	16.43
seawater	2.0	64.0	3.18	9.24	9.9	65.61	16.60
seawater	2.0	66.0	3.28	9.34	9.9	65.61	16.41
seawater	2.0	68.0	3.38	9.44	9.9	65.61	16.58
seawater	2.0	70.0	3.48	9.54	9.9	65.61	16.61
seawater	2.0	72.0	3.58	9.64	9.9	65.61	16.56
seawater	2.0	74.0	3.68	9.74	9.9	65.61	16.61
seawater	2.0	76.0	3.78	9.84	9.9	65.61	16.54
seawater	2.0	78.0	3.88	9.94	9.9	65.61	16.55
seawater	2.0	80.0	3.98	10.04	9.9	65.61	16.55

Appendix L. Coreflooding Oil Recovery Plot with Differential Pressures using 0.03 wt% Nanofluid



Appendix M. Coreflood Experiment Using 0.05 wt% Nanofluid on Berea Sandstone Raw Data

Injection Type	Volume Injected (per min) mL	Cumulative Volume injected mL	Pore Volume Injected mL	Total Pore Volume Injected	Cumulative Oil Produced mL	% Oil Recovery	ΔP
seawater	0.0	0.0	0.00	0.00	0.0	0.00	12.54
seawater	2.0	2.0	0.10	0.10	0.2	1.35	13.05
seawater	2.0	4.0	0.20	0.20	0.5	3.38	15.04
seawater	2.0	6.0	0.30	0.30	1.3	8.46	18.04
seawater	2.0	8.0	0.41	0.41	2.5	16.91	18.15
seawater	2.0	10.0	0.51	0.51	5.1	34.50	18.73
seawater	2.0	12.0	0.61	0.61	6.5	43.97	18.64
seawater	2.0	14.0	0.71	0.71	6.9	46.67	18.35
seawater	2.0	16.0	0.81	0.81	7.5	50.73	18.06
seawater	2.0	18.0	0.91	0.91	7.7	52.08	17.68
seawater	2.0	20.0	1.01	1.01	7.8	52.76	17.75
seawater	2.0	22.0	1.12	1.12	8.0	54.11	16.75
seawater	2.0	24.0	1.22	1.22	8.0	54.11	16.56
seawater	2.0	26.0	1.32	1.32	8.0	54.11	16.54
seawater	2.0	28.0	1.42	1.42	8.0	54.11	16.28
seawater	2.0	30.0	1.52	1.52	8.0	54.11	16.35
seawater	2.0	32.0	1.62	1.62	8.0	54.11	16.35
seawater	2.0	34.0	1.72	1.72	8.0	54.11	16.28
seawater	2.0	36.0	1.83	1.83	8.0	54.11	16.25
seawater	2.0	38.0	1.93	1.93	8.0	54.11	16.43
seawater	2.0	40.0	2.03	2.03	8.0	54.11	16.34
seawater	2.0	42.0	2.13	2.13	8.0	54.11	16.35
seawater	2.0	44.0	2.23	2.23	8.0	54.11	16.26
seawater	2.0	46.0	2.33	2.33	8.0	54.11	16.28
seawater	2.0	48.0	2.44	2.44	8.0	54.11	16.25
seawater	2.0	50.0	2.54	2.54	8.0	54.11	16.25
seawater	2.0	52.0	2.64	2.64	8.0	54.11	16.26
seawater	2.0	54.0	2.74	2.74	8.0	54.11	16.35
seawater	2.0	56.0	2.84	2.84	8.0	54.11	16.42
seawater	2.0	58.0	2.94	2.94	8.0	54.11	16.40
seawater	2.0	60.0	3.04	3.04	8.0	54.11	16.36

seawater	2.0	62.0	3.15	3.15	8.0	54.11	16.25
seawater	2.0	64.0	3.25	3.25	8.0	54.11	16.21
seawater	2.0	66.0	3.35	3.35	8.0	54.11	16.19
seawater	2.0	68.0	3.45	3.45	8.0	54.11	16.19
seawater	2.0	70.0	3.55	3.55	8.0	54.11	16.08
seawater	2.0	72.0	3.65	3.65	8.0	54.11	16.07
seawater	2.0	74.0	3.75	3.75	8.0	54.11	16.05
seawater	2.0	76.0	3.86	3.86	8.0	54.11	16.03
seawater	2.0	78.0	3.96	3.96	8.0	54.11	16.13
nanofluid	2.0	2.0	0.10	4.06	8.0	54.11	16.31
nanofluid	2.0	4.0	0.20	4.16	8.0	54.11	16.41
nanofluid	2.0	6.0	0.30	4.26	8.2	55.47	16.51
nanofluid	2.0	8.0	0.41	4.36	8.4	56.82	16.61
nanofluid	2.0	10.0	0.51	4.46	8.6	58.17	16.64
nanofluid	2.0	12.0	0.61	4.57	8.7	58.85	16.66
nanofluid	2.0	14.0	0.71	4.67	8.8	59.53	16.62
nanofluid	2.0	16.0	0.81	4.77	9.0	60.88	16.51
nanofluid	2.0	18.0	0.91	4.87	9.0	60.88	16.55
nanofluid	2.0	20.0	1.01	4.97	9.1	61.55	16.68
nanofluid	2.0	22.0	1.12	5.07	9.2	62.23	17.37
nanofluid	2.0	24.0	1.22	5.17	9.4	63.58	17.56
nanofluid	2.0	26.0	1.32	5.28	9.5	64.26	17.76
nanofluid	2.0	28.0	1.42	5.38	9.8	66.29	17.68
nanofluid	2.0	30.0	1.52	5.48	9.9	66.97	17.48
nanofluid	2.0	32.0	1.62	5.58	10.2	69.00	17.70
nanofluid	2.0	34.0	1.72	5.68	10.2	69.00	17.83
nanofluid	2.0	36.0	1.83	5.78	10.2	69.00	17.91
nanofluid	2.0	38.0	1.93	5.88	10.2	69.00	18.01
nanofluid	2.0	40.0	2.03	5.99	10.2	69.00	18.12
seawater	2.0	2.0	0.10	6.09	10.2	69.00	18.21
seawater	2.0	4.0	0.20	6.19	10.2	69.00	18.22
seawater	2.0	6.0	0.30	6.29	10.2	69.00	18.23
seawater	2.0	8.0	0.41	6.39	10.2	69.00	18.17
seawater	2.0	10.0	0.51	6.49	10.2	69.00	18.26
seawater	2.0	12.0	0.61	6.60	10.2	69.00	18.36
seawater	2.0	14.0	0.71	6.70	10.2	69.00	18.42
seawater	2.0	16.0	0.81	6.80	10.2	69.00	18.46
seawater	2.0	18.0	0.91	6.90	10.2	69.00	18.49
seawater	2.0	20.0	1.01	7.00	10.2	69.00	18.52

seawater	2.0	22.0	1.12	7.10	10.2	69.00	18.53
seawater	2.0	24.0	1.22	7.20	10.2	69.00	18.53
seawater	2.0	26.0	1.32	7.31	10.2	69.00	18.55
seawater	2.0	28.0	1.42	7.41	10.2	69.00	18.55
seawater	2.0	30.0	1.52	7.51	10.2	69.00	18.56
seawater	2.0	32.0	1.62	7.61	10.2	69.00	18.56
seawater	2.0	34.0	1.72	7.71	10.2	69.00	18.55
seawater	2.0	36.0	1.83	7.81	10.2	69.00	18.57
seawater	2.0	38.0	1.93	7.91	10.2	69.00	18.57
seawater	2.0	40.0	2.03	8.02	10.2	69.00	18.58
seawater	2.0	42.0	2.13	8.12	10.2	69.00	18.58
seawater	2.0	44.0	2.23	8.22	10.2	69.00	18.58
seawater	2.0	46.0	2.33	8.32	10.2	69.00	18.56
seawater	2.0	48.0	2.44	8.42	10.2	69.00	18.57
seawater	2.0	50.0	2.54	8.52	10.2	69.00	18.57
seawater	2.0	52.0	2.64	8.62	10.2	69.00	18.57
seawater	2.0	54.0	2.74	8.73	10.2	69.00	18.58
seawater	2.0	56.0	2.84	8.83	10.2	69.00	18.57
seawater	2.0	58.0	2.94	8.93	10.2	69.00	18.57
seawater	2.0	60.0	3.04	9.03	10.2	69.00	18.56
seawater	2.0	62.0	3.15	9.13	10.2	69.00	18.55
seawater	2.0	64.0	3.25	9.23	10.2	69.00	18.55
seawater	2.0	66.0	3.35	9.33	10.2	69.00	18.54
seawater	2.0	68.0	3.45	9.44	10.2	69.00	18.54
seawater	2.0	70.0	3.55	9.54	10.2	69.00	18.53
seawater	2.0	72.0	3.65	9.64	10.2	69.00	18.54
seawater	2.0	74.0	3.75	9.74	10.2	69.00	18.53
seawater	2.0	76.0	3.86	9.84	10.2	69.00	18.55
seawater	2.0	78.0	3.96	9.94	10.2	69.00	18.54
seawater	2.0	80.0	4.06	10.04	10.2	69.00	18.55

Appendix N. Coreflood Experiment Using 0.05 wt% Nanofluid on Hebron Core Raw Data

Injection Type	Volume Injected (per min) mL	Cumulative Volume injected mL	Pore Volume Injected mL	Total Pore Volume Injected	Cumulative Oil Produced mL	% Oil Recovery	ΔP
seawater	0.0	0.0	0.00	0.00	0.0	0.00	11.96
seawater	2.0	2.0	0.09	0.09	0.0	0.00	12.68
seawater	2.0	4.0	0.18	0.18	0.3	2.23	14.72
seawater	2.0	6.0	0.27	0.27	0.8	5.93	15.74
seawater	2.0	8.0	0.36	0.36	1.8	13.35	16.75
seawater	2.0	10.0	0.45	0.45	2.6	19.28	16.98
seawater	2.0	12.0	0.53	0.53	3.5	25.96	17.37
seawater	2.0	14.0	0.62	0.62	4.5	33.38	17.71
seawater	2.0	16.0	0.71	0.71	5.5	40.80	17.65
seawater	2.0	18.0	0.80	0.80	6.1	45.25	17.65
seawater	2.0	20.0	0.89	0.89	6.5	48.21	17.61
seawater	2.0	22.0	0.98	0.98	6.6	48.95	17.33
seawater	2.0	24.0	1.07	1.07	6.7	49.70	17.10
seawater	2.0	26.0	1.16	1.16	6.7	49.70	15.41
seawater	2.0	28.0	1.25	1.25	6.7	49.70	15.30
seawater	2.0	30.0	1.34	1.34	6.7	49.70	15.11
seawater	2.0	32.0	1.42	1.42	6.7	49.70	15.29
seawater	2.0	34.0	1.51	1.51	6.7	49.70	15.43
seawater	2.0	36.0	1.60	1.60	6.7	49.70	15.46
seawater	2.0	38.0	1.69	1.69	6.7	49.70	15.53
seawater	2.0	40.0	1.78	1.78	6.7	49.70	15.56
seawater	2.0	42.0	1.87	1.87	6.7	49.70	15.56
seawater	2.0	44.0	1.96	1.96	6.7	49.70	15.53
seawater	2.0	46.0	2.05	2.05	6.7	49.70	15.36
seawater	2.0	48.0	2.14	2.14	6.7	49.70	15.40
seawater	2.0	50.0	2.23	2.23	6.7	49.70	15.27
seawater	2.0	52.0	2.31	2.31	6.7	49.70	15.20
seawater	2.0	54.0	2.40	2.40	6.7	49.70	15.17
seawater	2.0	56.0	2.49	2.49	6.7	49.70	15.30
seawater	2.0	58.0	2.58	2.58	6.7	49.70	15.22
seawater	2.0	60.0	2.67	2.67	6.7	49.70	15.26

seawater	2.0	62.0	2.76	2.76	6.7	49.70	15.29
seawater	2.0	64.0	2.85	2.85	6.7	49.70	15.35
seawater	2.0	66.0	2.94	2.94	6.7	49.70	15.36
seawater	2.0	68.0	3.03	3.03	6.7	49.70	15.24
seawater	2.0	70.0	3.12	3.12	6.7	49.70	15.21
seawater	2.0	72.0	3.20	3.20	6.7	49.70	15.16
seawater	2.0	74.0	3.29	3.29	6.7	49.70	15.20
seawater	2.0	76.0	3.38	3.38	6.7	49.70	15.21
seawater	2.0	78.0	3.47	3.47	6.7	49.70	15.29
seawater	2.0	80.0	3.56	3.56	6.7	49.70	15.35
seawater	2.0	82.0	3.65	3.65	6.7	49.70	15.28
seawater	2.0	84.0	3.74	3.74	6.7	49.70	15.27
seawater	2.0	86.0	3.83	3.83	6.7	49.70	15.24
seawater	2.0	88.0	3.92	3.92	6.7	49.70	15.24
seawater	2.0	90.0	4.01	4.01	6.7	49.70	15.21
nanofluid	2.0	2.0	0.09	4.09	6.7	49.70	15.11
nanofluid	2.0	4.0	0.18	4.18	6.7	49.70	15.13
nanofluid	2.0	6.0	0.27	4.27	6.7	49.70	15.13
nanofluid	2.0	8.0	0.36	4.36	6.7	49.70	15.61
nanofluid	2.0	10.0	0.45	4.45	6.7	49.70	16.10
nanofluid	2.0	12.0	0.53	4.54	6.8	50.44	16.63
nanofluid	2.0	14.0	0.62	4.63	6.9	51.18	16.92
nanofluid	2.0	16.0	0.71	4.72	7.4	54.89	17.01
nanofluid	2.0	18.0	0.80	4.81	7.7	57.11	16.97
nanofluid	2.0	20.0	0.89	4.90	7.9	58.60	17.18
nanofluid	2.0	22.0	0.98	4.98	8.1	60.08	17.28
nanofluid	2.0	24.0	1.07	5.07	8.3	61.56	17.28
nanofluid	2.0	26.0	1.16	5.16	8.3	61.56	17.32
nanofluid	2.0	28.0	1.25	5.25	8.3	61.56	17.32
nanofluid	2.0	30.0	1.34	5.34	8.3	61.56	17.34
nanofluid	2.0	32.0	1.42	5.43	8.3	61.56	17.36
nanofluid	2.0	34.0	1.51	5.52	8.3	61.56	17.39
nanofluid	2.0	36.0	1.60	5.61	8.3	61.56	17.48
nanofluid	2.0	38.0	1.69	5.70	8.3	61.56	17.59
nanofluid	2.0	40.0	1.78	5.79	8.3	61.56	17.59
nanofluid	2.0	42.0	1.87	5.87	8.3	61.56	17.58
nanofluid	2.0	44.0	1.96	5.96	8.3	61.56	17.58
nanofluid	2.0	46.0	2.05	6.05	8.3	61.56	17.61
seawater	2.0	2.0	0.09	6.14	8.3	61.56	17.59

seawater	2.0	4.0	0.18	6.23	8.3	61.56	17.57
seawater	2.0	6.0	0.27	6.32	8.3	61.56	17.59
seawater	2.0	8.0	0.36	6.41	8.3	61.56	17.59
seawater	2.0	10.0	0.45	6.50	8.3	61.56	17.57
seawater	2.0	12.0	0.53	6.59	8.3	61.56	17.57
seawater	2.0	14.0	0.62	6.68	8.3	61.56	17.59
seawater	2.0	16.0	0.71	6.76	8.3	61.56	17.58
seawater	2.0	18.0	0.80	6.85	8.3	61.56	17.57
seawater	2.0	20.0	0.89	6.94	8.3	61.56	17.58
seawater	2.0	22.0	0.98	7.03	8.3	61.56	17.60
seawater	2.0	24.0	1.07	7.12	8.3	61.56	17.65
seawater	2.0	26.0	1.16	7.21	8.3	61.56	17.61
seawater	2.0	28.0	1.25	7.30	8.3	61.56	17.60
seawater	2.0	30.0	1.34	7.39	8.3	61.56	17.62
seawater	2.0	32.0	1.42	7.48	8.3	61.56	17.60
seawater	2.0	34.0	1.51	7.57	8.3	61.56	17.59
seawater	2.0	36.0	1.60	7.65	8.3	61.56	17.47
seawater	2.0	38.0	1.69	7.74	8.3	61.56	17.46
seawater	2.0	40.0	1.78	7.83	8.3	61.56	17.44
seawater	2.0	42.0	1.87	7.92	8.3	61.56	17.48
seawater	2.0	44.0	1.96	8.01	8.3	61.56	17.52
seawater	2.0	46.0	2.05	8.10	8.3	61.56	17.52
seawater	2.0	48.0	2.14	8.19	8.3	61.56	17.52
seawater	2.0	50.0	2.23	8.28	8.3	61.56	17.54
seawater	2.0	52.0	2.31	8.37	8.3	61.56	17.54
seawater	2.0	54.0	2.40	8.46	8.3	61.56	17.53
seawater	2.0	56.0	2.49	8.54	8.3	61.56	17.57
seawater	2.0	58.0	2.58	8.63	8.3	61.56	17.55
seawater	2.0	60.0	2.67	8.72	8.3	61.56	17.54
seawater	2.0	62.0	2.76	8.81	8.3	61.56	17.56
seawater	2.0	64.0	2.85	8.90	8.3	61.56	17.54
seawater	2.0	66.0	2.94	8.99	8.3	61.56	17.54
seawater	2.0	68.0	3.03	9.08	8.3	61.56	17.53
seawater	2.0	70.0	3.12	9.17	8.3	61.56	17.52
seawater	2.0	72.0	3.20	9.26	8.3	61.56	17.55
seawater	2.0	74.0	3.29	9.35	8.3	61.56	17.55
seawater	2.0	76.0	3.38	9.43	8.3	61.56	17.56
seawater	2.0	78.0	3.47	9.52	8.3	61.56	17.57
seawater	2.0	80.0	3.56	9.61	8.3	61.56	17.60
seawater	2.0	82.0	3.65	9.70	8.3	61.56	17.59

seawater	2.0	84.0	3.74	9.79	8.3	61.56	17.57
seawater	2.0	86.0	3.83	9.88	8.3	61.56	17.58
seawater	2.0	88.0	3.92	9.97	8.3	61.56	17.60
seawater	2.0	90.0	4.01	10.06	8.3	61.56	17.43

Appendix O. Coreflood Experiment Using HCl/Seawater Mixture on Berea Sandstone Raw Data

Injection Type	Volume Injected (per min) mL	Cumulative Volume injected mL	Pore Volume Injected mL	Total Pore Volume Injected	Cumulative Oil Produced mL	% Oil Recovery	ΔP
seawater	0.0	0.0	0.0	0.0	0.0	0.00	13.42
seawater	2.0	2.0	0.10	0.10	0.0	0.00	14.47
seawater	2.0	4.0	0.19	0.19	1.2	7.79	14.98
seawater	2.0	6.0	0.29	0.29	2.7	17.53	15.99
seawater	2.0	8.0	0.39	0.39	4.5	29.22	16.51
seawater	2.0	10.0	0.48	0.48	5.9	37.98	16.51
seawater	2.0	12.0	0.58	0.58	7.2	46.75	17.03
seawater	2.0	14.0	0.68	0.68	8.0	51.62	17.54
seawater	2.0	16.0	0.78	0.78	8.6	55.51	17.34
seawater	2.0	18.0	0.87	0.87	8.6	55.51	14.15
seawater	2.0	20.0	0.97	0.97	8.6	55.51	14.15
seawater	2.0	22.0	1.07	1.07	8.6	55.51	14.16
seawater	2.0	24.0	1.16	1.16	8.6	55.51	14.17
seawater	2.0	26.0	1.26	1.26	8.6	55.51	14.95
seawater	2.0	28.0	1.36	1.36	8.6	55.51	14.13
seawater	2.0	30.0	1.45	1.45	8.6	55.51	14.12
seawater	2.0	32.0	1.55	1.55	8.6	55.51	14.10
seawater	2.0	34.0	1.65	1.65	8.6	55.51	14.09
seawater	2.0	36.0	1.75	1.75	8.6	55.51	14.07
seawater	2.0	38.0	1.84	1.84	8.6	55.51	14.06
seawater	2.0	40.0	1.94	1.94	8.6	55.51	14.02
seawater	2.0	42.0	2.04	2.04	8.6	55.51	14.01
seawater	2.0	44.0	2.13	2.13	8.6	55.51	14.03
seawater	2.0	46.0	2.23	2.23	8.6	55.51	13.98
seawater	2.0	48.0	2.33	2.33	8.6	55.51	13.84
seawater	2.0	50.0	2.42	2.42	8.6	55.51	13.79
seawater	2.0	52.0	2.52	2.52	8.6	55.51	14.08
seawater	2.0	54.0	2.62	2.62	8.6	55.51	14.11
seawater	2.0	56.0	2.72	2.72	8.6	55.51	14.14
seawater	2.0	58.0	2.81	2.81	8.6	55.51	14.13
seawater	2.0	60.0	2.91	2.91	8.6	55.51	14.12

seawater	2.0	62.0	3.01	3.01	8.6	55.51	14.10
seawater	2.0	64.0	3.10	3.10	8.6	55.51	14.08
seawater	2.0	66.0	3.20	3.20	8.6	55.51	14.06
seawater	2.0	68.0	3.30	3.30	8.6	55.51	14.05
seawater	2.0	70.0	3.39	3.39	8.6	55.51	14.02
seawater	2.0	72.0	3.49	3.49	8.6	55.51	14.01
seawater	2.0	74.0	3.59	3.59	8.6	55.51	13.99
seawater	2.0	76.0	3.69	3.69	8.6	55.51	14.00
seawater	2.0	78.0	3.78	3.78	8.6	55.51	14.07
seawater	2.0	80.0	3.88	3.88	8.6	55.51	14.09
seawater	2.0	82.0	3.98	3.98	8.6	55.51	14.11
seawater	2.0	84.0	4.07	4.07	8.6	55.51	14.62
nanofluid	2.0	2.0	0.10	4.17	8.7	56.49	14.45
nanofluid	2.0	4.0	0.19	4.27	8.7	56.49	14.36
nanofluid	2.0	6.0	0.29	4.36	8.7	56.49	14.35
nanofluid	2.0	8.0	0.39	4.46	8.7	56.49	14.35
nanofluid	2.0	10.0	0.48	4.56	8.7	56.49	14.37
nanofluid	2.0	12.0	0.58	4.66	8.7	56.49	14.37
nanofluid	2.0	14.0	0.68	4.75	8.7	56.49	14.38
nanofluid	2.0	16.0	0.78	4.85	8.7	56.49	14.39
nanofluid	2.0	18.0	0.87	4.95	8.7	56.49	14.41
nanofluid	2.0	20.0	0.97	5.04	8.7	56.49	14.40
nanofluid	2.0	22.0	1.07	5.14	8.7	56.49	14.40
nanofluid	2.0	24.0	1.16	5.24	8.7	56.49	14.39
nanofluid	2.0	26.0	1.26	5.33	8.7	56.49	14.41
nanofluid	2.0	28.0	1.36	5.43	8.7	56.49	14.41
nanofluid	2.0	30.0	1.45	5.53	8.7	56.49	14.41
nanofluid	2.0	32.0	1.55	5.63	8.7	56.49	14.41
nanofluid	2.0	34.0	1.65	5.72	8.7	56.49	14.40
nanofluid	2.0	36.0	1.75	5.82	8.7	56.49	14.41
nanofluid	2.0	38.0	1.84	5.92	8.7	56.49	14.41
nanofluid	2.0	40.0	1.94	6.01	8.7	56.49	14.41
nanofluid	2.0	42.0	2.04	6.11	8.7	56.49	14.42
seawater	2.0	2.0	0.10	6.21	8.7	56.49	14.41
seawater	2.0	4.0	0.19	6.30	8.7	56.49	14.42
seawater	2.0	6.0	0.29	6.40	8.7	56.49	14.41
seawater	2.0	8.0	0.39	6.50	8.7	56.49	14.41
seawater	2.0	10.0	0.48	6.60	8.7	56.49	14.42
seawater	2.0	12.0	0.58	6.69	8.7	56.49	14.42

seawater	2.0	14.0	0.68	6.79	8.7	56.49	14.42
seawater	2.0	16.0	0.78	6.89	8.7	56.49	14.42
seawater	2.0	18.0	0.87	6.98	8.7	56.49	14.42
seawater	2.0	20.0	0.97	7.08	8.7	56.49	14.42
seawater	2.0	22.0	1.07	7.18	8.7	56.49	14.42
seawater	2.0	24.0	1.16	7.27	8.7	56.49	14.31
seawater	2.0	26.0	1.26	7.37	8.7	56.49	14.42
seawater	2.0	28.0	1.36	7.47	8.7	56.49	14.42
seawater	2.0	30.0	1.45	7.57	8.7	56.49	14.41
seawater	2.0	32.0	1.55	7.66	8.7	56.49	14.41
seawater	2.0	34.0	1.65	7.76	8.7	56.49	14.41
seawater	2.0	36.0	1.75	7.86	8.7	56.49	14.42
seawater	2.0	38.0	1.84	7.95	8.7	56.49	14.41
seawater	2.0	40.0	1.94	8.05	8.7	56.49	14.41
seawater	2.0	42.0	2.04	8.15	8.7	56.49	14.42
seawater	2.0	44.0	2.13	8.24	8.7	56.49	14.41
seawater	2.0	46.0	2.23	8.34	8.7	56.49	14.41
seawater	2.0	48.0	2.33	8.44	8.7	56.49	14.11
seawater	2.0	50.0	2.42	8.54	8.7	56.49	14.41
seawater	2.0	52.0	2.52	8.63	8.7	56.49	14.41
seawater	2.0	54.0	2.62	8.73	8.7	56.49	14.31
seawater	2.0	56.0	2.72	8.83	8.7	56.49	14.42
seawater	2.0	58.0	2.81	8.92	8.7	56.49	14.32
seawater	2.0	60.0	2.91	9.02	8.7	56.49	14.42
seawater	2.0	62.0	3.01	9.12	8.7	56.49	14.41
seawater	2.0	64.0	3.10	9.21	8.7	56.49	14.41
seawater	2.0	66.0	3.20	9.31	8.7	56.49	14.42
seawater	2.0	68.0	3.30	9.41	8.7	56.49	14.41
seawater	2.0	70.0	3.39	9.51	8.7	56.49	14.42
seawater	2.0	72.0	3.49	9.60	8.7	56.49	14.42
seawater	2.0	74.0	3.59	9.70	8.7	56.49	14.42
seawater	2.0	76.0	3.69	9.80	8.7	56.49	14.42
seawater	2.0	78.0	3.78	9.89	8.7	56.49	14.42
seawater	2.0	80.0	3.88	9.99	8.7	56.49	14.41
seawater	2.0	82.0	3.98	10.09	8.7	56.49	14.39